INFORMATION TO USERS

This material was produced from a microfilm copy of the original document. While the most advanced technological means to photograph and reproduce this document have been used, the quality is heavily dependent upon the quality of the original submitted.

The following explanation of techniques is provided to help you understand markings or patterns which may appear on this reproduction.

1. The sign or "target" for pages apparently lacking from the document photographed is "Missing Page(s)". If it was possible to obtain the missing page(s) or section, they are spliced into the film along with adjacent pages. This may have necessitated cutting thru an image and duplicating adjacent pages to insure you complete continuity.

2. When an image on the film is obliterated with a large round black mark, it is an indication that the photographer suspected that the copy may have moved during exposure and thus cause a blurred image. You will find a good image of the page in the adjacent frame.

3. When a map, drawing or chart, etc., was part of the material being photographed the photographer followed a definite method in "sectioning" the material. It is customary to begin photoing at the upper left hand corner of a large sheet and to continue photoing from left to right in equal sections with a small overlap. If necessary, sectioning is continued again — beginning below the first row and continuing on until complete.

4. The majority of users indicate that the textual content is of greatest value, however, a somewhat higher quality reproduction could be made from "photographs" if essential to the understanding of the dissertation. Silver prints of "photographs" may be ordered at additional charge by writing the Order Department, giving the catalog number, title, author and specific pages you wish reproduced.

5. PLEASE NOTE: Some pages may have indistinct print. Filmed as received.

University Microfilms International
300 North Zeeb Road
Ann Arbor, Michigan 48106 USA
St. John's Road, Tyler's Green
High Wycombe, Bucks, England HP10 8HR

RESONANCE RAMAN STUDIES OF VISUAL PIGMENTS

by

APOSTOLOS GEORGE DOUKAS

A dissertation submitted to the Graduate Faculty in Physics in partial fulfillment of the requirements for the degree of Doctor of Philosophy, The City University of New York.

1977

The manuscript has been read and accepted for the Graduate Faculty in Physics in satisfaction of the dissertation requirement for the degree of Doctor of Philosophy.

Sept. 12 1977
date

Robert Callender
Chairman of Examining Committee

Sept. 12, 1977
date

Myriam P. Sarachik
Executive Officer

Supervisory Committee

The City University of New York

Abstract

RESONANCE RAMAN STUDIES OF VISUAL PIGMENTS

by

Apostolos George Doukas

Adviser: Professor Robert Callender

We have developed a general technique which allows Raman measurements of any photosensitive material solution. The technique involves the imposition of a molecular velocity transverse to the laser exciting beam sufficient to insure that any given molecule moves through the beam so that it has little probability of absorbing a photon. This technique has been used to obtain resonance Raman spectra of all-trans, 13-cis, 9-cis, 11-cis protonated and unprotonated Schiff bases with n-butylamine in solution, extracts of bovine rhodopsin in cetyltrimethylamonium bromide, metarhodopsin I and metarhodopsin II vesicles, and the pigments PM568 and M412 from the purple membrane protein of Halobacterium Halobium.

The analysis indicate that the chromophore in metarhodopsin I and metarhodopsin II assumes an essentially all-trans conformation. The main difference between the two forms as it concerns the chromophore being in the deprotonation of the Schiff base in the metarhodopsin I to metarhodopsin II transition. An earlier finding that the conformation of the chromophore in rhodopsin is similar to that of 11-cis protonated Schiff base in solution has been confirmed.

The resonance Raman study of purple membrane system (PM568 and M412) contradicts earlier chemical-extraction experiments. The conformation of the chromophore in the two forms as indicated by the Raman spectra, does not resemble any of the proposed models. However, the deprotonation of the Schiff base in the PM568 to M412 transition has been confirmed. The mechanism by which the visual pigments and purple membrane system regulate their color has been studied. It has been confirmed that this regulation is achieved by delocalization of the electrons of the chromophore. This explanation has also been extended to metarhodopsin I and metarhodopsin II.

ACKNOWLEDGEMENTS

To Professor Robert Callender the author wishes to express his sincere appreciation for the direction, valuable suggestions and encouragement given in the preparation of this thesis. His ideas have been a central and essential part of these experiments.

In addition I would like to express my special thanks to Randy Fenstermacher, Dick Leigh, Jo-Lien Yang, Bea Aton, Anthony Yudd and Mike Pettei.

Finally, the close support of the entire staff of the machine shop of the Department of Physics and Mr. H. Schimatz of the glass blowing shop of the Department of Chemistry have been invaluable during the course of this work.

TABLE OF CONTENTS

LIST OF TABLES

LIST OF FIGURES

Introduction

Resonance Raman spectroscopy has come into prominence as a tool of studying macromolecules in the last few years. The unique advantage of the resonance Raman spectroscopy is that it can specifically probe the absorption site of the molecule. The vibrational modes that couple with the electronic transition are selectively enhanced while the rest of the molecule does not contribute to the Raman spectrum. Thus the Raman spectrum contains information specifically about the structure of the absorption site and its interaction with the rest of the molecule.

Resonance Raman spectroscopy has been restricted so far to coloured molecular systems like bovine rhodopsin (Lewis et al., 1973; Oseroff and Callender, 1974; Mathies et al., 1976; Callender et al., 1976), hemoglobin (Strekas and Spiro, 1972a; Spiro and Strekas, 1972, 1974; Brunner et al., 1972; Spiro, 1975a) cytochrome c (Yamamoto et al., 1973; Strekas and Spiro, 1972b; Brunner, 1973; Collins et al; 1973; Pezolet et al., 1973, Adar and Erecinska, 1974; Nafie et al., 1973; Spiro, 1975b) chlorophyl (Lutz and Breton, 1973), and the purple membrane protein of Halobacterium Halobium (Mendelsohn, 1973, 1976; Lewis et al., 1974; Mendelsohn et al., 1974, Aton et al., 1977). However, it may be possible in the future to study specific parts of molecules that do not absorb in the visible by incorporating a dye in the molecule. This method has already been used in the study of proteins that do not fluoresce (Weber and Teale, 1959; Chadwick et al., 1960; see also Udenfriend, 1969).

The purpose of this work is to extend the resonance Raman spectroscopy to the study of the visual pigments, in particular, the bovine rhodopsin its intermediates

metarhodopsin I and metarhodopsin II, under close to physiological conditions. We also extend the same techniques we have developed in the study of the visual pigments to the study of the purple membrane system from the bacterium of Halobacterium Halobium. The resonance Raman spectra of the visual pigments and the purple membrane system constitutes one aspect of this work. Another aspect is the assignment of the Raman bands to particular vibrational modes and the interpretation of the Raman spectra of the visual pigments and the purple membrane system. We propose to approach this problem using the Raman spectra of model compounds such as retinals and Schiff bases of retinals in solution and crystals.

This work is divided into three parts. The first part includes (a) a short introduction of the Raman and resonance Raman effect. (b) A review of the bovine rhodopsin system and its physiological role as a light transducer. (c) A review of the purple membrane protein from the bacterium Halobacterium Halobium and its physiological role as a photosynthetic pigment. In the second part difficulties arising from the photolabile nature of these systems are discussed and the molecular flow technique is introduced. A detailed description of the samples and the experimental conditions of the Raman measurements is also included. Finally, in the third part the resonance Raman spectra of the model compounds, visual pigments and the purple membrane system are presented and discussed.

Section I

Raman Effect

In the Raman effect monochromatic radiation is impigned on a molecule. The scattered radiation contains components that are shifted in frequency by amounts corresponding to the normal mode frequencies of the molecule. The shifts (vibrational frequencies) are independent of the frequency of the incident radiation. Two identical patterns, as far as the vibrational frequencies are concerned, are observed, one on each side of the incident light frequency. The pattern on the low-frequency side of the exciting light is known as stokes lines while the pattern on the high-frequency side is known as anti-stokes lines. Raman spectroscopy is complementary to the infrared absorption spectroscopy in that it measures vibrational frequencies. When the incident radiation frequency lies on or near a particular absorption band, Raman effect is known as resonance Raman. Resonance Raman is not qualitatively different from Raman effect. However, changes in the spectrum appear due to cross section enhancement of particular normal modes.

Since the discovery of the Raman effect in 1928 (Raman and Krishnan, 1928) a considerable amount of theoretical work has been done on the Raman and resonance Raman spectroscopy (Van Vleck, 1929; Placzek, 1934; Rea 1960; Albrecht, 1961; Peticolas et. al., 1970; Tang and Albrecht, 1968, 1970; Mingardi and Siebrand, 1973, 1974, 1975; Johnson and Peticolas, 1976). In the core of the theory lies the Kramer-Heiseberg-Dirac dispersion equation. In 1934 Placzek formulated a comprehensive outline of the theory of Raman and Rayleigh scattering.

The approach is semiclassical in which the radiation field is treated classically and the molecule quantum mechanically. The elements of the scattering tensor for the m to n transition are given by

$$(\alpha_{\rho\sigma})_{mn} = \frac{1}{h} \sum_r \left[\frac{\langle r|M_\rho|n\rangle\langle m|M_\sigma|r\rangle}{\nu_{rm} - \nu_L} + \frac{\langle m|M_\rho|r\rangle\langle r|M_\sigma|n\rangle}{\nu_{rn} + \nu_L} \right] \quad (1)$$

where the subscripts ρ, σ refer to a cartesian coordinate system fixed in the molecule, m, r, n to the initial intermediate and final energy states. M_ρ M_σ are the scalar components of the dipole moments $\bar{M} = \sum_j e_j \bar{r}_j$, $\bar{r}_j$, the position vector of the j electron, ν_L is the laser frequency and $\nu_{rm} = (E_r - E_m)/h$. Finally, the summation is carried over all intermediate states, electronic and vibrational. Figure 1, gives the production of the Raman effect. The transition to the intermediate state is virtual, and it does not matter whether it is energetically possible. The total intensity of the scattered light (4π solid angle) after averaging over all orientations is given by

$$I_{mn} = \frac{2^7 \pi^5}{3^2 c^4} I_o (\nu_L + \nu_{mn})^4 \sum_{\rho\sigma} |(\alpha_{\rho\sigma})_{mn}|^2 \quad (2)$$

The principal dispersion of the Raman scattered radiation is determined by two factors. The term $(\nu_L + \nu_{mn})^4$ and $1/(\nu_{rm} - \nu_L)^2$. When the laser frequency is much lower than an electronic transition the term $(\nu_L + \nu_{mn})^4$ predominates. As the laser frequency approaches the energy of an electronic transition one of the terms in the summation of Equation 1 becomes important.

Figure 1

The production of Raman effect for stokes lines. $|m\rangle$, $|n\rangle$, and $|r\rangle$ represent the initial, final, and one of the intermediate states respectively. Dashed lines indicate virtual transitions.

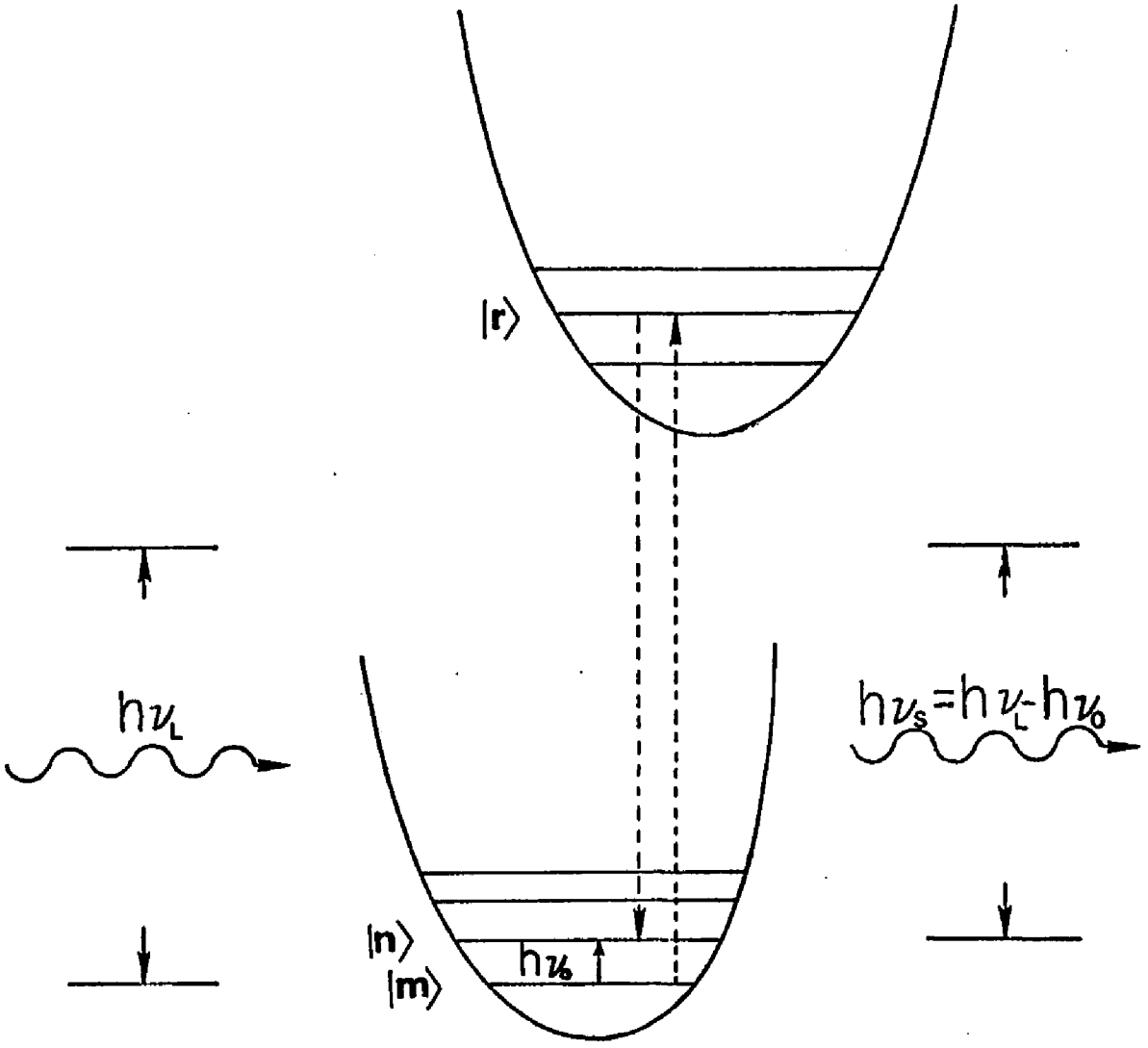
|r⟩
hν_L
hν_s=hν_L-hν_0
|n⟩
|m⟩
hν_0

In the latter case the summation over the electronic states is dropped and the sum over the vibrational states is restricted to the manifold of the electronic state in resonance with the laser. A term of the bandwidth Γ is usually added to the denominator to keep the polarizability tensor finite. The second term of Equation 1 can also be neglected. Equation 1 can be then written as

$$(\alpha_{\rho\sigma})_{mn} = \frac{1}{h} \sum_{K} \frac{\langle K|M_\rho|n\rangle\langle m|M_\sigma|K\rangle}{\nu_{Km} - \nu_L + i\Gamma} \qquad (3)$$

Finally the population distribution of the vibrational states should be included in the intensity (Equation 3) to give the right intensities for the antistokes lines.

The Born-Oppenheimer approximation is introduced next into Equation 1. Every state can be separated into (a) an electronic part which is a function of nuclear, Q, and electronic, r, coordinates and (b) a vibrational part which is a function of the nuclear coordinate only (see, for example, Tang and Albrecht, 1970). We change the notation to take into account both parts as follows:

$$|m\rangle \equiv |m\rangle|m_j\rangle, \quad |n\rangle \equiv |n\rangle|n_i\rangle, \quad |r\rangle \equiv |r\rangle|r_k\rangle \qquad (4)$$

where i, j, k are the vibrational wave function within the manifolds of the corresponding electronic states n, m and r. Taking into account that initial and final states belong to the same electronic state, Equation 1 can be rewritten as:

$$(\alpha_{\rho\sigma})_{mn} = \frac{1}{h}\sum_{(rk)}\left[\frac{\langle rk|\langle r|M_\rho|m\rangle|mi\rangle\langle mj|\langle m|M_\sigma|r\rangle|rk\rangle}{\nu_{rk,mj} - \nu_L} + \right.$$

(5)

$$\left. + \frac{\langle mj|\langle m|M_\rho|r\rangle|rk\rangle\langle rk|\langle r|M_\sigma|m\rangle|mi\rangle}{\nu_{rk,mi} + \nu_L}\right]$$

At this point it is customary to carry the integration over the nuclear coordinates by expanding the electronic transition moment $\langle r|M_\rho|m\rangle$ about the nuclear equilibrium coordinates. The expansion can be carried out in Taylor's series with no further analysis. Thus $\langle r|M_\rho|m\rangle$ can be expanded into

$$\langle r|M_\rho|m\rangle \equiv (M_\rho)_{rm} =$$

(6)

$$= (M_\rho)^\circ_{rm} + \sum_\alpha \frac{\partial (M_\rho)^\circ_{rm}}{\partial Q_\alpha} + (0)\sum_{\alpha,\beta}\frac{\partial^2 (M_\rho)^\circ_{rm}}{\partial Q_\alpha \partial Q_\beta}$$

where $(M_\rho)^\circ_{rm}$ stands for the transitions moment at the equilibrium position and Q_α for the displacements of the αth normal mode. Alternatively, the expansion can be formulated within the first-order perturbation theory. If H is the electronic hamiltonian which is an implicit function of the nuclear coordinates $(\partial H/\partial Q_\alpha)Q_\alpha$ is the perturbing operator (Albrecht, 1961). This expansion, known as Herzberg-Teller, applied to the transition moment gives:

$$(M_p)_{rm} = (M_p)^{\circ}_{rm} + \sum_{r \neq t} f_{rt}(Q)\,(M_p)^{\circ}_{tm} \qquad (7)$$

where $f_{rt}(Q) = \sum_{\alpha} \frac{Q_\alpha \epsilon^{\alpha}_{rt}}{E_r - E_t}$. ϵ^{α}_{rt} is a perturbation energy per unit displacement of the th mode due to the mixing of equilibrium configuration of the electronic states $|r\rangle$ and $|t\rangle$ under vibrational perturbation. From (7) and (5) the equation for the polarizability tensor is derived (Albrecht, 1961)

$$(\alpha_{p\sigma})_{mn} = A + B + C \qquad (8)$$

where

$$A = \frac{1}{h} \sum_{(rk)} \left(\frac{1}{\nu_{rk,mj} - \nu_L} + \frac{1}{\nu_{rk,mi} + \nu_L} \right) \times$$

$$\times \left[(M_p)^{\circ}_{rm} (M_\sigma)^{\circ}_{rm} \langle mj|rk\rangle\langle rk|mi\rangle \right] \qquad (9)$$

$$B = \frac{1}{h} \sum_{(rk)} \left(\frac{1}{\nu_{rk,mj} - \nu_L} \right) \sum_{t \neq r} f_{mt} \left[(M_p)^{\circ}_{mr} (M_\sigma)^{\circ}_{mt} \langle mi|rk\rangle\langle rk|Q|mj\rangle + \right.$$

$$\left. + (M_\sigma)^{\circ}_{mr} (M_p)^{\circ}_{mt} \langle mj|rk\rangle\langle rk|Q|mi\rangle \right] \qquad (10)$$

$$C = \frac{1}{h} \sum_{(rk)} \left(\frac{1}{\nu_{rk,mi} + \nu_L} \right) \sum_{t \neq r} f_{mt} \left[(M_p)^{\circ}_{mr} (M_\sigma)^{\circ}_{mt} \langle mj|rk\rangle\langle rk|Q|mi\rangle + \right.$$

$$\left. + (M_\sigma)^{\circ}_{mr} (M_p)^{\circ}_{mt} \langle mi|rk\rangle\langle rk|Q|mj\rangle \right] \qquad (11)$$

In the off-resonance case where $\nu_{rk,mj} \gg \nu_L$ we can approximate $\nu_{rk,mj} = \nu_L$. The A term goes to zero and the B and C terms are the major contributors to the Raman scattering. As it can be seen from Equation (10), the B and C term contain contributions from more than one electronic state. The relative contributions of A and B terms close to resonance for various systems still remains an open question. (Albrecht and Hurtley, 1971; Rinai et al., 1971a; Inagaki et al., 1974; Johnson and Peticolas, 1976). It is expected that for polyenes the A term (Equation 9) is the major contributor of the Raman intensity, particularly, for the main intense absorption band (Warshel and Karplus, 1974; see also Warshel, 1977). This has been confirmed for the case of β - carotene (Inagaki et al., 1974).

According to Equation (1) the intensity of the scattered radiation depends on the transition amplitudes for the absorption and emission of the intermediate states. Terms that belong to different states can reinforce, weaken or cancel each other. However, the corresponding transitions must be allowed. A given pair of pure electronic states will not contribute to Raman intensity unless a dipole transition, coupling them is allowed. In the resonance region the Raman scattering tensor involves only a few, perhaps one intermediate states. Thus, in general, only part of the Raman spectra will be enhanced upon approaching resonance.

The theoretical study of the Raman effect described thus far cannot be used as a tool for the assignment of the normal modes. Recently however, new theoretical techniques (Warshel and Karplus, 1972, 1972b, 1974; Kakitani, 1974;

Warshel, 1977) may facilitate the interpretation of the Raman spectra. The techniques involve a formal separation of σ and π electrons, with the former represented by an empirical potential of the form $1/2K\,(Q - Q_0)^2$ and the latter by a semiempirical model of Pariser-Parr-Pople type corrected for orbital overlap. The potential of the π electrons can be written in analytical form (Warshel and Karplus, 1972b; Warshel, 1973) as follows:

$$V_{\pi} = \sum_{\ell} 2P_{\ell}\beta\left(\exp-\alpha(b_{\ell} - b_{o})\right)\left|\cos\phi_{\ell}\right| \tag{12}$$

where b_{ℓ} is the ℓth bond of the π electron, ϕ_{ℓ} the corresponding torsional angle, P_{ℓ} the bond order character and β a negative constant.

The vibrational normal modes can be derived by solving the following equation (Lifson and Warshel, 1968):

$$F(Q)\bar{Y}_s = 2\pi\nu_s\bar{Y}_s \tag{13}$$

where $F_{\alpha\beta} = \left(\partial^2 V/\partial Q_{\alpha}\partial Q_{\beta}\right)(m_{\alpha}m_{\beta})^{1/2}$, ν_s is the vibrational frequency, $\bar{Y}_s$ is the corresponding normal mode vector and V stands for the sum of σ and π electron potential calculated at the equilibrium. Warshel and Karplus have studied the systems of β-ionone, retinal and Schiff bases of retinal (Warshel and Karplus, 1973, 1977) using this technique. The assignments are not very accurate yet. The difficulties stem from the uncertainty about the potential surfaces of the ground states and the errors introduced by the reduction of a complete set of intermediate states to a few terms.

Another approach to mode assignment is based on the observation that some bonds or groups have similar frequencies in different molecules. Table (1) gives some of the observed frequencies. The values usually hold within $\pm$ 100 cm^{-1}. However, it should be kept in mind that the constancy of the frequencies holds only when the group or the bond is in the same environment and there is no strong coupling between different vibrations. In this work, extensive use is made of this approach by comparing spectra of model chromophores with that of the visual pigments.

Table 1

Characteristic vibrations of various groups.

(A) Stretching vibrations.

(B) Bending vibrations.

(Herzberg, 1945)

A	Cm^{-1}	B	Cm^{-1}
≡C—H	3300	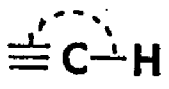	700
=C—H	3020	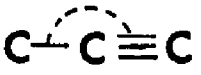	300
-C—H	2960	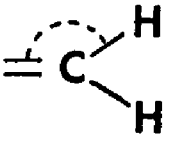	1100
—O—H	3680	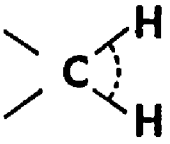	1450
—S—H	2570	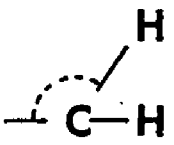	1000
=N—H	3350	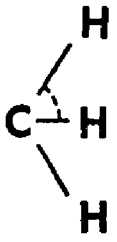	1450
=C=O	1700		
—C≡N	2100		
—C≡C—	2050		
=C=C=	1650		
=C—C=	900		
=C—F	1100		
=C—Cl	650		
=C—Br	500		
=C—I	500		

Visual Pigments

The visual pigments are located in the rods and cones. The rod consists of an inner segment that contains the nucleus and mitochondria and an outer segment (ROS) attached by a number of small fibrils. Figure 2 gives a schematic picture of the rods and cones of the vertebrates. The length of the outer segment is 10-50 μm and the diameter 1-6 μm. Rhodopsin is located in the outer segment on the membrane of the disks. The number of the disks in the outer segment varies from species to species and is of the order of 500-2000. Low angle X-ray diffraction gives a distance between adjacent disks of 300Å and thickness of 150Å (Blasie et al., 1965; Robertson, 1966). There is some small difference of the X-ray diffraction pattern between dark - and light - adapted retina (Corless, 1972; see also Worthington, 1973). The most well studied system is the bovine visual pigment rhodopsin. Other systems of vertebrate rhodopsin share the general properties of the bovine rhodopsin (Hubbard et al., 1959; Abrahamson and Fager, 1973). In what follows we shall describe the bovine rhodopsin. For recent reviews see also Ebrey and Honig (1975) and Worthington (1974).

Rhodopsin is a glycoprotein. It consists of a chromophore 11-cis retinal dehyde (11-cis retinal) covalently bound to a protein (opsin), a single polypeptide chain. The linkage is a protonated aldimine bond (Schiff base)(Lewis et al., 1973; Oseroff and Callender, 1974). In addition an oligosacharide is covalently bound to opsin (Heller and Lawrence, 1970). The lipid of the disk membrane is also an important part of rhodopsin. Composition studies of vertebrate membranes

Figure 2

Schematic diagram of cones and rods of vertebrates.

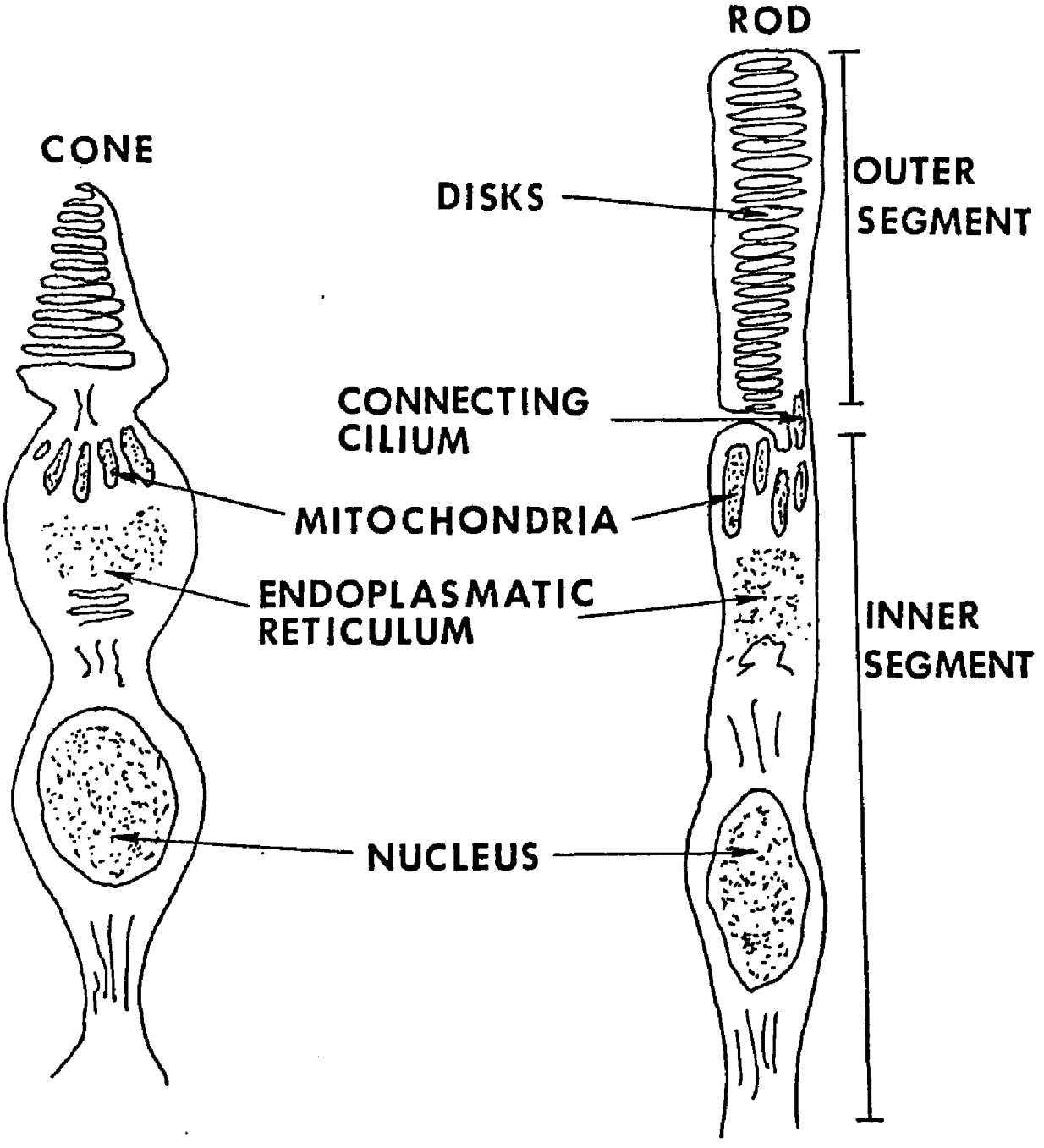
ROD
CONE
DISKS
OUTER SEGMENT
CONNECTING CILIUM
MITOCHONDRIA
ENDOPLASMATIC RETICULUM
INNER SEGMENT
NUCLEUS

summarized by Daemen (1973) and Abrahamson and Fager (1973) show that 40% of the dry weight of the outer segment is lipid and 60% protein, mostly rhodopsin (Papermaster and Dryer, 1974). The bulk of the lipid component belongs to phospholipids. The lipid component can be removed. The removal, however, affects some of the properties of rhodopsin namely the thermal stability (Daemen, 1973) and regeneration (Zorn and Futterman 1971; Shichi, 1971; Hong and Hubbell, 1973).

Rhodopsin is embedded in the disk membrane. Rough calculations based on the molecular weight and the dry weight of rhodopsin in the ROS suggest that the density of rhodopsin molecules is extremely high (see, for example, Bridges, 1970). In addition the rhodopsin molecule have considerable freedom of rotational (Brown, 1972; Cone, 1972) and translational (Poo and Cone, 1974) movement which is temperature dependent (Blasie and Worthington, 1969; Worthington, 1971). This suggests that rhodopsin molecule behave like a two-dimensional liquid. In addition, to the rotational and translational mobility of rhodopsin on the plane of the membrane, there is the hypothetical possibility that rhodopsin can flip-flop from one side of the membrane to the other. There is no evidence, however, at present to support this possibility.

The three-dimensional structure of rhodopsin is presently unknown. This information can only be obtained by a complete X-ray structure determination, and so far it has not been possible to even crystallize rhodopsin. There are, however, alternative techniques that can be employed to provide information about the shape of the molecule. Recent experiments have suggested that

rhodopsin may be asymmetric. Evidence is provided by (a) low angle X-ray measurements (Blaurock and Wilkins, 1969); (b) efficiency of the energy transfer from the aromatic amino acids to the chromophore of the bleached and reduced rhodopsin (Ebrey, 1971); (c) efficiency of the energy transfer between dye labelled sites of rhodopsin (Wu and Stryer, 1972; Renthal et al., 1973). The results are not conclusive yet. Eisenger and Dale (1974) have pointed out that distances obtained from energy transfer measurements as in (c) depend critically on the values of orientation factors used in the calculations. It is noteworthy, however, that all the results point to the same direction. This internal consistency reduces the uncertainty associated with the measurements. Based on (c), Wu and Stryer (1972) proposed that rhodopsin molecule is ellipsoidal, at least 75 Å long with a hydrophilic and a hydrophobic end. Given the length of the molecule, rhodopsin could easily span the disk membrane.

The amino acids composition for bovine rhodopsin is known and is given in Table (2). As it has been found for other membrane proteins, rhodopsin has also a higher percentage of hydrophobic amino acids. When the molecular weight of the retinal and the oligosacharide is added to that of the polypeptide chain, it gives a molecular weight for rhodopsin of about 36,000 daltons. This is in agreement to the value of 40,000 daltons reported by Hubbard (1954). The binding site of the chromophore is the ϵ-amino group of lysine (Fager et al., 1972; DeGrip et al., 1973). The stability of the Schiff base linkage over a wide pH range (3.9-9.6).(Radding and Wald, 1956a) and its resistance to sodium borohydride (Bownds and Wald, 1965) as well as the resistance of the polyene chain

Table 2

Amino acid composition of bovine rhodopsin

Polar		Non-Polar	
Lys	10	Gly	21
His	5	Ala	25
Arg	8	Val	22
Asp	22	$MetSO_3$	10
Glu	30	Ile	14
Thr	24	Leu	22
Ser	18	Phe	26
Tyr	16	Pro	18
$CySO_3H$	10	Trp	4
	143		162

Total 305 amino acids

(Ebrey and Honig, 1975)

to lipoxidase enzyme (Wald and Hubbard, 1960) suggest that the Schiff base linkage and part of the polyene chain are enfolded inside a three-dimensional frame of the polypeptide chain.

So far only 11-cis retinal (see Figure 17d, e) and 3 dehydro 11-cis retinal have been found in natural visual pigments. A number of other compounds (Figure 3), however, have been successfully attached to the protein to form artificial visual pigments (Lewin and Thomson, 1967; Blatz et al., 1969; Nelson et al., 1970; Chan et al., 1974; Ebrey et al., 1975; Crouch et al., 1975). These experiments suggest that the binding site is not specific to 11-cis retinal. There are restrictions, however, on the length (Blatz et al., 1969) and isomeric form. In addition, the presence of the ring is very important in enabling the attachment. Attempts to combine opsin with the polyene chain even with the right isomeric form have failed (Blatz et al., 1969). It is noteworthy that 5, 6 - monoepoxy-retinaldehyde can be utilized in vivo to form pigment. In experiments on retinal-deficient rats fed on diets supplemented with the 5, 6 - monoepoxy derivative a small amount of light sensitive pigment with absorption at 467 nm was formed (Lewin and Thomson 1967). In addition the monoepoxy pigment appears to be physiologically active.

Absorption of a photon isomerizes the chromophore (Wald, 1968), and initiates a series of intermediates (Figure 4) leading to the detachment of chromophore from the opsin. This process is called bleaching because pigments absorb in the visible while the final product, retinal and opsin, absorb in the UV. The first intermediate is bathorhodopsin (also called prelumirhodopsin)

Figure 3

Conformation of some of retinal analogues that can combine with opsin to form artificial visual pigments. 11-cis (a) 5, 6 - monoepoxyretinal, (b) 13-desmethyl-14-methylretinal, (c) 14-methylretinal, (d) 9, 13-dicis-retinal.

a.

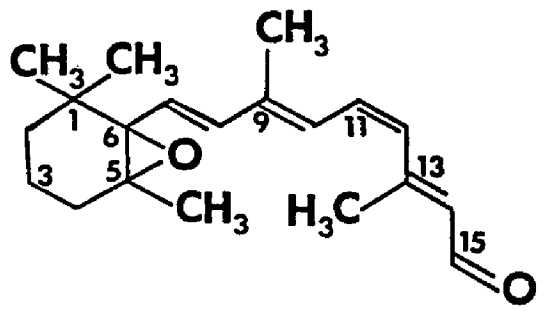
CH3
CH3 CH3
1
6
9
11
O
5
3
13
CH3
H3C
15
O

b.

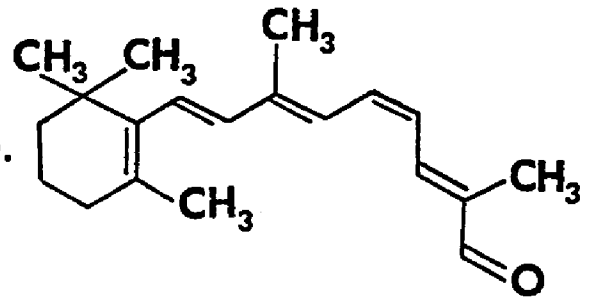
CH3
CH3 CH3
CH3
CH3
O

c.

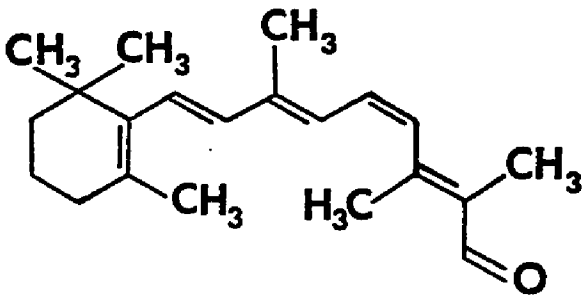
CH3
CH3 CH3
CH3
CH3
H3C
O

d.

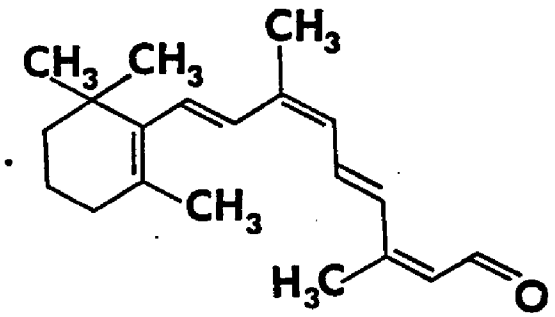
CH3
CH3 CH3
CH3
H3C
O

Figure 4

The bleaching sequence of rhodopsin. Rhodopsin and isorhodopsin are placed lowest in the figure to indicate that they have lower free energy than their common photoproducts (see text). Numbers in parentheses give absorption maxima, left side numbers give the time of formation of the intermediates, right side numbers give the temperatures below which the intermediates are stable.

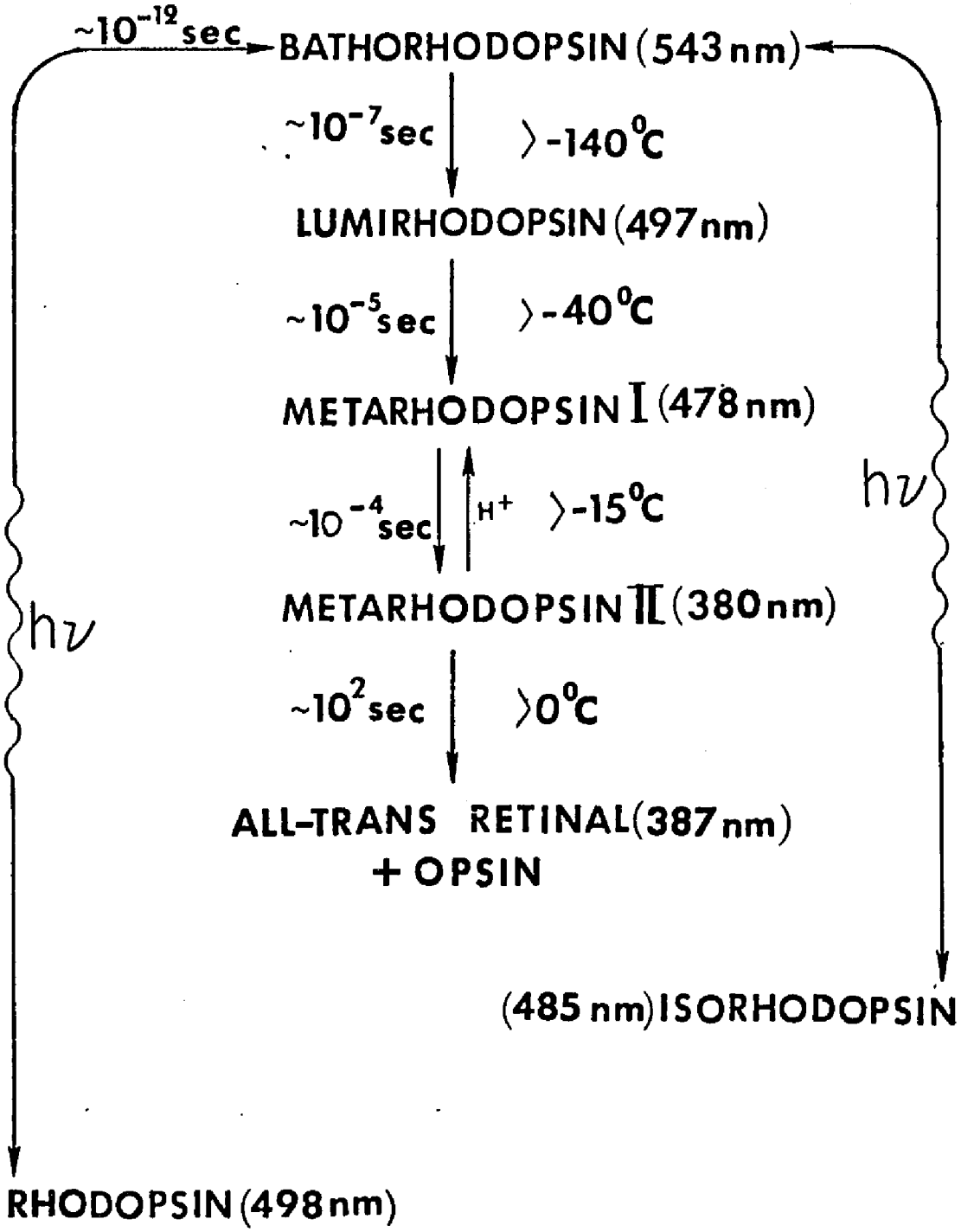
~10⁻¹²sec
BATHORHODOPSIN (543 nm)
~10⁻⁷sec
> -140°C
LUMIRHODOPSIN (497nm)
~10⁻⁵sec
> -40°C
METARHODOPSIN I (478 nm)
~10⁻⁴sec
H⁺
> -15°C
METARHODOPSIN II (380nm)
~10²sec
> 0°C
ALL-TRANS RETINAL (387 nm)
+ OPSIN
hν
hν
(485 nm) ISORHODOPSIN
RHODOPSIN (498nm)

(Yoshizawa and Wald, 1963). Study of the kinetics using picosecond laser pulses show that bathorhodopsin is formed in less than 6 psec (Busch et al., 1972). The existence of an even faster first intermediate hypsorhodopsin (Yoshizawa and Horiuchi, 1973) has not been verified yet. The first step from rhodopsin to bathorhodopsin is purely photochemical. It has been so far assumed that 11-cis retinal is isomerized to all-trans. Bathorhodopsin can absorb a photon and convert back to rhodopsin or to another pigment isorhodopsin (Yoshizawa and Wald, 1963). Isorhodopsin contains the 9-cis retinal (see Figure 17c) as a chromophore and follows the same bleaching sequence as rhodopsin.

Resonant Raman studies of bathorhodopsin (Oseroff and Callender, 1974) show that the Schiff base is protonated but otherwise are incompatible with a pure all-trans form for the chromophore. Honig and Ebrey (1976) and coworkers (Rosenfeld, et al., 1977a, b) have reviewed the alternative mechanisms of the photochemical reaction and concluded that the cis-trans isomerization (not necessarily a pure trans) is consistent with the experimental evidence. In addition they suggest that rhodopsin and bathorhodopsin share a common excited state.

The next intermediate in the bleaching sequence is lumirhodopsin (Hubbard et al., 1959; Yoshizawa and Wald, 1963). Lumirhodopsin is the least studied intermediate. Study of the kinetics of thermal decay of lumirhodopsin (see, for example, Abrahamson and Ostroy, 1967; Abrahamson, 1973) are inconclusive and there is disagreement in the constant rates observed by the various authors. They tend to indicate, however, that no major conformational changes in the

protein take place, at least up to the stage of lumirhodopsin. Ebrey and Honig (1972) have reached the same conclusion by studying the ultraviolet transitions in the rhodopsin spectrum.

The stages of metarhodopsin I and metarhodopsin II are of the most interesting because they are correlated with neural activity. Metarhodopsin I and II are in thermal equilibrium. The equilibrium depends on the temperature, pH, solvent and the species of rhodopsin but it is not affected by light (Matthews et al., 1963). Increase in temperature, in acidity (within pH stability range) or in ionic strength as well as replacement of water by glycerol shift the equilibrium toward metarhodopsin II.

The study of kinetics of metarhodopsin I to metarhodopsin II reaction shows a large change of entropy (Matthews et al., 1963). This tends to imply that there is a considerable unfolding of the protein which up to the stage of metarhodopsin I was protecting the chromophore. It should be noted that at the metarhodopsin II stage the Schiff base can be reduced by sodium borohydride and hydrolyzed by hydroxylamine. In contrast studies of circular dichroism (CD) of rhodopsin, metarhodopsin I and metarhodopsin II at their longest absorption band (Waggoner and Stryer, 1971) show no significant change. These results have been interpreted as implying that a significant portion of local environment of the chromophore remains unchanged in the transition from rhodopsin to metarhodopsin I and metarhodopsin II.

Flow photocalorimetry can supply important information about the energetics of the intermediate stages. So far it has been applied to metarhodopsin I and

metarhodopsin II. Cooper and Converse, (1976), have found that metarhodopsin I and II are energetically higher than rhodopsin and the formation of metarhodopsin II involves the uptake of one hydrogen ion from the solution (see also Matthews et al., 1963).

In the final stage of the bleaching sequence the all-trans retinal detaches from the opsin. In vitro the retinal can recombine with any of the free amino groups of the opsin. In vivo, however, all-trans retinal is reduced to all-trans retinol through the action of an enzyme dehydrogenase coupled with NADH or NADP (see, for example, Bridges, 1970). What happens next is still a matter of controversy. It was originally assumed that all-trans retinol transported to the pigment epithelium where all-trans retinol is isomerized back to 11-cis retinol. Subsequently, 11-cis retinol returned to the rod for reoxidation and incorporation with the opsin.(Dowling, 1960). A number of observations, however, cast doubt on the validity of this hypothesis. The regeneration of cone pigments can take place without the pigment epithelium being present (Goldstein, 1967); 11-cis retinol is not easily oxidized to 11-cis retinal (Daemen et al., 1974). Some of the all-trans retinal is reisomerized before reduction to retinol (Zimmerman et al., 1974).

This work will be primarily concerned with the initial changes of the rhodopsin molecule following the absorption of a photon. The key question to be answered is the understanding of the mechanisms of the nervous excitation. Two excitations have been reported in the literature, (a) the early receptor potential (ERP) (Brown and Murakami, 1964); (b) the electroretinogram (ERG) (Hecht et al., 1942;

see also Brown et al., 1965). The first is a biphasic potential that is generated prior to the formation of metarhodopsin I. Studies on model membranes indicate that ERP is originated from capacitative charge displacements of oriented rhodopsin molecules (Trissl et al., 1977). The ERG has a latency of msec so it must be generated prior to the slow hydrolysis of the metarhodopsin II. It is for this reason that the stage of conversion of metarhodopsin I to metarhodopsin II becomes significant. The ERG is associated with the transfer of information from the retina to the brain.

Many theories have been developed to explain the generation of ERG (see, for example, Bonting, 1969). In the last few years, however, the ionic theory has gained wide support and it is the only generally accepted theory today (see, for example, Hagins, 1972; Ebrey and Honig, 1975). Figure 5 summarizes the main points. The vertebrate receptors maintain a large steady current, mostly Na^{+} moving into the rods. This dark current is so large that it is calculated to be equivalent to a turnover of all the cations in a rod in 45 sec (Hagins, 1972).

The concentration of Na^{+} ions is kept low inside the rods by the action of Na^{+} ATP pump at the inner rod segment. At the same time the concentration of Ca^{++}, the assumed transmitter substance, (see, for example, Smith et al., 1977) is kept low by a Ca^{++} ATP pump (Mason et al., 1974). The effect of the light is to open the pores and release Ca^{++} in the intradisk space. The identity of the pores is still unresolved. The Ca^{++} block the entrance to the Na^{+} hyperpolarizing the membrane. This excitation is transferred through layers of neural cells such as horizontal, bipolar, ganglion cells to the optic nerve and the brain (Figure 6).

Figure 5

Schematic diagram of the assumed mechanism for excitation in the vertebrate rods and cones (see text). (A) Dark adapted rod. (B) Light adapted rod. (Hagins, 1972)

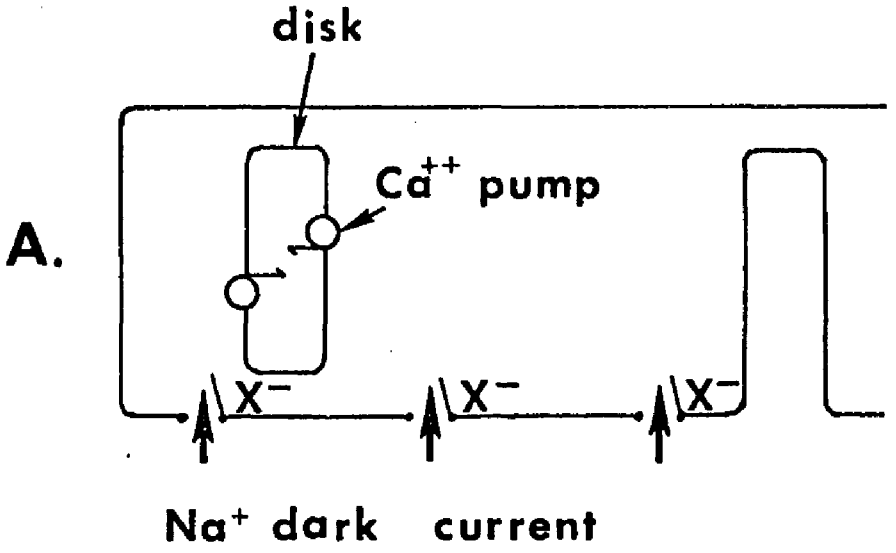
A.
disk
Ca^{++} pump
X^-
X^-
X^-
Na^+ dark current

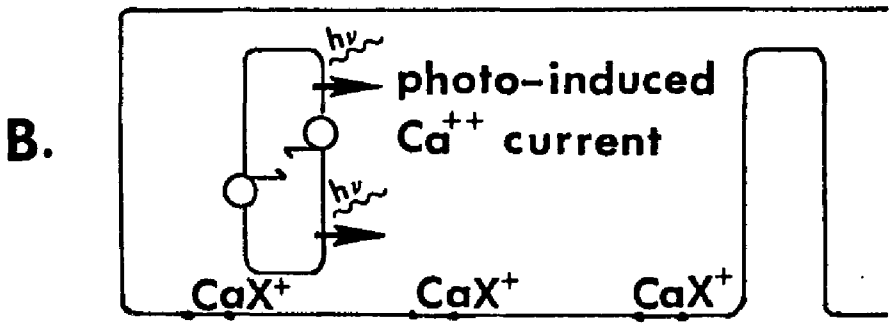
B.
hν
photo-induced
Ca^{++} current
hν
CaX^+
CaX^+
CaX^+

Figure 6

Schematic diagram of a cross section of the vertebrate retina.

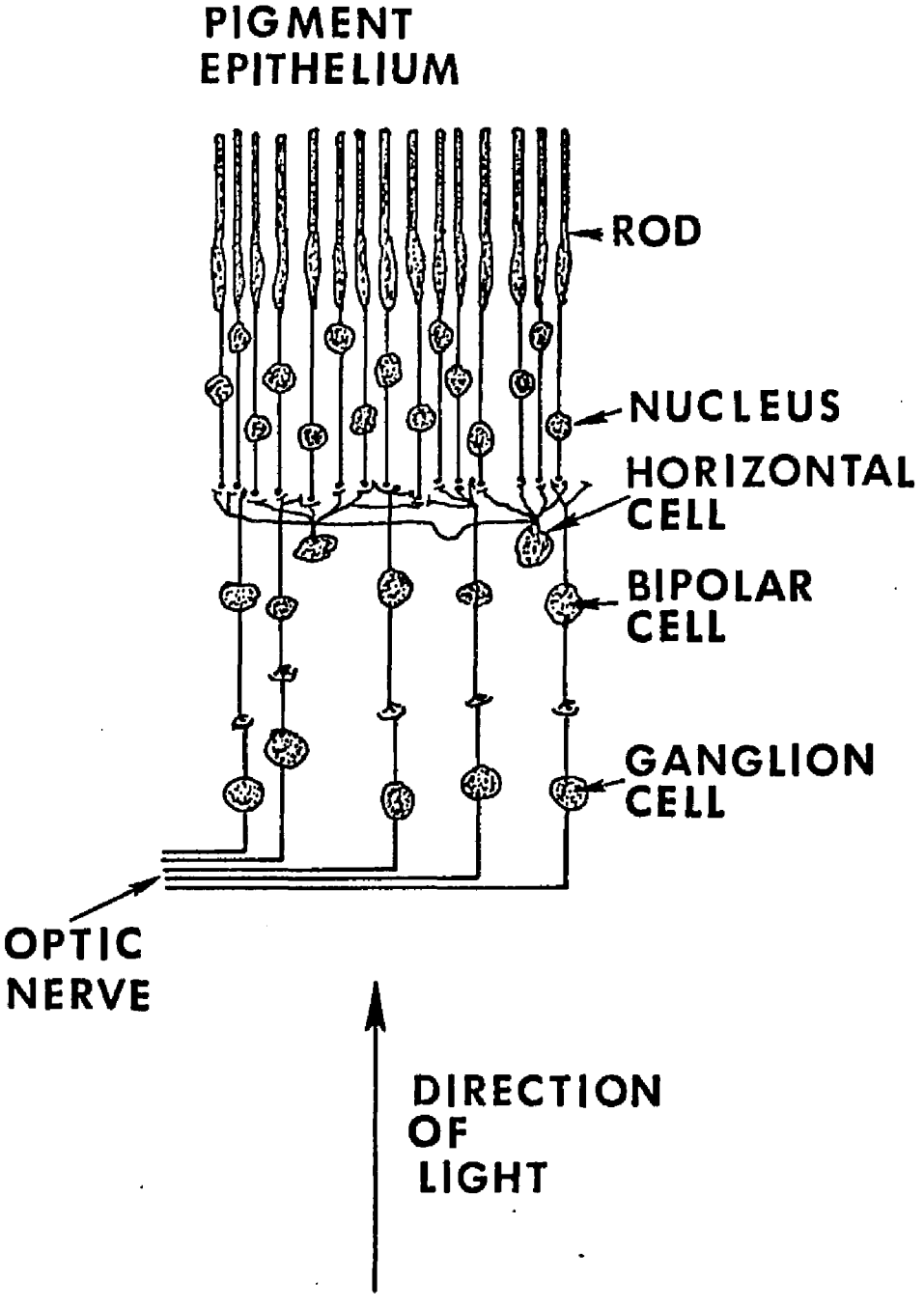
PIGMENT
EPITHELIUM
ROD
NUCLEUS
HORIZONTAL
CELL
BIPOLAR
CELL
GANGLION
CELL
OPTIC
NERVE
DIRECTION
OF
LIGHT

Bacteriorhodopsin

A new photosynthetic pigment that has been recently studied is the purple membrane from the bacterium Halobacterium Halobium, often referred to as bacteriorhodopsin (Oesterhelt and Stoeckinius, 1971). The name is justified by the similarities between the visual pigment rhodopsin and the purple membrane protein. Both, for example, contain the retinal as a chromophore although in different isomeric forms (Oesterhelt and Stoeckinius, 1971; Pettel et al., 1977). The similarities, however, should not be overemphasized. The biochemical roles of the two pigments are quite different. Rhodopsin is a photosensor; absorption of light triggers the biochemical changes. The mechanism, however, is supported energetically by other sources. Bacteriorhodopsin, in contrast, utilizes the energy of the light to supply the bacteria with the energy requirements (Oesterhelt and Stoeckinius, 1973). For recent reviews, see Stoeckinius, 1976; Henderson, 1977.

H. Halobium is a rod shaped bacteria about .5 μm in diameter and 5 μm long. It requires high concentration of NaCl and lower concentration of K Cl and Mg Cl_2 for growth. Light stimulates the synthesis of purple patches on the membrane. The purple membrane contains a single rhodopsin-like protein. In contrast to the amorphous state of the visual pigment membrane, the purple membrane is a two dimensional crystal, with an hexagonal P_3 structure (Blaurock and Stoeckinius, 1971). Each unit cell contains three bacteriorhodopsin molecules that span the whole membrane.

Bacteriorhodopsin consists of a chromophore all-trans retinaldehyde (Pettel et al., 1977; and in this work) connected to the protein via a protonated Schiff

linkage (Lewis et al., 1974). The binding site is the ϵ-amino group of lysine (Oesterhelt, 1971). The retinal chromophore interacts further with the protein so that its absorption maximum is shifted towards a longer wavelength. In addition the Schiff base of the intact complex is protected inside the protein from sodium borohydride and hydroxylamine.

Recent X-ray (Henderson, 1975; Blaurock, 1975) and electron microscopy studies (Henderson and Unwin, 1975) have elucidated the structure of the pigment and its environment. The protein in the membrane is composed of seven closely packed, α-helical segments perpendicular to the plane of the membrane. The α-helices span most of the width of the membrane (Henderson and Unwin, 1975).

Absorption of a photon initiates a series of intermediate stages (Figure 7) (Lozier et al., 1975), which, contrary to what happens in the visual pigments, form a closed cycle. The first step in this reaction is purely photochemical. Study of the kinetics show that the rise time of first intermediate is less than 10 psec (Kaufmann et al., 1976) while the whole cycle is completed in $\sim$10 msec. The cycling of the pigment is accompanied by release and uptake of protons, inhibition of respiration (Oesterhelt and Stoeckinius, 1973) and increases in intracellular adenosine triphosphate (ATP) (Danon and Stoeckinius, 1974). It has been postulated that the purple membrane functions as a light driven pump. Absorption of a photon by bacteriorhodopsin causes the ejection of a proton from the cell. This establishes an electrochemical gradient across the cell membrane, which can drive ATP synthesis or some other metabolic process (see, for example, Mitchell, 1972).

Figure 7

Photoreaction cycle of the light adapted form of the purple membrane protein of Halobacterium Halobium. Bold face numbers give the absorption maxima of the intermediates. Wavy lines indicate photoreactions, solid lines indicate thermal (dark) reactions. Times of formation of the intermediates are given along the arrows.

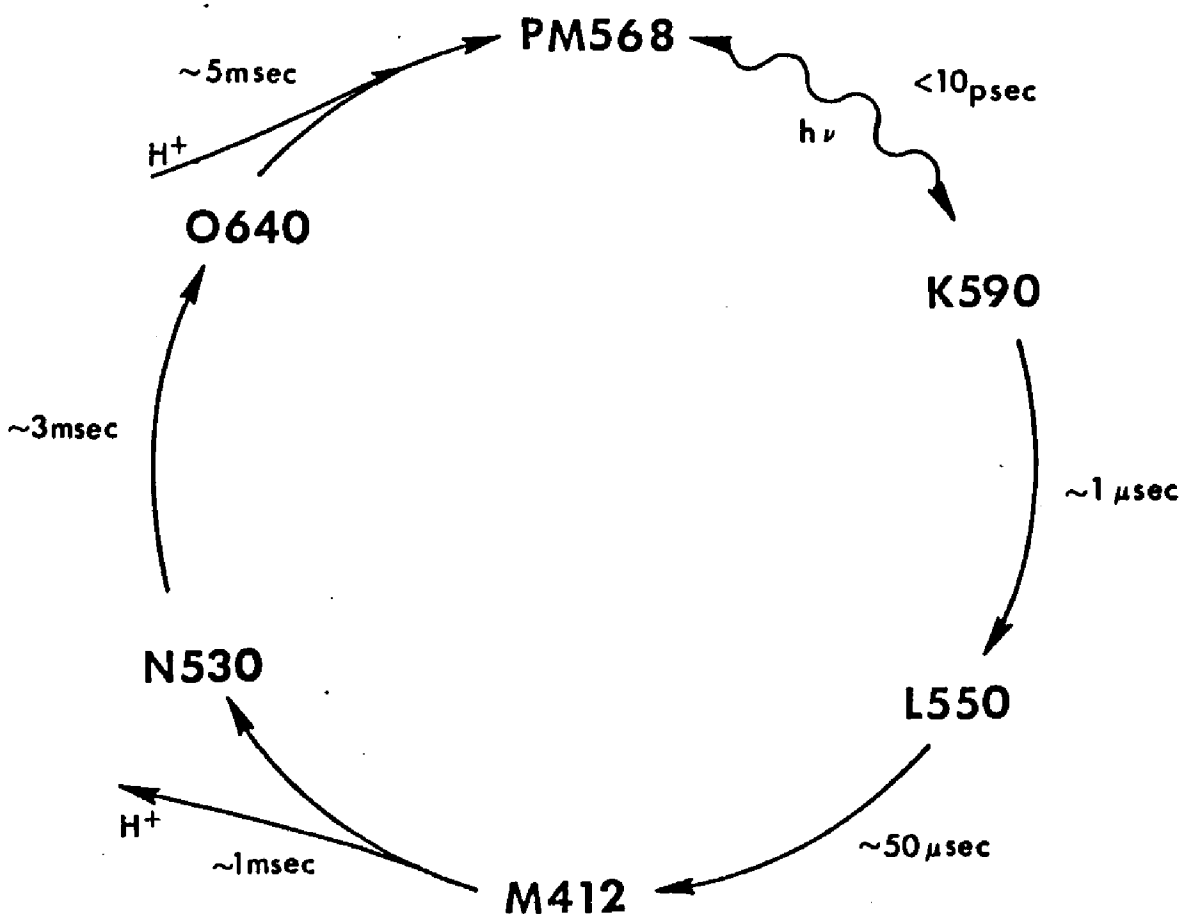
PM568
<10psec
hν
K590
~1 μsec
L550
~50 μsec
M412
~1msec
H+
N530
~3msec
O640
~5msec
H+

Additional evidence is provided from studies on reconstituted purple membrane vesicles. Racker and Stoeckinius (1974) have shown that vesicles formed in the presence of bacteriorhodopsin transpose protons across the membrane upon illumination. They have also demonstrated that inclusion of ATPase of bovine heart mitochondria during reconstitution enables the vesicles to calalyze ATP formation from adenosine diphosphate (ADP) and Pi.

Section II

Experimental

A typical Raman apparatus consists of a laser, a double monochromator and a photomultiplier tube connected to photon-counting electronics (Figure 8). The laser beam can be focused to a few microns in diameter, making possible the study of very small samples. The scattered light is collected and focused on the entrance slit of the monochromator. This modern instrumentation has simplified the Raman measurements. However, the nature of the sample introduces a new complexity. The samples, visual pigments and most of the model compounds, are extremely photolabile. Thus, the light probe alters the composition of the sample. This problem is intensified in resonance Raman spectroscopy where the probe beam must be close to the absorption band to take advantage of the resonance enhancement.

To illustrate the severity of the problem of the photolability we shall calculate the rate of the photons absorbed by a rhodopsin molecule in a typical stationary Raman experiment. The number of photons absorbed per second is given by

$$\frac{I_o \sigma_A}{\pi r_o^2} \tag{14}$$

where I_0 is the laser intensity, r_0 the radius of the laser beam (assuming circular beam for simplicity) and σ_A the absorption cross section at the laser wavelength. The absorption cross section is related to the molar extinction coefficient by

$$\sigma_A (cm^2) = 3.821 \times 10^{-21} \epsilon (M\ell^{-1} cm^{-1}) \tag{15}$$

Figure 8

Schematic diagram of a Raman apparatus. ν_L and ν_s are the frequencies of the exciting and scattered light, respectively. ν_o is the vibrational frequency of a sample normal mode.

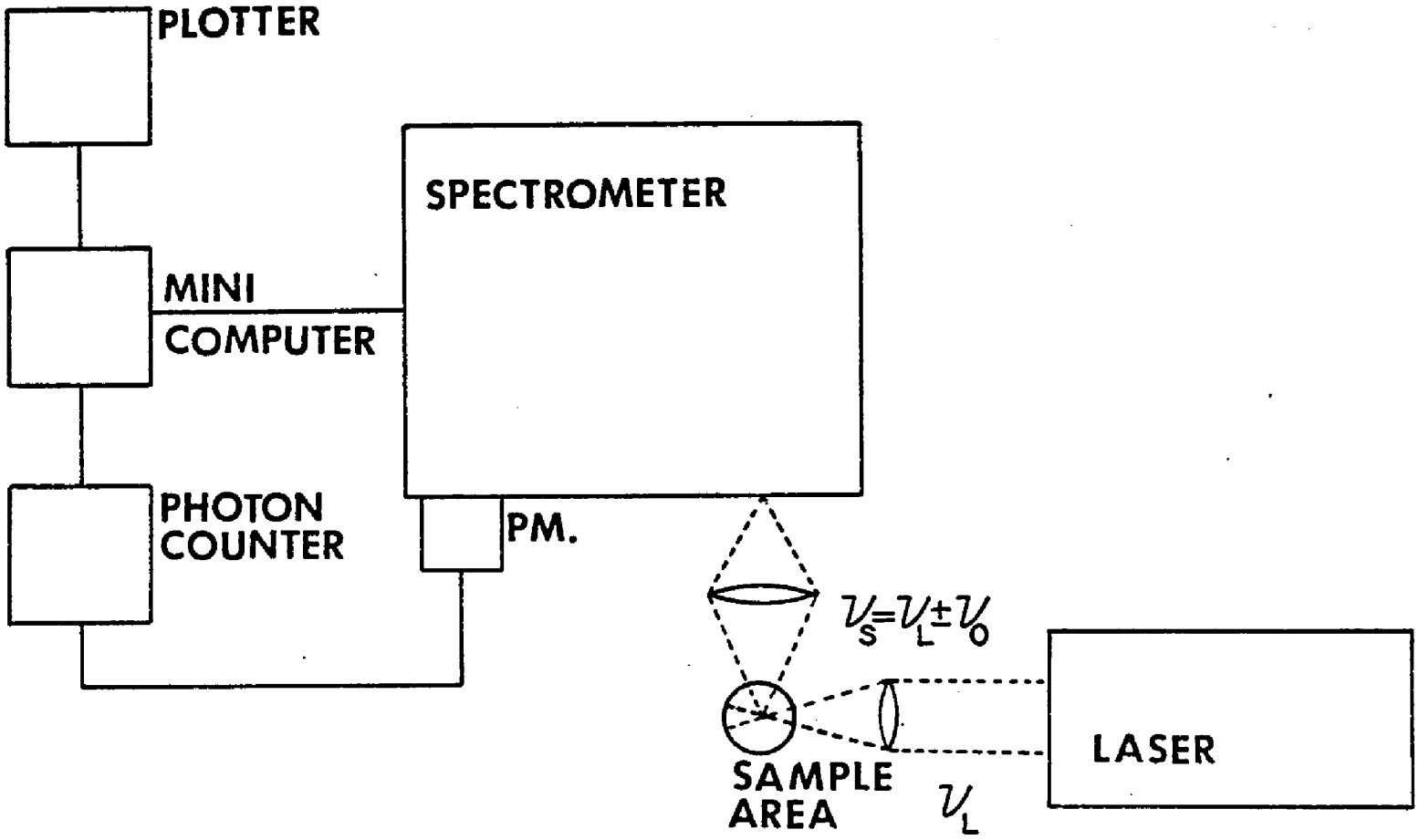
PLOTTER
SPECTROMETER
MINI
COMPUTER
PHOTON
COUNTER
PM.
$\nu_S = \nu_L \pm \nu_0$
LASER
SAMPLE
AREA
ν_L

For a laser wavelength at 568.2 nm ($\epsilon_{570} \approx 14000$) power level of 10mW and beam radius, 40 μm, we find that the rate of the absorbed photons per molecule is 10^4. The mean time between successive absorption is .1 msec.

Molecules in solutions are not stationary, however. They move in and out of the laser beam by diffusion or possibly by convection currents. To a first approximation, the molecular diffusion time to travel a distance r_o is given by:

$$\frac{6\pi\eta d r_o^2}{KT} \tag{16}$$

where η is the solvent viscosity, d the molecular radius, K the Boltzmann constant and T the absolute temperature. Taking d = 25Å (we assume a globular protein of 50Å diameter) $\eta = 10^{-2}$P (for water), T = 300°K, $r_o = 40\mu$m the transit time across the beam is 25 sec. This assumes the best possible case namely molecules travelling transverse to the beam. The quantum yield of rhodopsin is close to one (Dartnall, 1972) and absorption of a photon can initiate the bleaching sequence (Figure 4). Thus, depending upon the temperature of the sample many intermediates are likely to be present in the beam. An additional complication arises from the fact that the intermediates of the bleaching sequence can absorb a photon and revert back to rhodopsin or isorhodopsin. In fact, the composition of the mixture depends in general, on the incident laser flux, the absorption cross section of each intermediate at the laser wavelength, the thermal decay rate and the quantum yields of each intermediate. The resulting Raman spectra, therefore, is difficult to interpret in terms of single species. It should be noted here that the Raman effect, even for resonance - enhanced cross-sections,

is an extremely weak phenomenon. We have measured, for example, that for rhodopsin the ratio of the cross-section of the most intense Raman line measured with the 568.2 nm krypton line to the absorption cross-section at 568.2 nm is approximately 3×10^{-9}. In this particular case, the rhodopsin molecule is more apt by a factor of approximately 10^8, to absorb a photon than to scatter a Raman photon.

Molecular Flow

A new technique, Molecular Flow, was developed independently by Mathies et al., (1976) and in this work (Callender et al., 1976). It eliminates problems associated with photolability and allows the measurement of Raman spectra of distinct species of photosensitive material in solutions. The basic idea of this technique (see Figures 9 and 26) is to impose a molecular velocity transverse to the laser beam so that the probability that any molecule will absorb a photon while travelling through the beam is small. In addition, the small percentage of the molecules that is photoisomerized is continuously replenished by new material. This way the Raman apparatus detects essentially only the pure initial sample.

Two parameters are important, (a) the probability that a molecule will isomerize in the laser beam, (b) the fraction of the total sample photoisomerized. The derivation of these parameters is given in the Appendix. The probability of photoisomerization of a molecule during a single transit through the center of the laser beam is given by:

$$P_m = \frac{I_0 \sigma_A \psi}{\sqrt{\pi}\, U_0 r_0} \qquad (17)$$

I_o is the laser intensity, σ_A the absorption cross section at the laser wavelength, Ψ the quantum yield of photoisomerization, U_b the bulk velocity and r_o the distance of 1/e points of the laser beam (assuming that the laser beam intensity profile is Gaussian, as it is in our case).

It should be noted that $P_m > 1$ corresponds to molecular absorption of more than one photon. This case is discounted here by assuming low laser intensity. P_m can be made arbitrarily small by a suitable choice of experimental parameters. It is for this reason that the molecular flow technique works. Very few molecules in the laser beam are photoisomerized, a necessary criterion for obtaining reliable Raman results.

At all times molecules are undergoing photoisomerization; as such they are effectively destroyed. The photoisomerized molecules continuously accumulate and though the photoisomerization in the beam might be negligible the accumulation of the destroyed molecules might increase to a level of introducing errors to the Raman spectra. The fraction of the total sample destroyed is given by:

$$\bar{P} = \frac{I_o (1-10^{-A}) \Psi T}{C_o V} \tag{18}$$

where A is the absorbance of the sample, C_o the concentration in molecules/cm^3, V the total sample volume, and T the time of Raman measurement. For small absorbances the exponential can be expanded and Equation 18 can be simplified:

$$\bar{P} = \frac{2.3 I_o A T \Psi}{C_o V} \tag{19}$$

$\bar{P}$ can be made arbitrarily small by a suitable choice of experimental parameters.

There are two advantages in making the absorbance small. (a) There is some evidence that the resonance Raman cross section drops more slowly than the absorption cross section as the laser frequency moves away from the absorption band (Fenstermacher and Callender, 1974). (b) The scattered Raman light is attenuated less in exiting from the sample.

Methods and Materials

Resonance Raman spectra were obtained in a 1401 Spex double monochromator, a cooled RCA 31034 photomultiplier tube and photon counting electronic apparatus interfaced to a PDP - 8e minicomputer. Part of the memory of the computer is reserved for data storage in discreet channels. Absorption spectra were taken in a CGA McPherson UV-VIS spectrophotometer equipped with a constant temperature cell holder. The temperature in the holder was controlled by a bath circulator Lauda Super K/2R and monitored by a thermocouple. The spectrophotometer was interfaced to the PDP-8e. The PDP-8e is connected to a PDP-10, greatly increasing the capabilities of the system for data analysis and storage.

A Coherent Radiation model 52B krypton ion laser, a Spectra - Physics model 165 argon ion laser and a Spectra - Physics model 370 tunable dye laser with rhodamine 6G were used to produce monochromatic radiation. The available frequencies span the range from UV(350.4nm) to the red (647.1nm). The laser beam was difracted on a grating to separate the discharge lines and the first order difracted beam was used to excite the sample. A right angle scattering geometry was used. Power levels were measured before the sample with a calibrated thermopile (Eppley Laboratories, Newport, R.I.).

The molecular flow apparatus (Figure 9) consists of a closed recilculating flow system driven by a small pump (Micro-pump model 12-41-303). The capillary tube that intersects the laser beam is the drawn end of the Pasteur pipet of 1.5 mm internal diameter. The velocity of the fluid in the capillary tube can be measured

Figure 9

Molecular flow apparatus. Laser exciting beam is directed perpendicular to the plane of the graph. Scattered light is collected at 90 degrees. Arrows indicate the direction of the molecular flow.

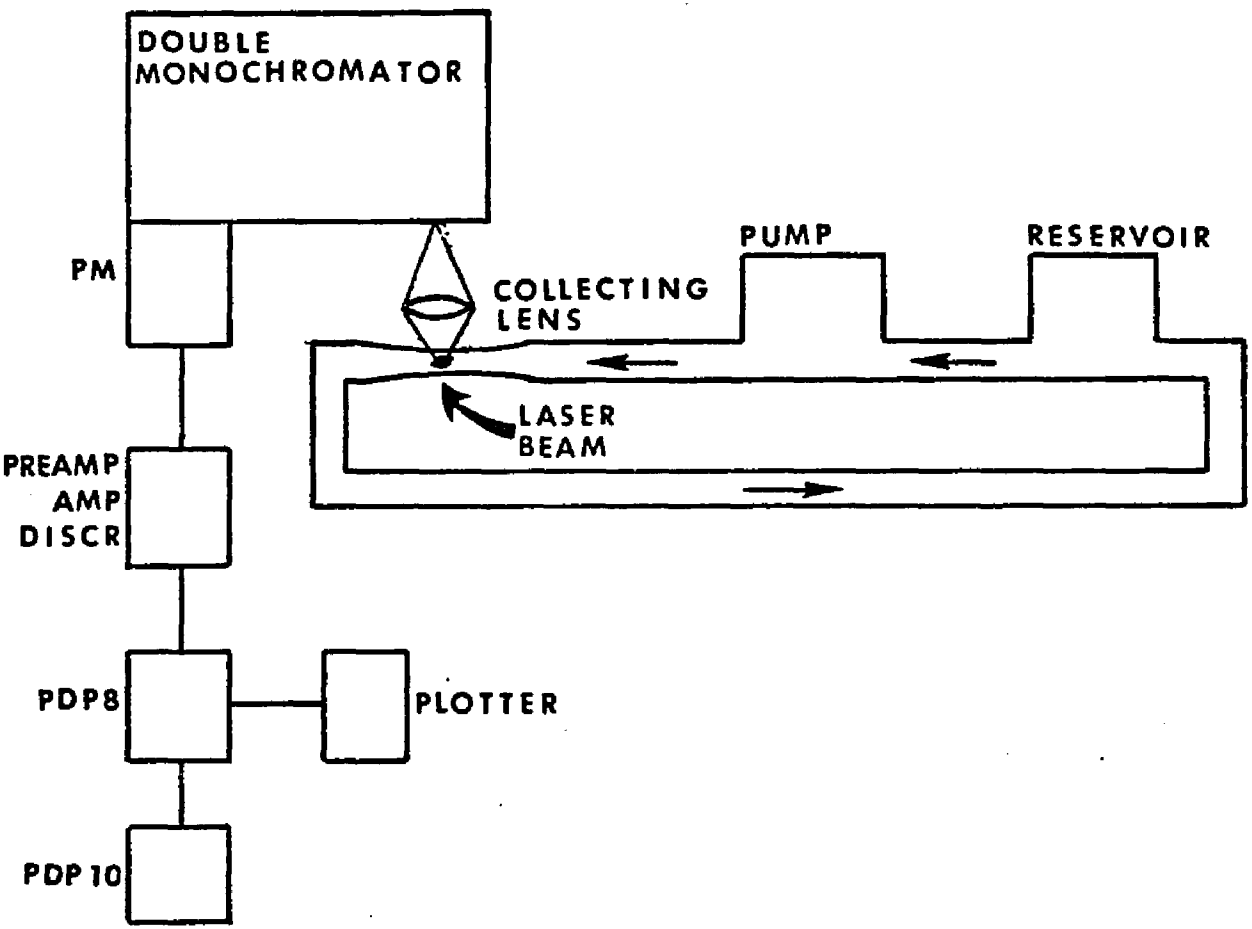
DOUBLE
MONOCHROMATOR
PM
COLLECTING
LENS
PUMP
RESERVOIR
LASER
BEAM
PREAMP
AMP
DISCR
PDP8
PLOTTER
PDP 10

by determining the bulk velocity. Typical values were between 500-600 cm/sec. The apparatus was slightly modified to enable Raman measurements of metarhodopsin I, metarhodopsin II and bacteriorhodopsin.

The incident laser beam was defocused on the capillary tube producing a 1/e beam radius of 40 ± 5 μm. The beam diameter and profile were determined by measuring the Rayleigh scattering of the flowing fluid with 10 μm monochromator slits while moving the laser beam transverse to the monochromator in known amounts. The magnification (x5.2) of the collecting lens was determined by replacing the sample with a microscope reticule and repeating the process. The beam diameter parallel to the beam axis was found not to vary by more than a few percent inside the capillary tube.

Low temperature Raman spectra were taken using a nitrogen cold finger dewar connected to the end of the flexible nitrogen/helium transfer line LT-3-110 (Air Products and Chemicals, Allentown, Pennsylvania). The sample was deposited in a concave depression in a temperature - controlled copper sample holder arranged for 90^{o} scattering from the face of the sample. The holder was cooled by a continuous stream of nitrogen gas. Temperature in the holder could be set between $-190^{o}C$ to $0^{o}C$ and maintained within $.5^{o}C$ of the set temperature.

The monochromator was calibrated by the known K_r^+ and A_r^+ laser lines. Line assignments are accurate to $\pm$ 3cm^{-1}. All the spectra presented here consist of digitally pooled data from multiple runs and all identified lines have been observed in several separate measurements. A typical single scan consisted of monochromator speed of 50 cm^{-1}/min and a channel duel time of 2.2 sec (an effective time constant of 12 sec) for a total of 512 channels.

Visual Pigments

Rhodopsin:

Bovine retinae were purchased from Hormel (Austin, Minnesota). ROS (rod outer segment) were prepared according to the procedures described in "Methods in Enzymology" (Hubbard et al., 1971). All procedures involving rhodopsin were carried out in red dim lights at room temperature.

ROS were homogenized to a thick paste. This was diluted with an equal volume of phosphate buffer .067M and pH ~7 with 40% sucrose (W/V). The suspension was centrifuged at ~20,000 rpm for 40 min and the turbid supernatant was discarded. The pellet was regrounded and suspended with the 40% (W/V) sucrose buffer. A thin layer of aqueous buffer was added on top of the homogenate in the centrifuge tube. The homogenate was centrifuged at ~17,000 rpm for 20 min. The ROS were collected with a syringe from the interface between the aqueous buffer and 40% (W/V) sucrose buffer. The collected fragments were washed with aqueous buffer centrifuged to a pellet and the whole process was repeated three to four times. Finally, the ROS were extracted in a solution of 1% cetyltrimethylamonium bromide (CTAB) (W/V) in potassium phosphate buffer .067M at pH 6.5 and .1M hydroxylamine. This was diluted five times with the same buffer without CTAB reaching .2% CTAB (W/V) concentration and absorbance of .5 O.D./cm, roughly equivalent to 10^{-5}M concentration of rhodopsin.

The purity of rhodopsin preparation is determined by the ratio of absorption at the maxima of the protein band (280nm) and the visible absorption band (500nm).

The lower this ratio the better the sample is. This ratio was for our samples about 3.5 out of 1.6 that has been reported in the literature for the best preparations. Figure 10 shows the absorption spectrum of a typical rhodopsin sample. It should be noted that the purity of rhodopsin is important in the Raman measurements. Low purity samples show an increased fluorescence background affecting adversely the signal to noise ratio.

Raman spectra of rhodopsin were taken in the molecular flow apparatus, previously described with the 568.2 nm line from the krypton laser and at a power level of 10mW. The temperature of the sample were kept at 17°C by immersing the reservoir in an ice bath. The procedure during the experiment was to obtain Raman spectra until the sample was 50% bleached. The entire sample was then completely bleached to retinal oxime and opsin and separate Raman measurements performed under identical conditions. It was found that the totally bleached sample gave a negligible Raman spectra apart from a broad background fluorescence and a small broad band around 1650 cm^{-1} which is a well known water line. We conclude that no significant Raman lines from the retinal oxime and opsin are contained in the rhodopsin spectrum. The rate of formation of retinal oxime was measured in a separate experiment by monitoring the absorbance at 365nm after a bleaching pulse of light. It was found that this time was faster than the molecular round trip transit time.

Figure 11 shows the Raman spectrum of a typical run of rhodopsin and the final spectrum composed of many digitally pooled runs after the fluorescence background was removed. The background was computer subtracted by least

Figure 10

Absorption spectra of (a) rhodopsin solution in potassium phosphate buffer .067M and .1M hydroxylamine at pH 8.0 2% CTAB (W/V), and (b) same sample bleached at room temperature. $A(280)/A(500) \approx 4$

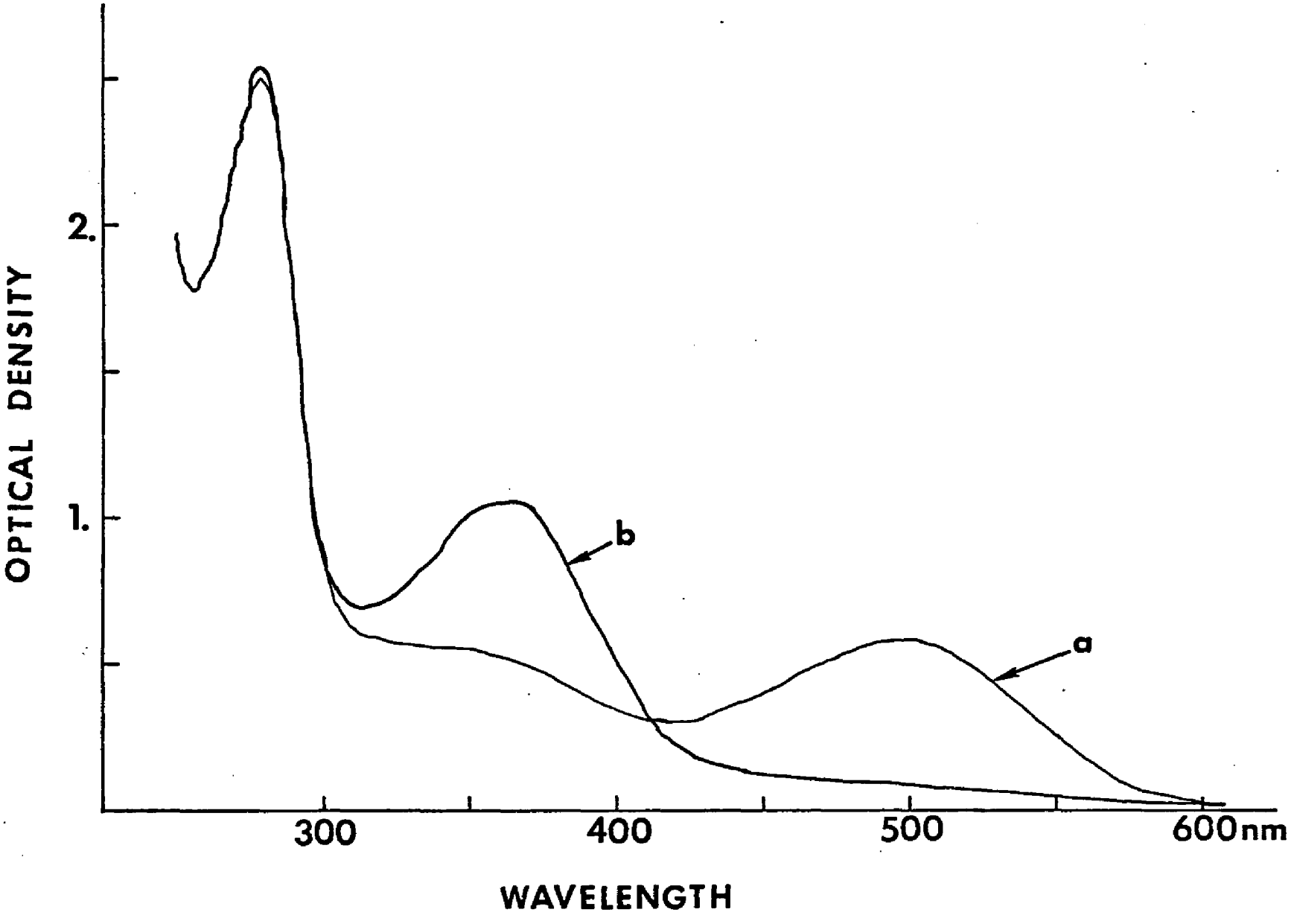
OPTICAL DENSITY
2.
1.
b
a
300
400
500
600nm
WAVELENGTH

Figure 11

(b) Resonance Raman spectrum of rhodopsin, a single run. Monochromator speed set at 100 cm^{-1}/min, dwell time 1.1 sec per channel. (a) Final spectrum composed of many digitally pooled runs. Fluorescence background has been subtracted (see text). Vertical arrow represents (b) 1000 counts, (a) 1600 counts.

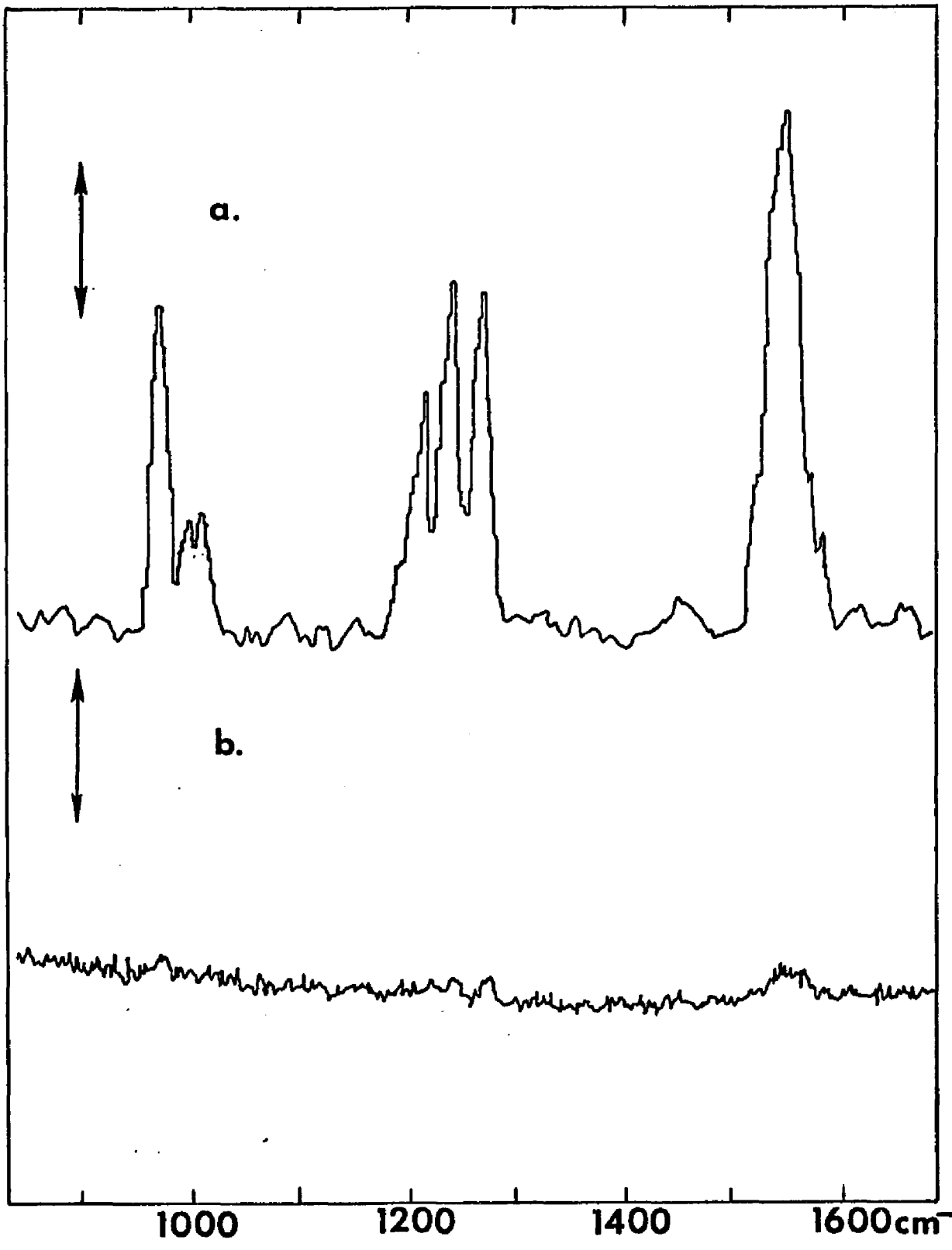
a.
b.
1000
1200
1400
1600cm⁻¹

square fitting a curve to a number of background points. The values of 512 equidistant points were subsequently calculated and subtracted from the corresponding channels of the raw data.

Metarhodopsin I and Metarhodopsin II

Metarhodopsin I was prepared from rhodopsin vesicles suspended in potassium phosphate buffer .067M at pH 8.0 and temperature +3°C. The suspension was irradiated with 568.2nm krypton line for sufficient time to ensure that a photosteady state was reached. Metarhodopsin I was identified and the stability tested by monitoring the absorption spectra of the suspension at +3°C.

Absorption measurements of suspension may introduce large errors due to light scattering. Figure 12a shows a typical absorption spectrum of rhodopsin in suspension. As it can be seen the absorption band at 500nm is only a few percent of the background making the assay of the composition of the suspension virtually impossible. The procedure that was followed was to record the absorption spectrum of the suspension with reference to air. The sample then was bleached at room temperature with a drop of hydroxylamine 1M being added to it and centrifuged. The supernatant, which included the retinal oxime was discarded and the pellet was resuspended in the same buffer to the same concentration and the absorption spectrum recorded. This spectrum was computer subtracted from the original spectrum of the suspension leaving an absorption spectrum without the background (Figure 12b).

This procedure was tested on a rhodopsin suspension. The absorption spectrum thus obtained was compared to the absorption spectrum of solubilized rhodopsin in 2% CTAB (W/V) in the same buffer and concentration (Figure 12c).

Figure 12

(a) Absorption spectra of rhodopsin vesicles in phosphate buffer (1), and the bleached sample (see text) (2). The baseline in both spectra has been suppressed by 1.5 O.D. (b) Absorption spectra of rhodopsin vesicles after the background has been computer subtracted. (c) Absorption spectra of solubilized rhodopsin in 2% CTAB (W/V) in phosphate buffer. Concentrations in (a) and (c) are the same.

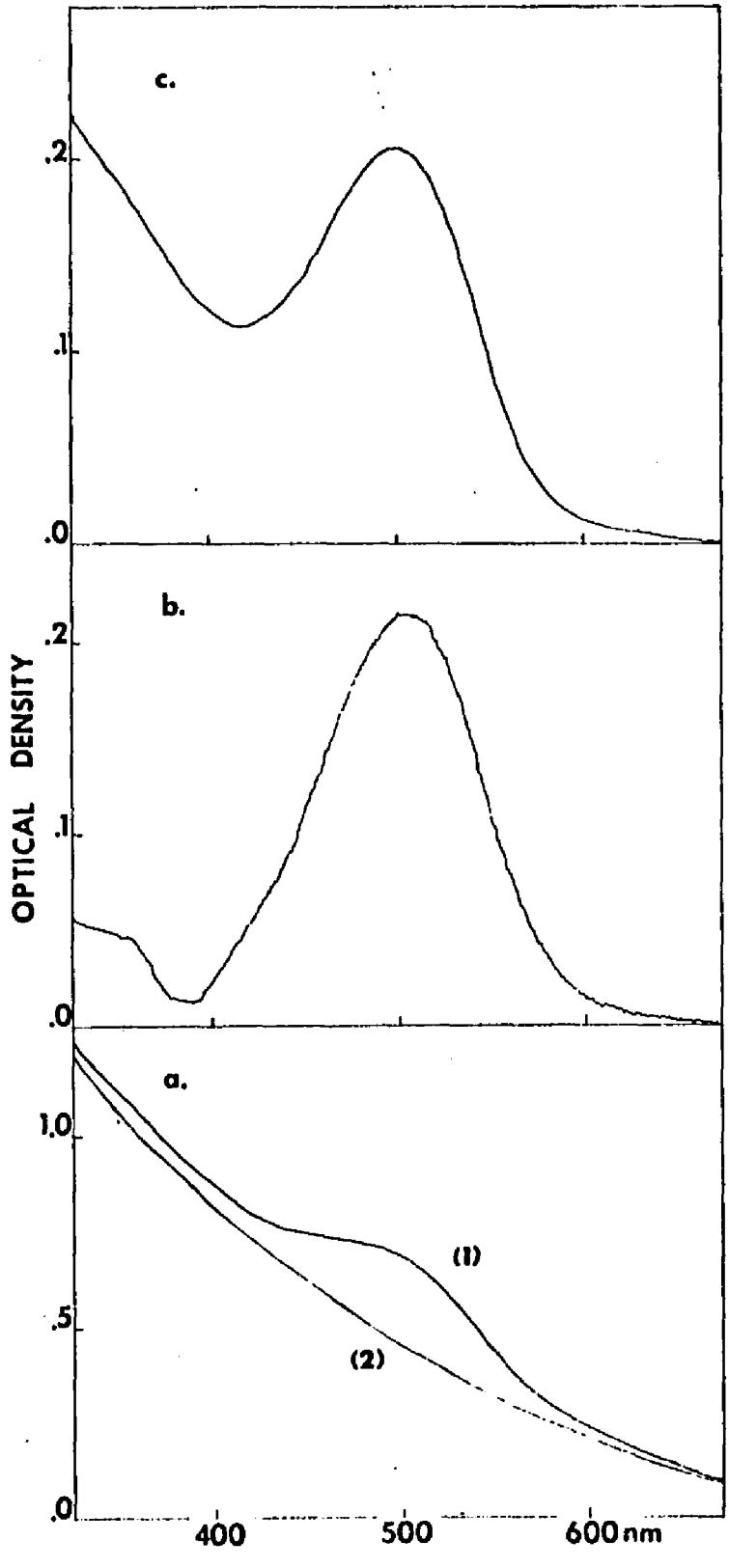
c.
.2
.1
.0
b.
.2
.1
.0
OPTICAL DENSITY
a.
1.0
.5
.0
(1)
(2)
400
500
600nm

The two absorption spectra are in good agreement.

The absorption band of rhodopsin upon irradiation with 568.2nm shifted to 480nm. The band decreased slowly, a few percent, over a period of an hour due probably to slow thermal reactions or possibly to precipitation of the vesicles. The sample was warmed up to room temperature in the dark and the absorption spectrum recorded. The absorption maxima of metarhodopsin I is 478nm (Matthews et al., 1963). From these spectra the composition of the suspension in the photosteady state was calculated to be 80% metarhodopsin I and 20% rhodopsin and isorhodopsin in good agreement with the values reported by Hubbard and Kropf (1958).

Metarhodopsin II was prepared and tested in a similar way. Rhodopsin vesicles were suspended in citrate (.067M) - potassium phosphate (.134M) buffer at pH 5.3 and irradiated at $+3^{o}C$ with the 568.2nm krypton laser line. The absorption spectra of the suspension were obtained as it has been previously described. The ratio of metarhodopsin II to metarhodopsin I was found to be 3/1. The absorption spectra remained unchanged for a period of two hours. The suspension was warmed up to room temperature in the dark and the absorption spectrum recorded again. No appreciable amount of rhodopsin or isorhodopsin was found.

A further test was performed to ensure the identity of metarhodopsin II. The pH of the irradiated vesicles was adjusted to 8.0 by titrating the suspension with small quantity of potassium hydroxide 2M. The operation was performed at $+3^{o}C$

under red dim lights. The absorption spectrum of the suspension was recorded at $+3^{o}C$. The 380nm band shifted to 478nm. As it was expected, metarhodopsin II was converted to metarhodopsin I. A small decrease of the optical density of the sample was attributed to a decrease in the concentration.

Raman measurements of metarhodopsin I and metarhodopsin II were taken in the molecular flow apparatus modified for that purpose. A cold bath circulator Lauda Super K/2R was included to cool the sample reservoir. The temperature was monitored by a thermocouple at the return port. The temperature at the solution was maintained at $+3^{o}C$. The temperature difference between the outgoing and the incoming sample was found in experimental runs, not to exceed $1^{o}C$. The sample was stirred inside the reservoir to prevent ice formation on the wall.

The reservoir was continuously irradiated with the 568.2nm krypton laser line expanded to illuminate the whole sample and at a power level of 250mW. The transfer time from the sample reservoir to the Raman measuring capillary tube was approximately 5 sec. This is much longer than the time of formation of metarhodopsin I ($\sim \mu$sec) or metarhodopsin II ($\sim$ m sec). We conclude, therefore, that the Raman obtained do not include any contributions from bathorhodopsin or lumirhodopsin intermediates. Typical concentration of samples were .3 - .5 O.D./cm. All samples were irradiated for 20 min prior to collecting Raman spectra.

The 476.2nm argon laser line was used to excite metarhodopsin I at a power level of 2mW. Under the conditions of the experiment less than 5% of the sample was photoconverted in the beam. Metarhodopsin II[2] spectra were obtained with

the 454.5nm argon laser line at a power level of 5-10mW. Since the absorption band of metarhodopsin II lies relatively far from the laser line no significant photoconversion in the laser beam is expected.

The procedure during the flow experiment was to accumulate the Raman spectra of multiple runs until the signal to noise ratio built to a sufficient level. The entire sample was warmed up to room temperature and bleached at the end of the experiment. Separate Raman measurements were performed then under otherwise identical conditions. The bleached sample gave a broad fluorescence background but no Raman structure was detected.

The Raman spectrum of metarhodopsin I contains components from rhodopsin and isorhodopsin. Under the conditions of the experiment the percentage of each of these two species is calculated to be roughly 10% (Hubbard and Kropf, 1958). The contribution of rhodopsin, however, to the Raman spectra may be expected to be relatively less, if the enhancement factor is taken into account. The contribution of isorhodopsin is more difficult to assess. Both metarhodopsin I and isorhodopsin are equally enhanced. The molar extinction coefficient of metarhodopsin I, however, is larger than that of isorhodopsin. This affects favourably the relative contribution of metarhodopsin I in the Raman spectra. In addition, comparison of the isorhodopsin Raman spectra (Oseroff and Callender, 1974; Mathies et al., 1976) and metarhodopsin I[1] reveals that the prominent bands are in different positions in the two spectra. The ratio of the main bands are better than 6/1. We conclude, therefore, that the Raman spectrum presented here is the Raman spectrum of metarhodopsin I, as far as the main features are concerned.

The contribution of metarhodopsin I to the metarhodopsin II^2 spectra is difficult to assess because of the different enhancement factors for the two species. The procedure that was followed was to computer subtract increasing amounts of the Raman spectrum of metarhodopsin I from the Raman spectrum of metarhodopsin II^2 without creating excessive valleys into the baseline. It was found, in this way, that the relative contribution of metarhodopsin I in the Raman spectrum of metarhodopsin II^2 was about 40-45%. This constitutes only an upper limit of the relative contribution of metarhodopsin I. It is not unreasonable, however, considering (a) the composition of the mixture of the two intermediates, (b) and that the Raman spectrum of metarhodopsin I is enhanced more due to the proximity of its absorption band to the exciting laser line. In addition, it was found that the main features of the Raman spectrum of metarhodopsin II are not very sensitive to the amount of the spectrum of metarhodopsin I subtracted.

Bacteriorhodopsin:

Cultures of Halobacterium Halobium of the R_1 mutant strain were grown and the purple membrane purified according to the procedures described by Becher and Cassim (1975). Two intermediates were studied: (a) the PM568 in the light adapted form and (b) the M412. The flow apparatus (Figure 9) was used for both intermediates.

For measurement of PM568, purple membrane suspended in distilled water was maintained at approximately 5°C by cooling the sample reservoir with a Lauda Super K-2/R circulator. The pigment in this reservoir was kept in the light-adapted state (PM568) by irradiating with light from a 60 watt incandescent bulb. After leaving the reservoir, the sample was in the dark for about 6 sec until it reached the exciting laser beam. The 568.2 nm krypton laser line was used at a power level of 1.5 mW. Under the conditions of the experiment, less than 5% of the sample was photoconverted during irradiation with the laser.

To record the M412 spectrum, NaCl was added to the purple membrane to make a 4.3 M solution and the pH was raised to approximately 10, greatly increasing the lifetime of this intermediate (Becher and Ebrey, 1977). The tubing from the sample reservoir to the Raman measuring capillary tube was shortened, reducing the transfer time to approximately 3 sec. The same lamp used for light adapting the purple membrane pigment was used to drive PM568 to M412, but now the sample reservoir was covered with yellow cellophane to remove most of the shorter wavelength light. The 454.5nm argon laser line was used at a power level of 2.6mW to measure the Raman spectra of M412. Under these conditions

less than 5% of the sample was photoconverted from M412 during irradiation with the laser. After the M412 Raman spectrum was recorded, the membrane suspension was placed in the dark for thirty minutes and then the Raman spectrum recorded with the 568.2nm laser line. This spectrum was indistinguishable from the spectrum of the PM568 without NaCl and high pH, demonstrating that the protein did not denature in NaCl and high pH.

Under the above conditions, the sample is not completely converted to M412. In order to determine the sample composition, the absorption spectra of the high salt, high pH purple membrane suspension were measured under conditions identical to that of the Raman experiments except that a 10nm flow spectrophotometer cuvette replaced the capillary tube of the Raman system. We estimate that a minimum of 80% of the pigment is in the M412 form. If opal glass is used to minimize the light scattering changes, a clear isosbestic point is obtained indicating that only PM568 and M412 are present. Since the 454.5nm laser irradiating line is much closer to resonance with the M412 absorption band than the PM568 absorption band, it can be expected that the M412 spectral features will dominate the composite Raman spectra more than its minimum composition of 80% would indicate. Examination of spectral features of the data (see below) show that the residual PM568 makes almost no contribution to this Raman spectrum.

Although the growth procedures for the bacteria are under conditions which minimize the amount of carotenoids present and nearly all of the carotenoids are associated with the purple membrane are removed in the purifying procedures,

it cannot be assumed that there is no carotenoid present in the sample which can then give rise to spurious Raman scattering. This is important since the laser lines used are in resonance with carotenoid absorption bands so that trace amounts can give rise to significant Raman scattering. The possible presence of carotenoid bands was assayed in the following manner. Raman spectra were taken of the sample washings, and the carotenoid present in these samples was found to be the (2, 2/2, 2) type as measured by Rimai et al., (1973) which has strong Raman bands at 1154 and 1510 cm^{-1}. These lines were not observed in the PM568 spectrum but were weakly present (less than 5% of the ethylenic intensity) in the M412 spectrum. To examine the carotenoids, stationary double beam measurements at room temperature of purple membrane (as used in the PM568 experiment above) were performed. A "probe" laser beam at 454.5nm and a "pump" laser beam at 568.2nm were used. The two beams were made coaxial by a beam splitter and passed through an aperture. The apertures ensured that each of the beams illuminated the same area of the sample. The ratio of the power levels of the "pump" to the "probe" was 10 to 1.

When the "pump" beam was not present the resulting spectra was essentially that of PM568. When the "pump" beam was included the spectrum of essentially M412 was obtained. However, the small Raman structure at 1154 and 1510 cm^{-1} was found not to change in these two runs. Thus, we conclude that these two lines found in the M412 spectrum are due to the carotenoid present in the sample. These two lines have been computer subtracted from the M412 spectrum.

Model Compounds

Retinals:

Retinals other than 11cis were purchased from Sigma Chemical Co. (St. Louis, Missouri) and used without further purification. The 11-cis isomer was a gift from the Hoffmann-La Roche company. The purity of the retinals was assayed by high pressure liquid chromatography (HPLC) (Chan et al., 1974) under the following conditions. A Walters Associates 6000 psi HPLC system equipped with a septum injector, and Laboratory Data Control 350nm detector was used with a μ-poracil one or two 1 ft. x .25 in. column(s). The solvent system was 1-4% (V/V) ether/n - hexane and the flow rate was adjusted to 1-2 ml/min. The retinal isomers present in the solution were identified by comparison with known standards. The compositions percentage were determined by measuring the areas under the curves by the cut-and-weigh method and divide them by their ϵ_{350} respective values. It was found that all-trans and 13-cis were better than 97% pure, 11-cis 95% and 9-cis 87% pure. A typical concentration of the retinal tetrachloride solution was 5mM.

Resonance Raman spectra of retinals were taken in the flow apparatus previously described. Sample temperature was maintained at 17°C by immersing the sample reservoir in an ice bath. The 520.8nm laser line at a power level of 1mW was used. The solutions of retinals were assayed by HPLC after each flow experiment. The degree of total photoisomerization was very small (less than 2%). The Raman spectrum of carbon tetrachloride were computer subtracted leaving the pure Raman spectra of the retinals.

The crystal Raman data were obtained by defocusing the 647.1nm laser beam to completely illuminate the crystals held in a sealed capillary tube. The sample was assayed after the Raman experiment by HPLC. No change in isomeric composition was observed in all cases.

Schiff Bases of Retinals

Retinal Schiff bases of all-trans, 13-cis and 11-cis were prepared by adding an excess amount of n-butylamine or monoethanolamine to the solution of the corresponding retinal in pure ethanol at $0^{o}C$. The solution was stirred for 2 hours under a stream of nitrogen. The completeness of the reaction was tested by the absorption spectra. Schiff bases absorb about 20nm to the shorter wavelengths of the retinals. The solution was dried for the complete removal of excess amine and the remaining powder was dissolved in absolute ethanol or carbon tetrachloride. Protonated Schiff bases were prepared by titrating the corresponding Schiff base in absolute ethanol with ethanol saturated with hydrogen chloride. The protonation was followed by the change in the absorption spectra.

Raman measurements of the retinal-n-butylamine Schiff bases protonated and unprotonated were taken in the molecular flow apparatus. Table 3 summarizes the conditions of the experiment, wavelength used, power level and concentration. The ethanol background spectrum was computer subtracted leaving the pure Raman spectra of the retinal Schiff bases.

Table 3

	Concentration moles	λ_L (nm)	Power (mW)
Schiff bases			
11-cis	C.T. 8.8×10^{-4}	476.2	1.2
all-trans	E.A. 3.5×10^{-3}	476.2	2
13-cis	E.A. 2.6×10^{-3}	476.2	2
Protonated Schiff bases			
11-cis	E.A. 2.4×10^{-4}	457.9	1
all-trans	E.A. 3.5×10^{-3}	647.1	3
13-cis	E.A. 2.6×10^{-4}	530.8	3

C.T. - solvent carbon tetrachloride

E.A. - solvent absolute ethyl alcohol

Footnotes

1. Metarhodopsin I followed by the superscript should be taken to mean the mixture of metarhodopsin I, rhodopsin and isorhodopsin previously described.

2. Metarhodopsin II followed by the superscript should be taken to mean the mixture of metarhodopsin I and metarhodopsin II previously described.

Section III

Results and Discussions

Model Compounds

Figures 13 - 16 show the resonance Raman spectra of all-trans, 13-cis, 9-cis and 11-cis retinal isomers in crystals and solution as well as their corresponding protonated and unprotonated Schiff bases. Previous experimental (Rinai et al., 1971b; Gill et al., 1971; Heyde et al., 1971; Callender et al., 1976; Mathies et al., 1977) and theoretical work (Tric, 1969; Rinai et al., 1973; Warshel and Karplus, 1974; 1977) have made possible some general spectral assignments (see also Callender and Honig, 1977). The fundamental vibrations of the retinals and their Schiff bases that have received the greatest attention in Raman studies are found between 800 and 1700 cm^{-1}. Traditionally, this region has been divided to (a) terminal end group (1600-1700 cm^{-1}), (b) the ethylenic mode region (1500 - 1620 cm^{-1}) and (c) the fingerprint region (900-1450 cm^{-1}). A low frequency region covers vibrations below 900 cm^{-1}.

Terminal End Group

The band in this region has been assigned to C=O stretching vibration for the retinals or C=N stretching vibration for the Schiff bases. The frequency of C=O vibration is insensitive to the conformation of the isomer (Figures 12, 13). It depends, however, on the state of the sample (e.g. powder or solution). In addition the frequency is affected by the polarity of the solvent. Polar solvents generally have the effect of decreasing the frequency of C=O vibration. This may be due to hydrogen bonding of the solvent to the oxygen of the carbonyl group.

Figure 13

Resonance Raman spectra of various retinal isomers as crystals. The exciting laser frequency is 647.1nm and, the resolution in all cases is 8 cm^{-1}.

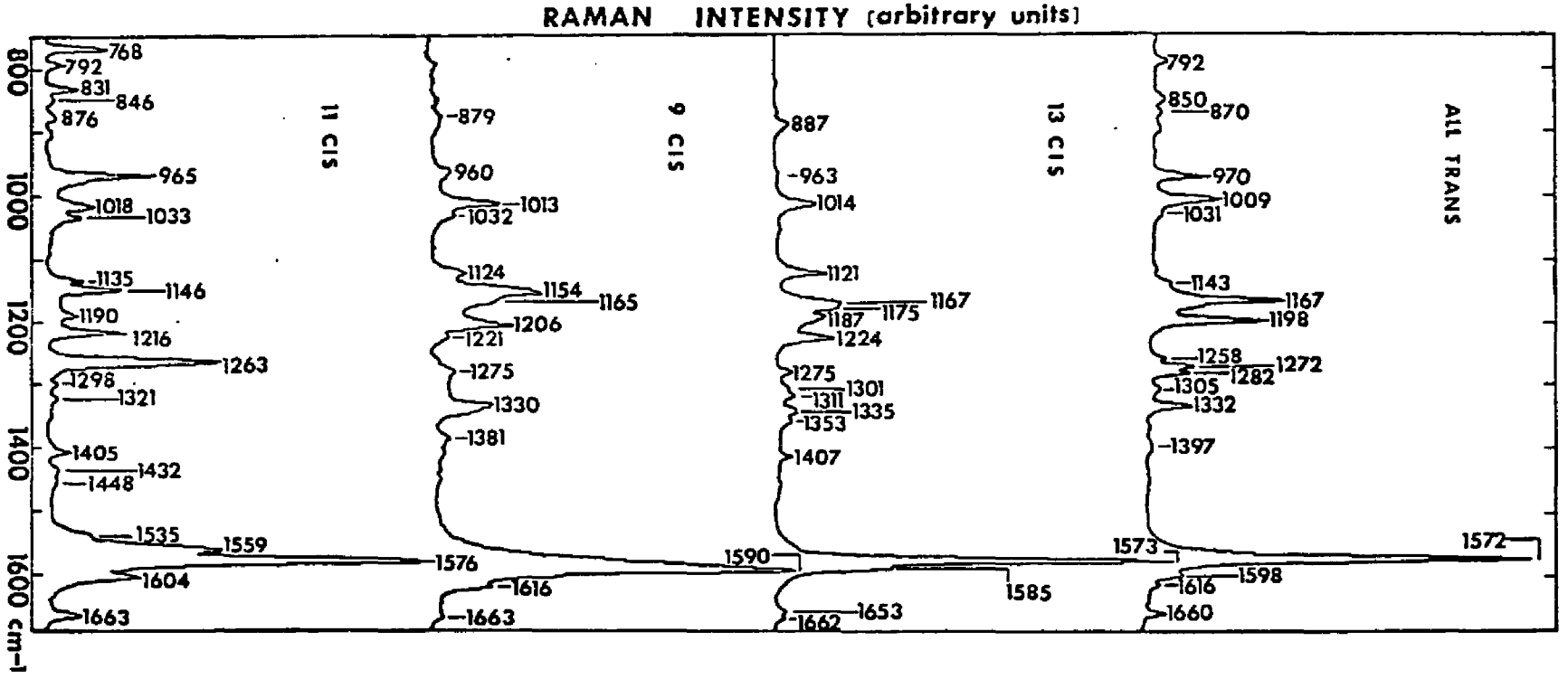
RAMAN INTENSITY (arbitrary units)
11 CIS
9 CIS
13 CIS
ALL TRANS
800
1000
1200
1400
1600 cm-1
768
792
831
846
876
965
1018
1033
1135
1146
1190
1216
1263
1298
1321
1405
1432
1448
1535
1559
1576
1604
1663
879
960
1013
1032
1124
1154
1165
1206
1221
1275
1330
1381
1616
1663
887
963
1014
1121
1167
1175
1187
1224
1275
1301
1311
1335
1353
1407
1590
1585
1653
1662
792
850
870
970
1009
1031
1143
1167
1198
1258
1272
1282
1305
1332
1397
1573
1572
1598
1616
1660

Figure 14

Resonance Raman spectra of various retinal isomers dissolved in carbon tetrachloride. The exciting laser frequency is 520.8nm, and the resolution in all cases is 12 cm^{-1}.

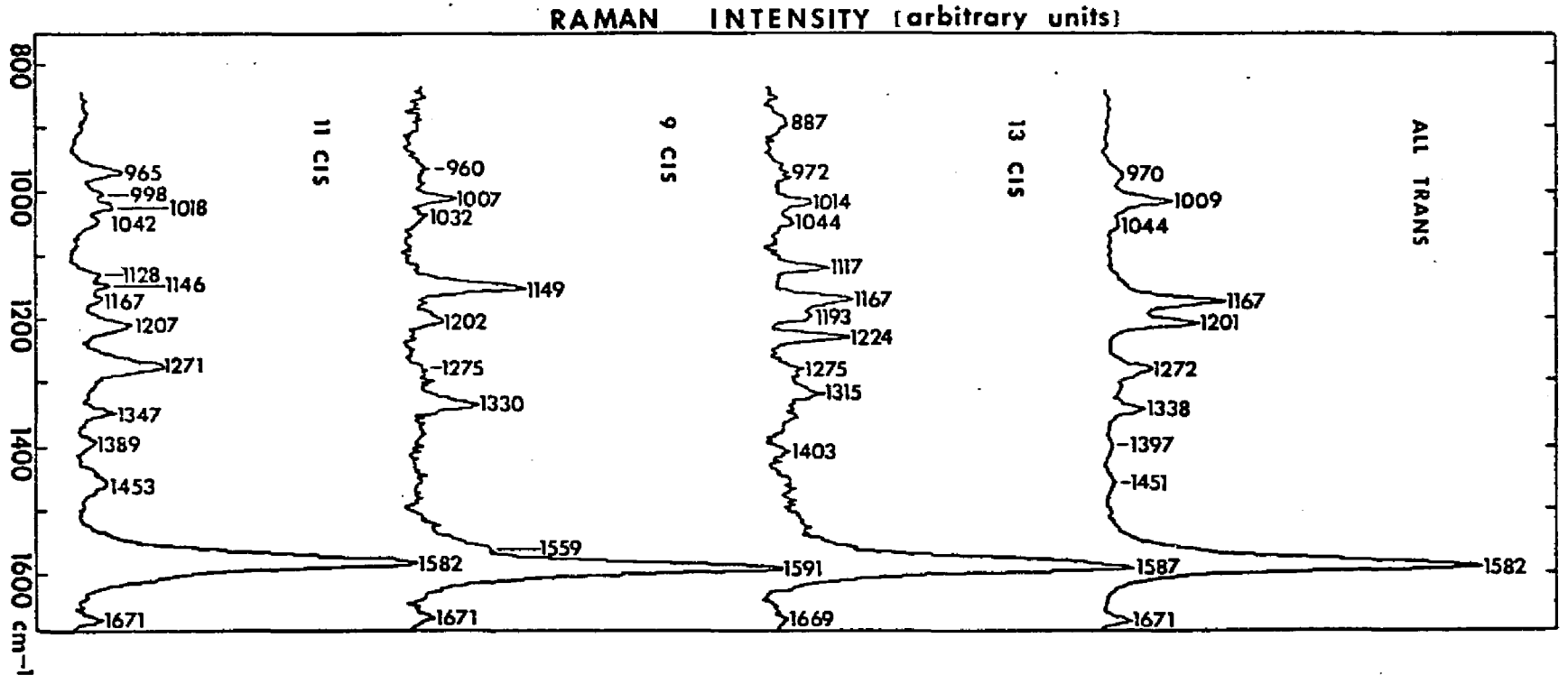
RAMAN INTENSITY (arbitrary units)
800
1000
1200
1400
1600 cm-1
11 CIS
965
998
1018
1042
1128
1146
1167
1207
1271
1347
1389
1453
1582
1671
9 CIS
960
1007
1032
1149
1202
1275
1330
1559
1671
13 CIS
887
972
1014
1044
1117
1167
1193
1224
1275
1315
1403
1591
1669
ALL TRANS
970
1009
1044
1167
1201
1272
1338
1397
1451
1587
1582
1671

Figure 15

Resonance Raman spectra of (A) 11-cis retinal-n-butylamine HCl, (B) all-trans retinal-n-butylamine HCl, and (C) 13-cis retinal-n-butylamine HCl. The resolution is (A) 9 cm^{-1}, (B) 4 cm^{-1}, and (C) 6 cm^{-1}.

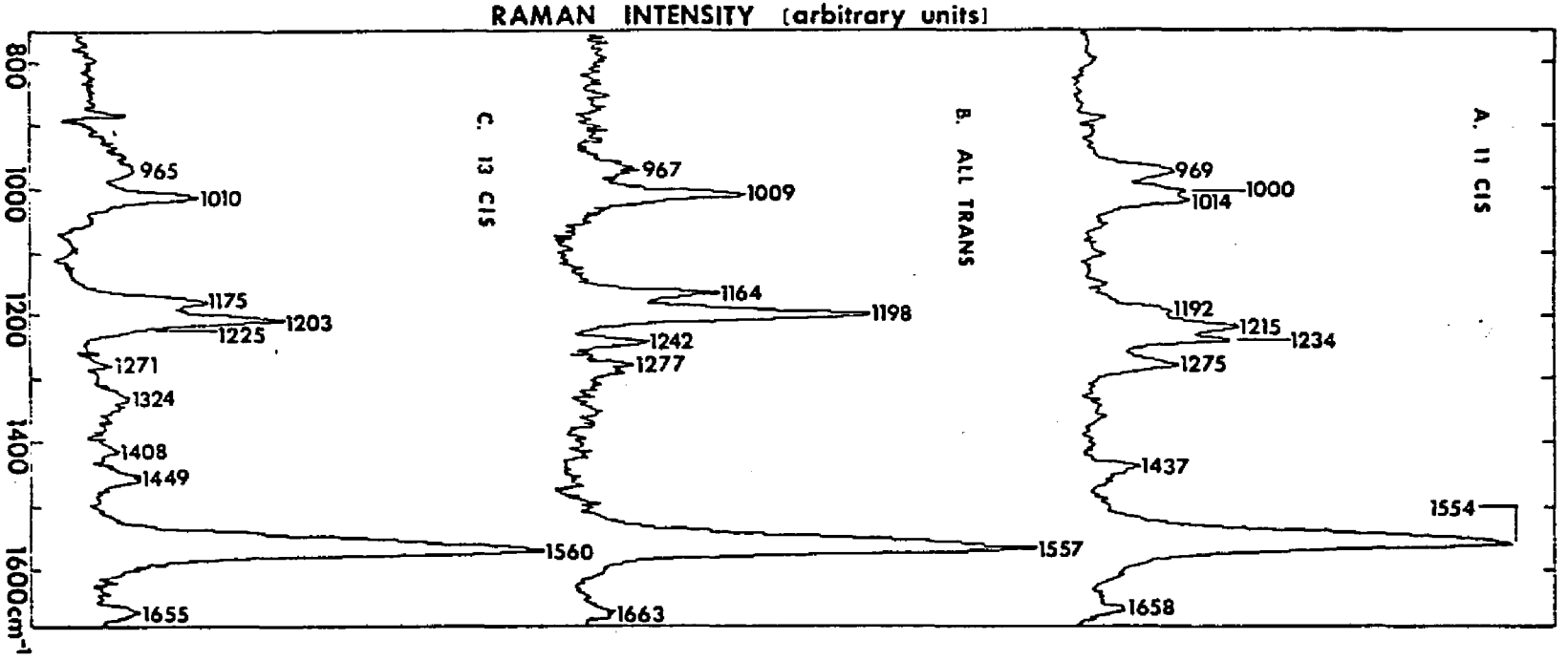
RAMAN INTENSITY (arbitrary units)
800
1000
1200
1400
1600 cm⁻¹
C. 13 CIS
965
1010
1175
1203
1225
1271
1324
1408
1449
1560
1655
B. ALL TRANS
967
1009
1164
1198
1242
1277
1557
1663
A. 11 CIS
969
1000
1014
1192
1215
1234
1275
1437
1554
1658

Figure 16

Resonance Raman spectra of (A) 11-cis retinal-n-butylamine, (B) all-trans retinal-n-butylamine, and (C) 13-cis retinal-n-butylamine. The resolution is (A) 9 cm^{-1}, (B) 7 cm^{-1}, and (C) 7 cm^{-1}.

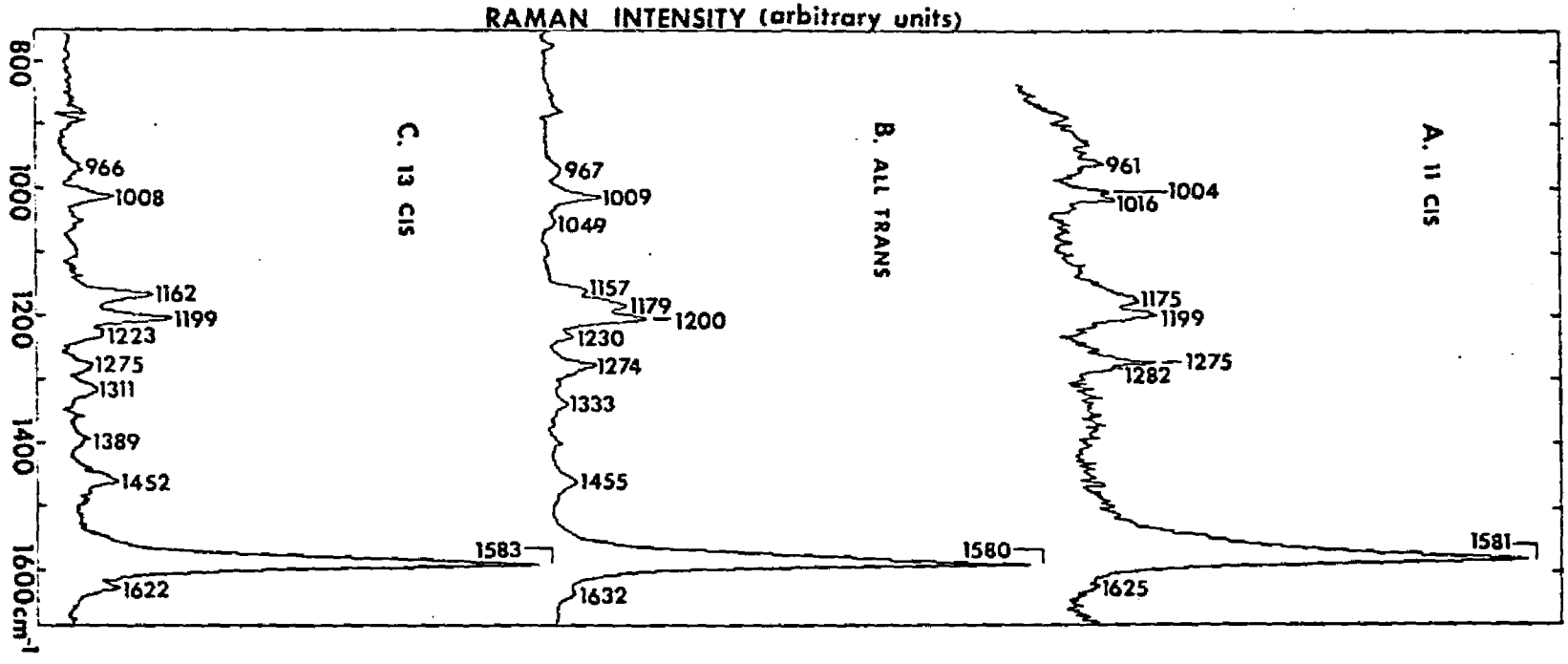
RAMAN INTENSITY (arbitrary units)
800
1000
1200
1400
1600 cm⁻¹
C. 13 CIS
966
1008
1162
1199
1223
1275
1311
1389
1452
1583
1622
B. ALL TRANS
967
1009
1049
1157
1179
1200
1230
1274
1333
1455
1580
1632
A. 11 CIS
961
1004
1016
1175
1199
1275
1282
1581
1625

It should be mentioned here that 13-cis retinal in crystal show a split C=O band but no explanation has been advanced to date.

In the Schiff bases of retinals (Figure 14) a weak band appears at 1620 cm^{-1} which has been assigned to the C=N stretching vibration. An important result is that the protonation of the Schiff base leads to a frequency increase of about 30 cm^{-1} (from 1620 cm^{-1} to 1650 cm^{-1}) (Figure 15). This observation facilitates the identification of the protonated and unprotonated forms of the Schiff base and has been used extensively in the study of the visual pigments. It should be mentioned here that the assignment of the band near to 1650 cm^{-1} in the protonated species to $C=\overset{+}{N}H$ stretching vibration has been demonstrated by Oseroff and Callender (1974). Deuteration of the Schiff base causes a predictable decrease in the stretching frequency from 1655 cm^{-1} to 1630 cm^{-1} (see for example, Herzberg, 1945).

Ethylenic Mode Region

Lines in this region have been assigned primarily to combinations of C=C stretching vibrations. These vibrations are the strongest observed in the Raman spectra of all polyenes. Their intensity is derived from large changes between the ground and excited state geometries. The number of possible lines is equal to the number of C=C double bonds. However, with the exception of 11-cis retinal and to a lesser extent of 13-cis the lines appear degenerate. Four C=C bands in the crystal spectra of 11-cis retinal are observed (Figure 12). This is perhaps due to twisting about the 12 - 13 single bond in this isomer (Figure 17),

Figure 17

Conformations of various isomers of retinal (X = O), its Schiff base (X = N), and its protonated Schiff base ($X=\overset{+}{N}H$). (a) all-trans; (b) 13-cis; (c) 9-cis; (d) 11-cis, 12-s-trans; (e) 11-cis, 12-s-cis. Arrows indicate flexible bonds whose equilibrium is not planar.

a.

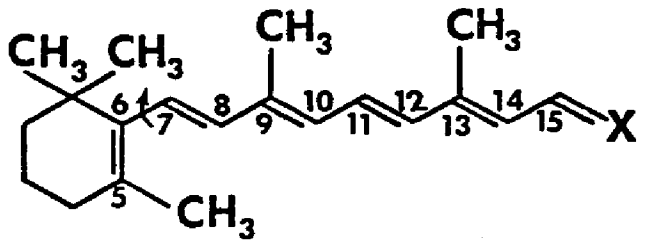
CH3 CH3
CH3
CH3
6
7
8
9
10
11
12
13
14
15
X
5
CH3

b.

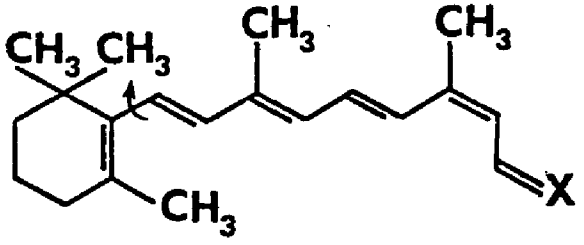
CH3 CH3
CH3
CH3
X
CH3

c.

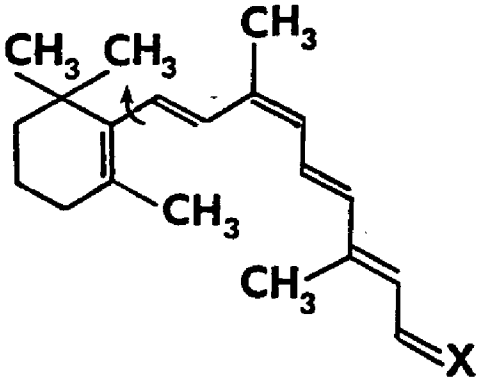
CH3 CH3
CH3
CH3
CH3
X

d.

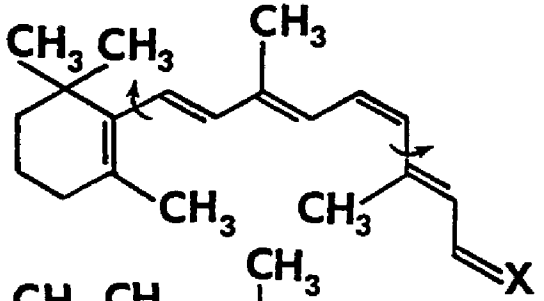
CH3 CH3
CH3
CH3
CH3
X

e.

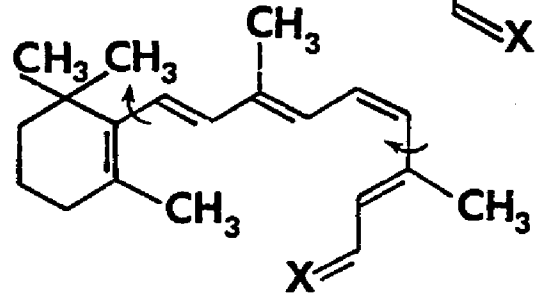
CH3 CH3
CH3
CH3
CH3
X

which could result in partial decoupling of the various C=C modes (Callender and Honig, 1977). It should be noted that to the extent that C=C bond of β-ionone is coupled to the electronic transition there could be five C=C bands in this region.

The relative positions of the measured lines for the 11-cis retinal 1535, 1559, 1576 and 1604 cm^{-1} are in good agreement with the calculated values 1565, 1646, 1660 and 1680 cm^{-1} (Warshel and Karplus, 1974). The absolute frequencies of the measured lines, however, are off by about 80 cm^{-1} from the calculated values reflecting some inaccuracy in the theoretical potential curves. In the solution spectra, the ethylenic lines either may broaden or their positions and Raman cross sections change so that the lines can not be separately resolved.

Fingerprint Region

Lines in this region are very sensitive to the isomeric form and the terminal group. For example, the conformation of 13-cis retinal is very similar to all-trans. However, the Raman spectra are different. An analysis of the Raman structure would lead to an understanding of the detailed conformation of the molecule and its interactions with the environment. This possibility still lies in the future. However, an aspect of the Raman spectra in this region, namely the characteristic spectral pattern for each isomer will be used extensively in the discussion of the visual pigments.

Vibrations in the fingerprint region are primarily C-C single bond stretches and C-C-H bends. The line near 1450 cm^{-1} has been assigned to asymmetric bending of the methyl hydrogen (Rinai et al., 1971b; Warshel and Karplus, 1974,

1976). The line near 960 cm^{-1} is observed in infrared measurements (Lunde and Zechmeister, 1955) and has been assigned to an active out-of-plane C-H bending vibration (Shepard and Sutherland, 1949; Rinai et al., 1971b), however, theoretical calculations (Warshel and Karplus, 1974) suggest that it is significantly coupled with the C-Me stretch. In addition, the lines near 1000 cm^{-1} have been assigned to C-Me stretching vibrations perpendicular to the polyene chain (Rinai et al., 1973). Other mode assignments are difficult to make and have not been made because they represent complicated group modes along the polyene chain.

Small differences that appear between solution and crystal spectra of the retinals can be attributed to different interactions of the retinal with the surrounding media and/or small differences in conformation. A weak positive correlation between the various lines and the absorption has been reported for the retinals (Heyde et al., 1971). This observation is consistent with a stiffening of the C-C single bonds with increased delocalization of the π electrons. The effect, however, is diluted by the large amount of the C-C-H bends coupled to C-C stretching vibrations.

We shall now turn our attention to the lines that have been assigned to C-Me stretching vibrations (1000-1050 cm^{-1}). An important observation in the spectrum of 11-cis retinal is the appearance of two lines at 998 and 1018 cm^{-1} in solution as compared with a single line at 1018 cm^{-1} in the crystal. The appearance of the two lines also persists in the protonated and unprotonated Schiff bases of this

isomer. In addition, all other isomeric forms have only a single band in this region.

Gill and co-workers (1971) interpreted the two bands in the spectrum of 11-cis retinal in solution as resulting from the different environments of the 9 - and 13 - methyl groups. X-ray studies of 11-cis retinal (Giraldi et al., 1971, 1972) have shown that the 11-cis retinal crystallizes in the 12-s-cis conformation (Figure 17e). The two mentioned methyl groups are in similar environments, in agreement to a single band appearing in the crystal Raman spectrum of 11-cis retinal. Theoretical (Honig and Karplus, 1971) and NMR studies (Patel, 1969; Rowan et al., 1974; Rowan and Sykes, 1974; Becker et al., 1974) indicate that both conformations 12-s-cis and 12-s-trans (Figure 17d) are present in the solution. The 13-methyl group, however, is in a different environment in the 12-s-trans conformation because of the steric hindrance between the 10-hydrogen and the 13-methyl group. Thus, the two methyl stretching vibrations can be expected to be different. Callender et al., (1976) has assigned the 998 and 1018 cm^{-1} bands to 13-methyl stretching and 9-methyl stretching vibrations. This assignment can be carried over to the Raman spectra of the protonated and unprotonated Schiff base of the 11-cis isomer.

Low Frequency Region

Lines below 900 cm^{-1} have been assigned to group skeletal, waging, torsional, and bending, out of the plane modes (Warshel and Karplus, 1974). Crystal of most isomers have considerable structure down to 50 cm^{-1} (Figure 18). Lines in this region are in general much weaker than in the other regions. It is evident

Figure 18

Low frequency Raman spectra of various retinal isomers as crystals. The exciting laser frequency is 647.1nm, and the resolution in all cases is 7 cm^{-1}.

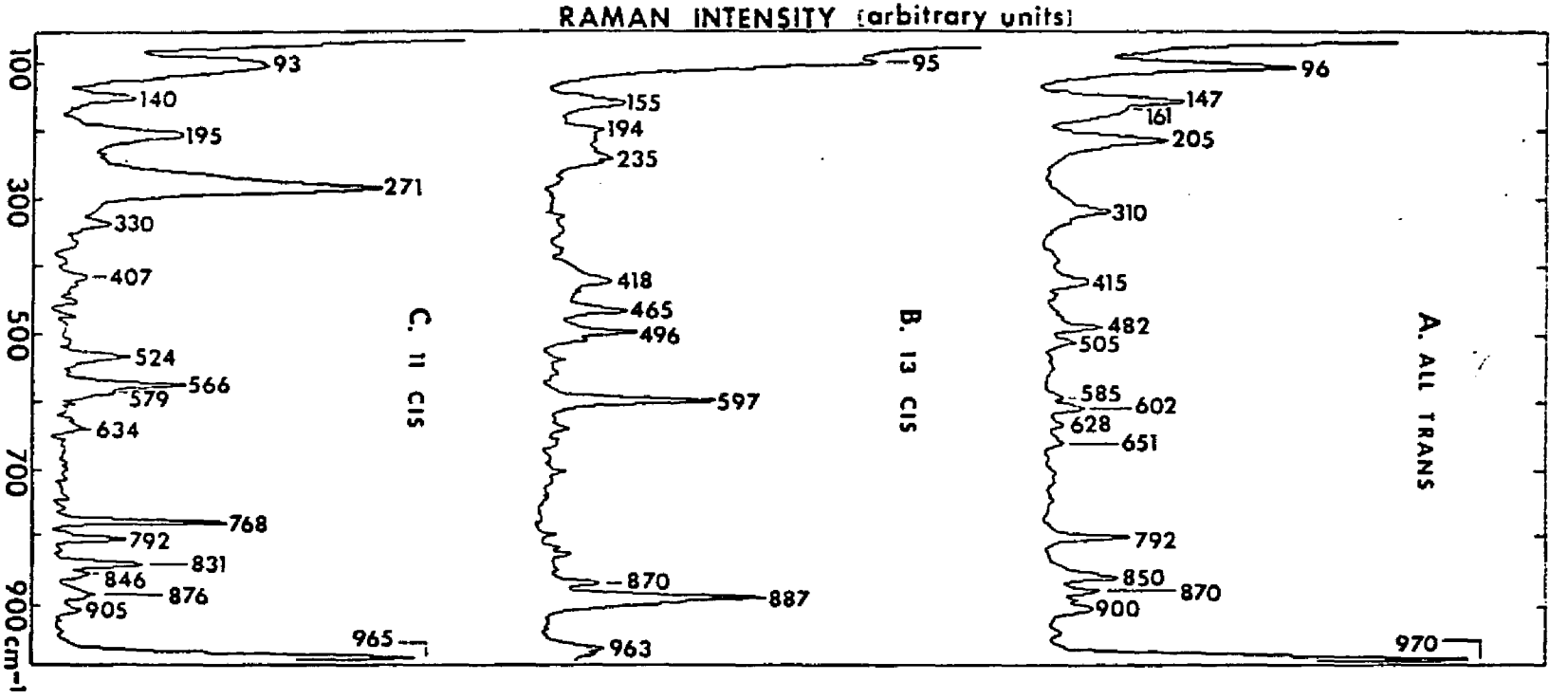
RAMAN INTENSITY (arbitrary units)
100
300
500
700
900 cm-1
93
140
195
271
330
407
524
566
579
634
768
792
831
846
876
905
965
C. 11 CIS
95
155
194
235
418
465
496
597
870
887
963
B. 13 CIS
96
147
161
205
310
415
482
505
585
602
628
651
792
850
870
900
970
A. ALL TRANS

that this region is also sensitive to the conformation of the molecule. A point of interest is the considerable structure about 800 cm^{-1} in 11-cis retinal not found with such strength in the other isomers. This may be a consequence of the highly non-planar conformation of this isomer due primarily to chain twisting about the 12C-13C bond. In addition, all retinal isomers exhibit considerable ring-chain twisting about the 6C-7C (Honig et al., 1971) bond which may be responsible for the appearance of low frequency modes of these isomers as well. The twisting of the 6C-7C is the result of the steric hindrances between the methyl groups in the ring and the proximal hydrogen along the chain. In addition, the steric hindrance between the 10H and $13CH_3$ causes the twisting about the 12C-13C bond in 11-cis retinal.

Visual Pigments

Rhodopsin, Metarhodopsin I and Metarhodopsin II

Figure 19 shows the resonance Raman spectra of rhodopsin, metarhodopsin I and metarhodopsin II. This is a very important figure since, a detailed analysis of the Raman structure leads to an understanding of the retinal conformation in the opsin matrix for rhodopsin and the two intermediates. In addition, the conformational changes of the intermediates could possibly give an insight into the mechanism that transduces the light into the nervous excitation.

The spectra of rhodopsin and the intermediates differ considerably, suggesting an extensive change in the conformation of the retinal and/or the interactions between the retinal and the opsin. In contrast the no-change of the CD spectra of the same compounds has been interpreted (Wu and Stryer, 1971) as implying stability of the local environment in the transition from rhodopsin to metarhodopsin I and metarhodopsin II. This example illustrates, perhaps, the advantages of the resonance Raman spectroscopy over other spectroscopic methods.

The Raman spectra of rhodopsin and the intermediates can be organized in a fashion similar to the spectra of the model compounds (e.g. Schiff base, ethylenic stretch and fingerprint region). Figures 20 - 22 compare the spectra of rhodopsin, metarhodopsin I and metarhodopsin II with the spectra of 11-cis protonated Schiff base, all-trans protonated Schiff base and all-trans unprotonated Schiff base respectively.

Figure 19

Resonance Raman spectra of (A) CTAB extracts of bovine rhodopsin taken with the 568.2nm laser line, (B) metarhodopsin I vesicles taken with the 476.2nm laser line, and (C) metarhodopsin II vesicles taken with the 454.5nm laser line. The resolution is (A) 10 cm^{-1}, (B) 7 cm^{-1}, and (C) 8 cm^{-1}.

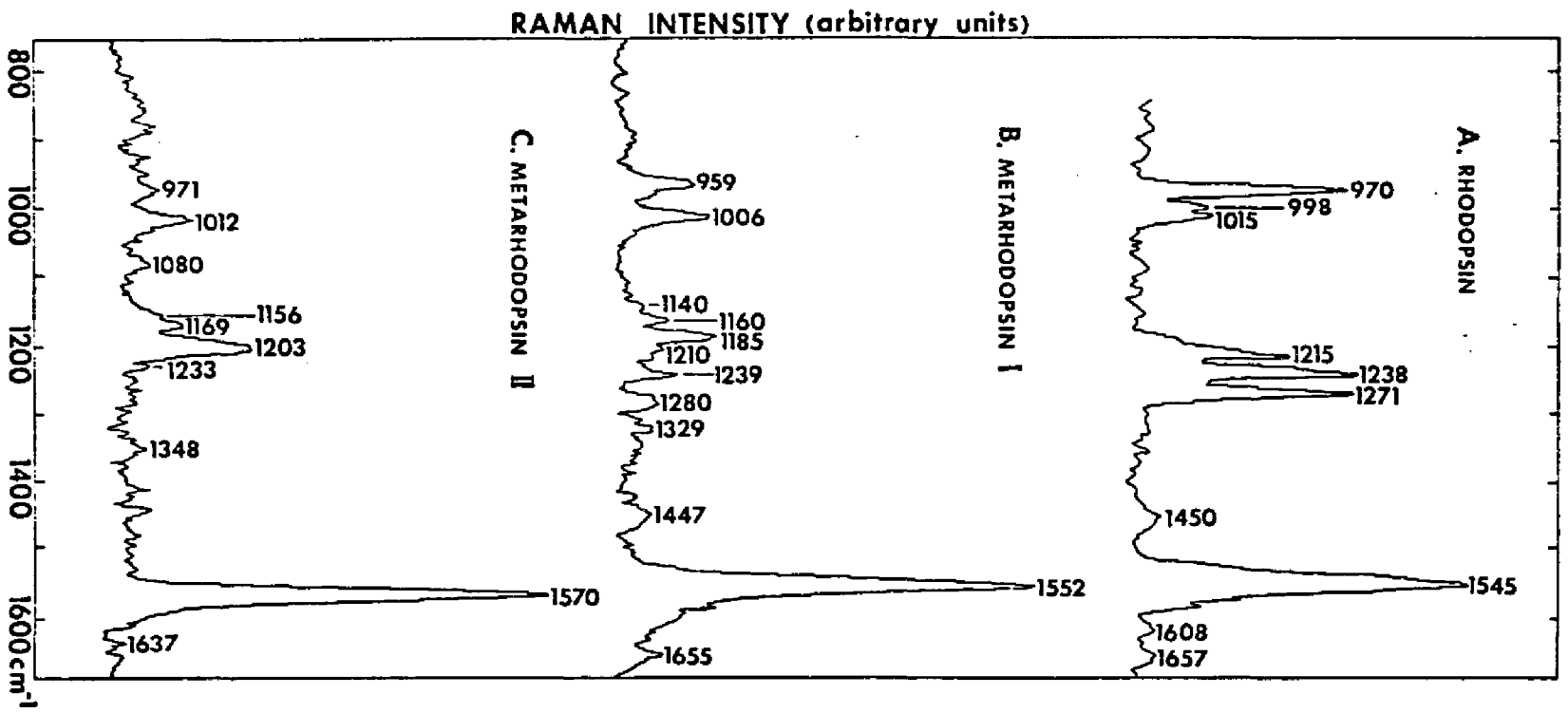
RAMAN INTENSITY (arbitrary units)
A. RHODOPSIN
970
998
1015
1215
1238
1271
1450
1545
1608
1657
B. METARHODOPSIN I
959
1006
1140
1160
1185
1210
1239
1280
1329
1447
1552
1655
C. METARHODOPSIN II
971
1012
1080
1156
1169
1203
1233
1348
1570
1637
800
1000
1200
1400
1600 cm⁻¹

Chromophore-Protein Linkage

Previous Raman studies have established that the retinal-opsin linkage of rhodopsin is a protonated Schiff base (Lewis et al., 1973; Oseroff and Callender, 1974; Mathies et al., 1976; Callender et al., 1976). The line at 1657 cm^{-1} in the spectrum of rhodopsin corresponds very closely to the 1660 cm^{-1} in the spectrum of 11-cis protonated Schiff base. In addition, a line at 1655 cm^{-1} appears in the spectrum of metarhodopsin I. Thus, the Raman spectra indicate that the chromophore remains connected to opsin via a protonated Schiff base through the metarhodopsin I intermediate. In addition, the data is consistent with a photocalorimetry study by Cooper and Converse (1976). They showed that formation of metarhodopsin I does not involve any changes in the net protonionization of the system.

A weak line at 1637 cm^{-1} appears in the spectrum of metarhodopsin II. The position of this line corresponds well to the 1632 cm^{-1} of the unprotonated all-trans Schiff base. The observation of this line is very important since it establishes directly that the metarhodopsin I to metarhodopsin II transition involves the deprotonation of the Schiff base. Previous work on metarhodopsins (Matthews et al., 1963; Cooper and Converse, 1976) have established that the metarhodopsin I to metarhodopsin II transition involves a net uptake of a proton. Thus, the Raman data confirm early suggestions that two protons are involved in this transition (Matthews et al., 1963), the second proton arising from the deprotonation of the Schiff base. The two proton acceptor groups become active in the metarhodopsin I stage. Prior to that intermediates appear to be pH insensitive within the stability range.

One of the active groups has a pK of 6.4 and has been tentatively identified as the imidazole group of histidine (Radding and Wald, 1956b; Matthews et al., 1963). It is likely that this acceptor group is close to the "surface" of the protein since the rhodopsin to metarhodopsin I transition correlates to only small changes in the conformation of the protein (Abrahamson and Ostroy, 1967; Abrahamson, 1973). It might be noted that in the squid rhodopsin system the metarhodopsin I to metarhodopsin II transition is accompanied by a net decrease of a proton (Kropf et al., 1959) possibly the proton of the Schiff base (Sulkes et al., 1976).

Cooper and Converse (1976) have recently suggested that metarhodopsin I to metarhodopsin II transition actually involves the hydrolysis of the Schiff base (forming retinal) with the chromophore bound non-covalently in the active site. The present Raman data argue strongly against this model. In summary, the arguments against are as follows: (a) the line at 1637 cm^{-1} which has been assigned in the C=N stretching vibration, (b) there is no line near 1670 cm^{-1} which would correspond to C=O stretching vibration of the aldehyde, and (c) overall the Raman spectrum of metarhodopsin II resembles that of all-trans unprotonated Schiff base rather than that of the retinal. In addition, Bownds and Wald (1965) have shown that the retinal-protein linkage can be reduced by sodium borohydride. It is difficult to see how this reaction can take place if the retinal is not covalently bound to the protein.

Conformation of the Protein-Bound Retinal

The discussion of the preceding chapter has shown that there is a close corre-

spondence in the Schiff base region between the visual pigments and Schiff bases of the retinals. In what follows we carry this analysis into the fingerprint region. As it has been mentioned before, this region is very sensitive to the conformation of the molecule. Thus, an analysis of this region can provide information about the conformation of the chromophore in the opsin matrix.

There is a close agreement (within a few wavenumbers) between the spectrum of rhodopsin and that of 11-cis protonated Schiff base (Figure 20). In addition, the spectrum of rhodopsin does not agree with any of the spectra of the other isomers protonated (see also Mathies et al., 1977) and unprotonated given here as well as the 9-cis protonated as reported by Mathies et al., (1977). This similarity between rhodopsin and 11-cis protonated Schiff base spectra, as it has been argued by Mathies et al., (1977), indicates that the conformation of the retinal in the ground state in the opsin matrix is very similar to the conformation of the 11-cis protonated Schiff base in solution. However, the protein may change the excited state of the chromophore inasmuch as the intensity of the Raman bands depend on both ground and excited states.

An important observation is the two bands at 998 and 1015 cm^{-1} in the rhodopsin spectrum. As we have discussed above these bands have been assigned to the 13 - and 9 - methyl stretching vibrations respectively, in the 12-s-trans conformation (Gill et al., 1971; Callender et al., 1976). By assuming that the chromophore in rhodopsin has a single conformation or that the 9 - and 13 - methyl stretching motions give rise to nearly equal Raman cross sections, these data suggest that the chromophore in rhodopsin is in the 12-s-trans conformation,

Figure 20

Resonance Raman spectra of (A) CTAB extracts of bovine rhodopsin, and (B) 11-cis retinal-n-butylamine HCl.

(P.S.B. = protonated Schiff base)

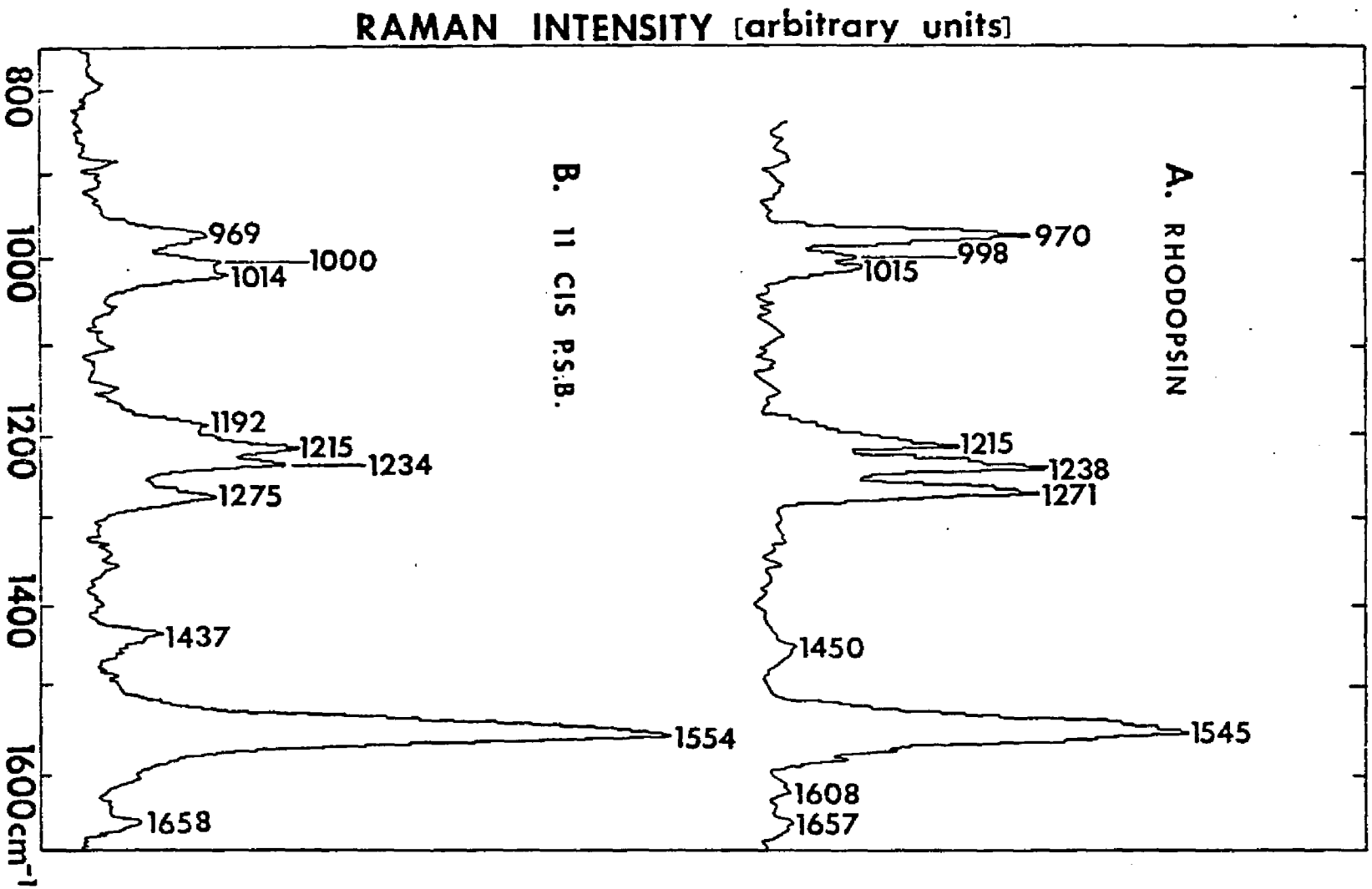
RAMAN INTENSITY [arbitrary units]
800
1000
1200
1400
1600 cm⁻¹
B. 11 CIS P.S.B.
969
1000
1014
1192
1215
1234
1275
1437
1554
1658
A. RHODOPSIN
970
998
1015
1215
1238
1271
1450
1545
1608
1657

perhaps distorted (Callender et al., 1976). Some recent studies, however, (Cookingham et al., 1977) as well as our studies on selectively deuterated retinals cast some doubt on this simple model. Our studies, though not inconsistent with the proposed conformation, indicate that modes in this region are extremely coupled.

Figure 21 shows the spectra of metarhodopsin I and all-trans protonated Schiff base. The all-trans protonated Schiff base has lines at 967, 1009, 1164, 1198, 1242, and 1277 cm^{-1} in the fingerprint region. All these lines except small changes in the position are repeated in the spectrum of metarhodopsin I. It is even more interesting that the majority of these lines show the same intensity pattern. The 967 cm^{-1} is an exception, but it is known that it is generally enhanced in visual pigments for reasons not as yet understood. The spectrum of metarhodopsin I contains weak lines at 1140, 1210 cm^{-1} which do not exist in the spectrum of all-trans protonated Schiff base. Some of these lines (like 1210 cm^{-1}) could be artifacts arising from small amounts of rhodopsin and isorhodopsin.

Figure 22 shows the spectra of metarhodopsin II, all-trans unprotonated Schiff base and all-trans retinal. It can be seen that the spectrum of metarhodopsin II resembles the spectrum of the Schiff base more than that of all-trans retinal. The spectrum of metarhodopsin II contains lines at 971, 1012, 1156, 1169, 1203 and 1233 cm^{-1} in the fingerprint region which are repeated in the Schiff base. Some of these lines appear in the Raman spectrum of all-trans retinal. However, the set of the three lines at 1156, 1169 and 1203 cm^{-1} is characteristic of the all-trans

Figure 21

Resonance Raman spectra of (A) metarhodopsin I vesicles, and (B) all-trans retinal-n-butylamine HCl.

(P.S.B. = protonated Schiff base)

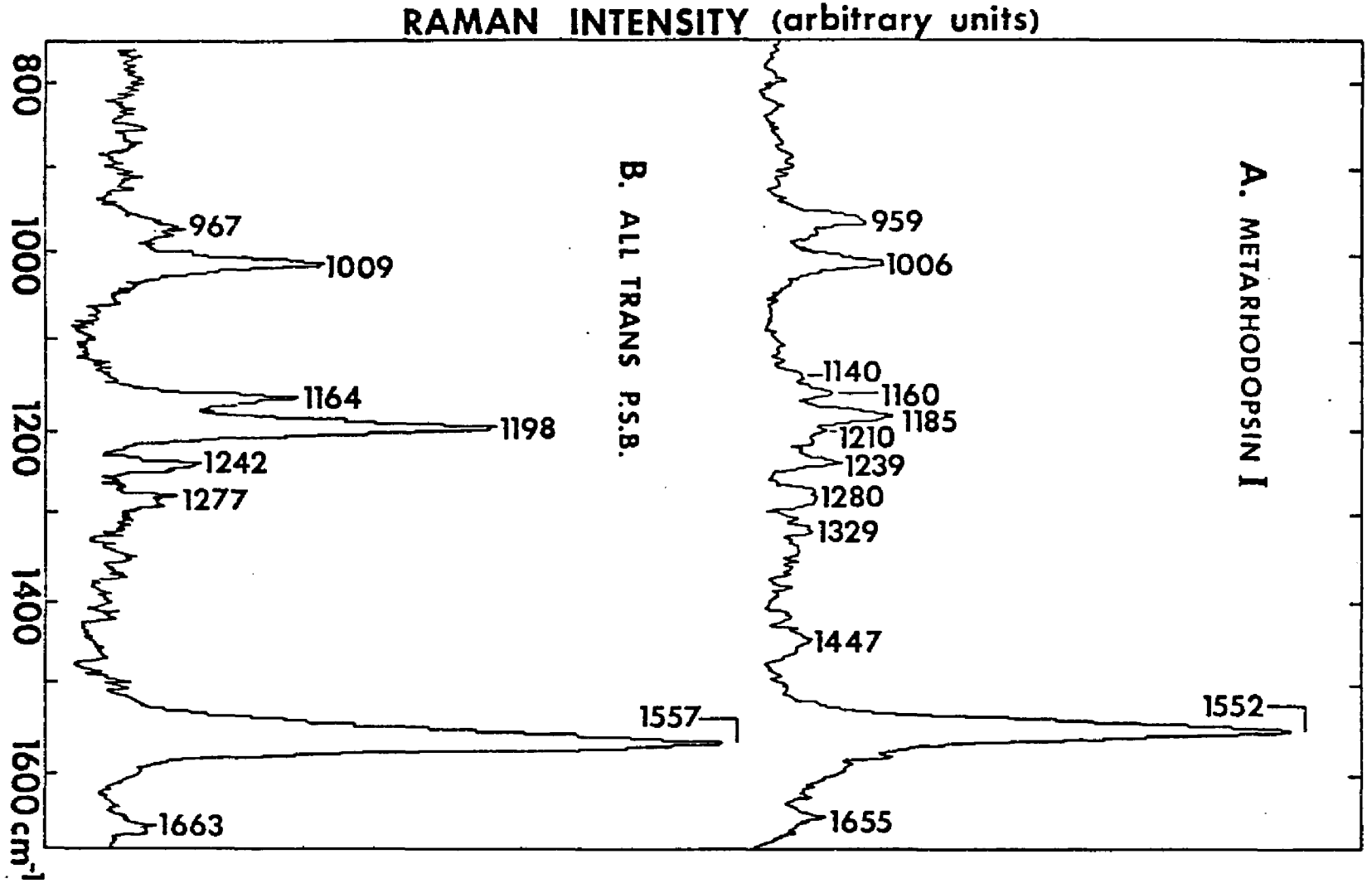
RAMAN INTENSITY (arbitrary units)
800
1000
1200
1400
1600 cm-1
B. ALL TRANS P.S.B.
967
1009
1164
1198
1242
1277
1557
1663
A. METARHODOPSIN I
959
1006
1140
1160
1185
1210
1239
1280
1329
1447
1552
1655

Figure 22

Resonance Raman spectra of (A) metarhodopsin II vesicles, (B) all-trans retinal-n-butylamine, and (C) all-trans retinal.

(S.B. = Schiff base)

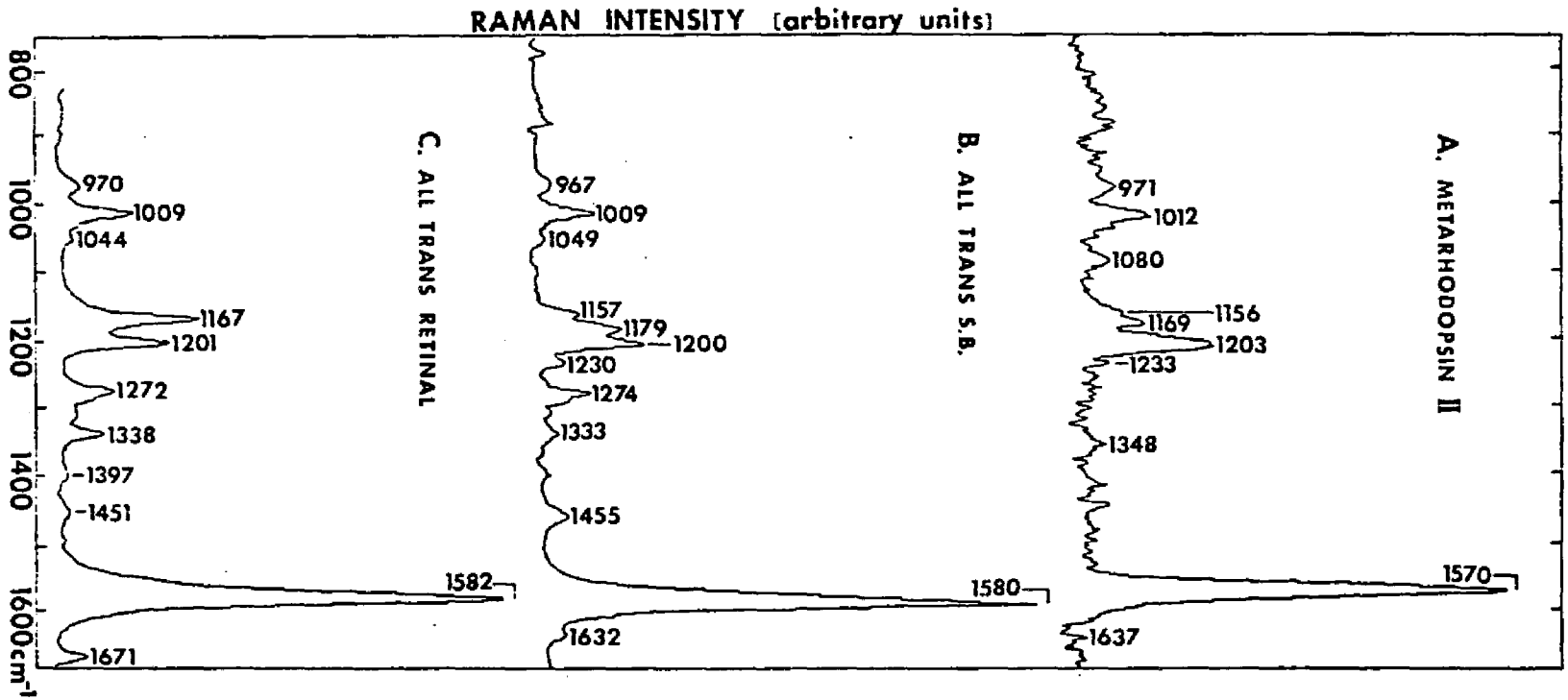
RAMAN INTENSITY (arbitrary units)
800
1000
1200
1400
1600cm⁻¹
C. ALL TRANS RETINAL
970
1009
1044
1167
1201
1272
1338
1397
1451
1582
1671
B. ALL TRANS S.B.
967
1009
1049
1157
1179
1200
1230
1274
1333
1455
1580
1632
A. METARHODOPSIN II
971
1012
1080
1156
1169
1203
1233
1348
1570
1637

Schiff base. In addition, the intensity pattern of the spectrum of metarhodopsin II resembles rather closely that of the all-trans Schiff base. The line at 1080cm^{-1} in the metarhodopsin II spectrum is not repeated in either. In addition, both Schiff base and retinal contain lines that are not found in the spectrum of metarhodopsin II.

Thus, as it appears from the Raman spectra, the conformation of the chromophore in the metarhodopsin I and metarhodopsin II is very similar to that of all-trans protonated and unprotonated Schiff base in solution respectively, The small changes in the line positions and intensities are very likely an indication of some residual chromophore-opsin interactions rather than of differences in the conformation between the pigments and the model compounds. As we have seen before, even small changes in the conformation produce disproportionately large changes in the Raman spectra (compare, for example, all-trans and 13-cis model compound). In conclusion, we can describe both metarhodopsins as having an essential all-trans conformation. Transition of metarhodopsin I to metarhodopsin II, as far as the chromophore is concerned, involves only the deprotonation of the Schiff base. It is also clear that there is unlikely any further retinal conformation changes from metarhodopsin II to final retinal hydrolysis since the chromophore detaches as all-trans retinal.

The 11-cis to all-trans isomerization of the chromophore has been the foundation of the primary photochemical event since the early works of Wald and coworkers (see, for example, Hubbard and Kropf, 1958; Yoshizawa and Wald, 1963; Hubbard et al., 1965; Wald, 1968). The early arguments were based on the photo-

reversibility between rhodopsin, isorhodopsin and bathorhodopsin. However, the Raman studies by Oseroff, Callender (1974) of bathorhodopsin do not support a pure all-trans conformation for the chromophore. The Raman data presented here are the first direct proof that the chromophore has assumed an all-trans conformation at least at the stage of metarhodopsin I. In addition, metarhodopsin I shows photoreversibility between rhodopsin and isorhodopsin. It is not unreasonable, therefore, to argue that since photoreversibility occurs in the transitions rhodopsin (11-cis) $\rightleftarrows$ metarhodopsin I (all-trans) $\rightleftarrows$ isorhodopsin (9-cis) a similar situation exists with metarhodopsin I replaced by bathorhodopsin.

It is appropriate at this point to ask the question as to what drives the thermal reactions in the bleaching sequence of rhodopsin. Photocalorimetry has shown that metarhodopsin I and metarhodopsin II are energetically higher than rhodopsin (Cooper and Converse, 1977). In addition, Rosenfeld et al., (1977a, b) have calculated that bathorhodopsin is at least 12Kcal/mole higher in energy than the ground state of rhodopsin. This energy must have been provided by the absorbed photon. The 11-cis to all-trans activation energy is only a few Kcal/mole (Hubbard, 1966; Kropf and Hubbard, 1970; Honig and Karplus, 1971). The absorbed photon, being of the order of 55 Kcal/mole, could provide sufficient energy to drive the thermal reactions. It is tempting to argue that the mechanism of energy storage lies in the strain of the distortion of the all-trans chromophore in bathorhodopsin. How this affects the conformation of the protein and drives the thermal reactions (e.g. energy transfer to apoprotein with breakage of secondary bonds and/or local melting) is a matter of speculation at this point.

Bacteriorhodopsin

Retinal-Protein Linkage

Figures 23a and 24a show the resonance Raman spectra of the light adapted form of the PM568 and the intermediate M412 of the purple membrane, respectively. For comparison purposes Raman spectra of the protonated and unprotonated Schiff bases of all-trans and 13-cis retinal are included. A comparative study of the spectra of the purple membrane system with those of the model compound can reveal certain chromophore properties of the membrane system.

In agreement with previous resonance Raman experiments of the purple membrane (Lewis et al., 1974; Mendelsohn, 1976) the present Raman data show that the chromophore is linked to the protein via a protonated Schiff base in the case of PM568 and via an unprotonated in the case of M412. Lewis et al., (1974) has demonstrated that the line at 1644 cm^{-1} moves approximately to 1622 cm^{-1} upon deuteration. This change in frequency is predicted from a simple reduced mass calculation (see, for example, Herzberg, 1945) where hydrogen of $C=\overset{+}{N}H$ stretching mode is replaced by deuterion. In addition, he associated the 1644 cm^{-1} line with PM568 and the 1623 cm^{-1} line with M412 by varying the composition of the PM568/M412 in mixtures and by measurements of excitation profile. In the present study, where each species is separately measured, this assignment is confirmed.

The Conformation of the Protein-Bound Chromophore

A comparative study of the Raman spectra of the visual pigments and of the model compounds (especially protonated and unprotonated Schiff bases) has proved

Figure 23

Resonance Raman spectra of (A) PM568 light-adapted purple membrane chromophore, (B) all-trans retinal-n-butylamine HCl, and (C) 13-cis retinal-n-butylamine HCl. The resolution is (A) 7 cm^{-1}, (B) 4 cm^{-1}, and (C) 6 cm^{-1}.

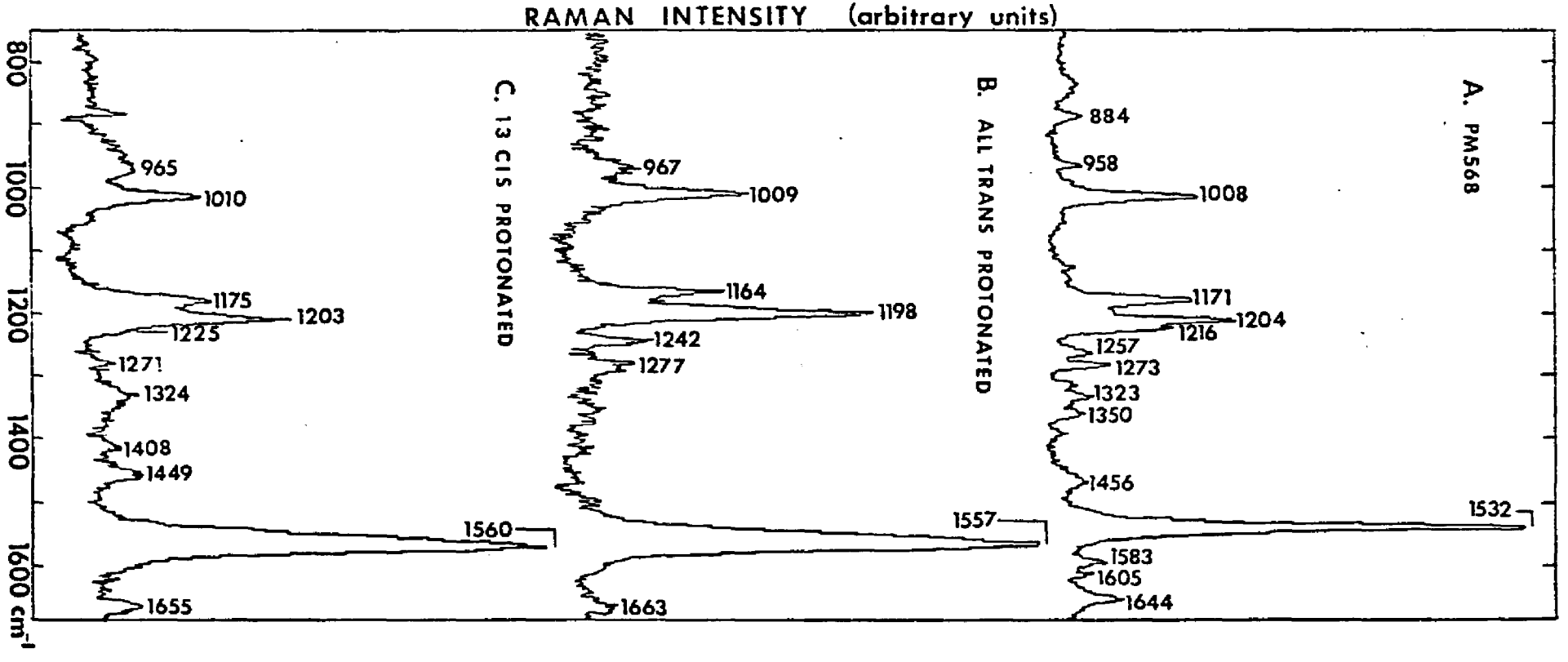
RAMAN INTENSITY (arbitrary units)
800
1000
1200
1400
1600 cm⁻¹
C. 13 CIS PROTONATED
965
1010
1175
1203
1225
1271
1324
1408
1449
1560
1655
B. ALL TRANS PROTONATED
967
1009
1164
1198
1242
1277
1557
1663
A. PM568
884
958
1008
1171
1204
1216
1257
1273
1323
1350
1456
1532
1583
1605
1644

Figure 24

Resonance Raman spectra of (A) M412 light-adapted purple membrane chromophore, (B) all-trans retinal-n-butylamine, and (C) 13-cis retinal-n-butylamine. The resolution is (A) 11 cm^{-1}, (B) 7 cm^{-1}, and (C) 7 cm^{-1}.

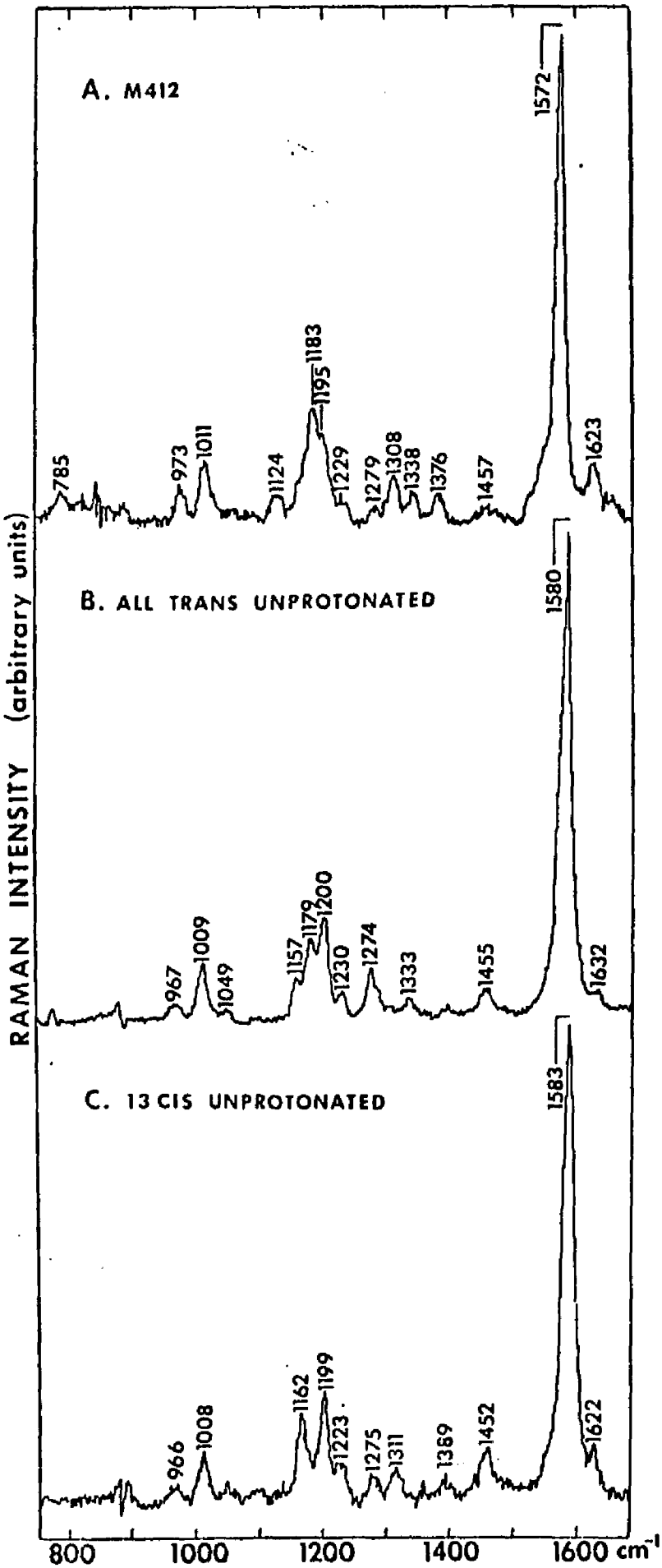
A. M412
785
973
1011
1124
1183
1195
1229
1279
1308
1338
1376
1457
1572
1623
B. ALL TRANS UNPROTONATED
967
1009
1049
1157
1179
1200
1230
1274
1333
1455
1580
1632
C. 13 CIS UNPROTONATED
966
1008
1162
1199
1223
1275
1311
1389
1452
1583
1622
RAMAN INTENSITY (arbitrary units)
800
1000
1200
1400
1600 cm⁻¹

to be very successful so far. This approach has helped to determine the conformation of the chromophore in rhodopsin, isorhodopsin (Mathies et al., 1977), metarhodopsin I and metarhodopsin II. The apparent conformational properties determined by Raman spectra of the chromophore in the purple membrane do not seem to be as clear.

In chemical extraction experiments (see, for example, Pilkiewicz et al., 1977) PM568 has been found to have an all-trans conformation (Pettei et al., 1977). M412, depending on the conditions, yields either 1:1 ratio of all-trans and 13-cis retinal or almost entirely 13-cis retinal (Pettei et al., 1977). It is reasonable, therefore, to compare the Raman spectra of PM568 and M412 to the all-trans and 13-cis Schiff bases protonated and unprotonated, respectively.

The PM568 Raman spectrum when compared with the protonated Raman data of Figure 23 reveals that there is not an exact correspondence with either the all-trans or 13-cis protonated Schiff base. The set of three lines in PM568 at 1171, 1204 and 1216 cm^{-1} corresponds rather closely to a similar set found in 13-cis but not in all-trans protonated Schiff base. In addition, the PM568 spectrum has more structure in the 1250-1400 cm^{-1} region than the protonated all-trans Schiff base spectrum. On the other hand, many of these lines have no correspondence in the 13-cis spectrum either. It should also be pointed out that the PM568 spectrum is quite different from the 11-cis (Figure 15) and 9-cis protonated Schiff base (Mathies et al., 1977). Thus, it appears that the conformation of the protein-bound chromophore of PM568 does not have the conformation of any of the isomers

of retinal protonated Schiff bases found in solution but rather has a conformation that relaxes to all-trans when the chromophore is extracted.

Similar observations apply to the M412 intermediate. The M412 spectrum is not in exact correspondence to either all-trans or 13-cis unprotonated Schiff bases. Overall there seems to be a closer correspondence of the 13-cis unprotonated Schiff base to the M412 spectrum. However, the line at 1183 cm^{-1} in the M412 spectrum is either not present or shifted to 1162 cm^{-1} in the 13-cis model compound. In addition, the M412 spectrum is quite different from the 11-cis Schiff base (Figure 16). From these results, it appears that the conformation of the chromophore of the M412 is closer to 13-cis but, like that of PM568 form, the conformation of the chromophore is not identical to that found in solution.

The role of the bacteriorhodopsin, is to convert the light energy into an electrochemical gradient across the membrane. The molecular mechanism by which it is attained is still a matter of speculation. The fact is that a proton is lost between the PM568 and M412 intermediates. Deuteron exchange studies of bacteriorhodopsin show that the exchange time of the proton of the Schiff base for a deuteron is slow in the dark. In the light, however, it is fast (Stoeckinius, 1975). These observations are consistent with the assumption that the proton of the Schiff base is involved in the establishment of the electrochemical gradient. It need not, however, be tied directly to the proton which is eventually ejected from the cell.

Color Regulation of the Visual-Pigments and Bacteriorhodopsin

Two of the most interesting problems related to the absorption properties of the visual pigments are: (a) the bathochromic shift and (b) the wavelength regulation of the absorption spectra. Retinals in solution absorb near 380nm when they are combined with opsin; the absorption of the formed pigment can be shifted from 50nm to as much as 200nm depending on the origin of the protein. It has already been established that the chromophore is connected to the protein via a protonated Schiff base. Protonation of the retinal Schiff bases induce a bathochromic shift of about 80nm (from 360 to 440nm). This bathochromic shift, however, is not large enough to account for the large shifts that observed in the visual pigments. A variety of mechanisms have been proposed that can induce additional bathochromic shifts (see, for example, Honig et al., 1976).

The regulation of the absorption maxima in the visual pigments and bacteriorhodopsin appears to be through the control of the delocalization of the π electron system. The first excited state is lowered in energy more than the ground state resulting in a bathochromic shift in the absorption maxima (see, for example, Honig and Ebrey, 1974). Electron delocalization also affects the character of the bonds of the polyene chain, decreasing the electron density of the double bonds and increasing the electron density of the single bonds. As a consequence, the frequency of the C=C stretching vibration is lowered. Thus, the position of C=C band is a sensitive indicator of the delocalization of the π electrons (Heyde et al., 1971; Gavin and Rice, 1971).

Small changes of the position of the ethylenic vibrations in the retinal isomers

(Figure 13) are not correlated with their corresponding absorption maxima at (383, 376, 375 and 378nm). This indicates that the differences are not due to the delocalization of π electrons, which is approximately the same for all isomers, but rather to different combination of vibrations making up the normal modes. Changes in the electronic distribution, however, induced by changes in the end group are expected to change the delocalization of the π electrons. This is what we observe in substituting the oxygen of the retinals with the less electronegative nitrogen of the corresponding Schiff base or again in the protonation of the nitrogen. The ethylenic frequencies of the protonated and unprotonated Schiff bases correlate very well with their absorption maxima (Figure 25). In addition, delocalization of the electrons can be directly observed in the effect of the bond alternation it causes. X-ray studies of all-trans retinal and its unprotonated and protonated Schiff base (Hamanaka et al., 1972; Mitsui and Hamanaka, 1975) show a significant change of the bond alternation especially between the unprotonated and protonated Schiff base.

Absorption studies on model compounds, mostly protonated Schiff bases, have shown that their absorption maxima depend on the environment of the molecule (Erikson and Blatz, 1968; Irving et al., 1970; Blatz et al., 1972; Blatz, 1972; Blatz and Mohler, 1972). In addition, theoretical calculation has shown that negative or positive charges placed in appropriate positions in the proximity of the chromophore can induce significant wavelength shifts (Wiesenfeld and Abrahamson, 1968; Waleh and Ingraham, 1973; Suzuki et al., 1974; Honig et al., 1976). In fact any mechanism that increases delocalization should induce

Figure 25

Correlation of ethylenic (C = C) stretching frequency of retinal based structures with the absorption maxima (see text). P.S.B. = protonated Schiff base, S.B. = Schiff base. ▲ visual pigments, ● model compounds.

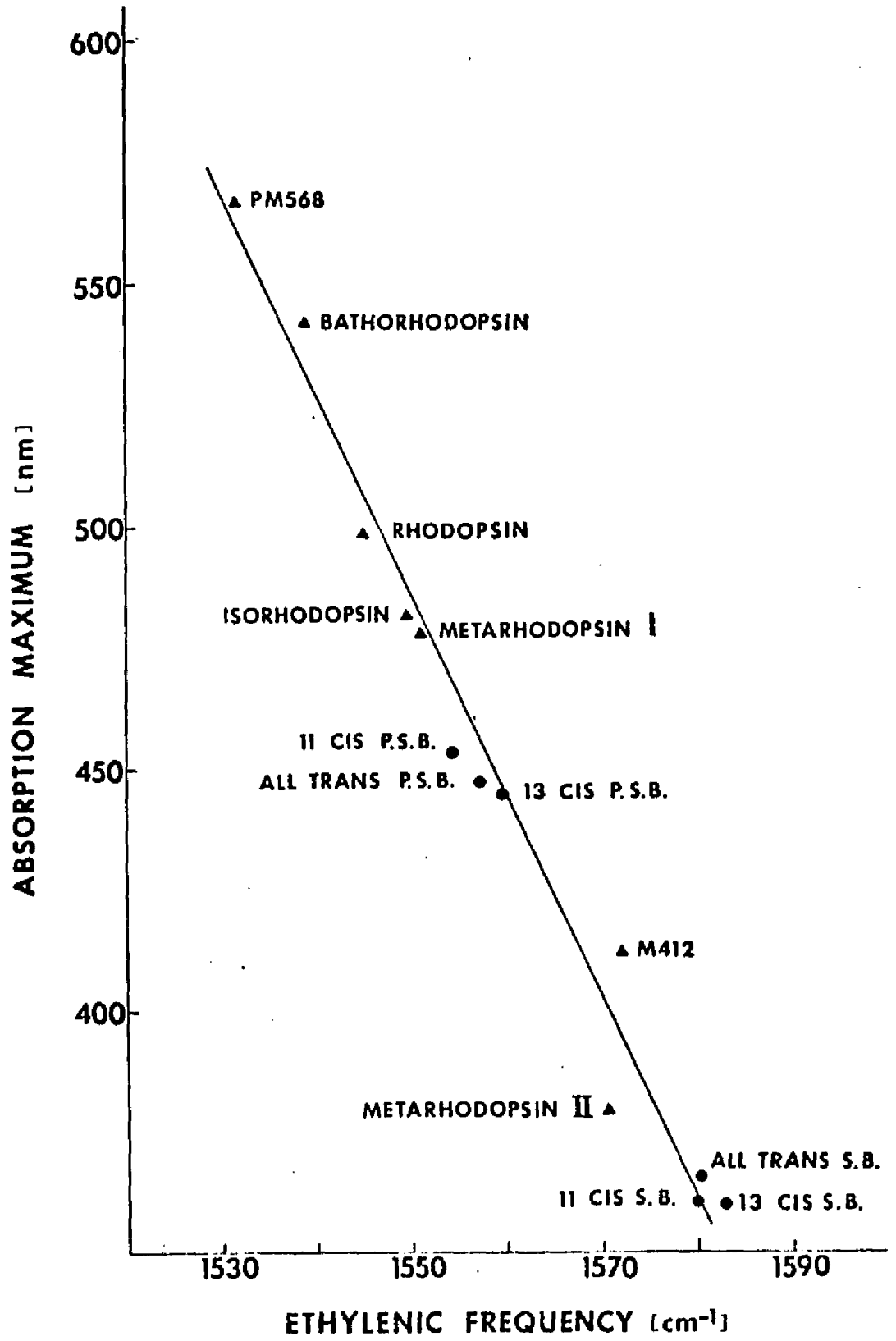
600
550
500
450
400
ABSORPTION MAXIMUM [nm]
PM568
BATHORHODOPSIN
RHODOPSIN
ISORHODOPSIN
METARHODOPSIN I
11 CIS P.S.B.
ALL TRANS P.S.B.
13 CIS P.S.B.
M412
METARHODOPSIN II
ALL TRANS S.B.
11 CIS S.B.
13 CIS S.B.
1530
1550
1570
1590
ETHYLENIC FREQUENCY [cm⁻¹]

bathochromic shifts in the absorption maxima. Thus, the protein by controlling the micro-environment of the chromophore in the opsin matrix, can regulate the absorption spectra of the pigments.

Figure 25 shows the correlation between the absorption maxima and the ethylenic frequencies for the protonated and unprotonated Schiff bases, rhodopsin, the metarhodopsins, PM568 and M412 pigments. Isorhodopsin and bathorhodopsin as reported by Oseroff and Callender (1974) have also been included. They all fall pretty much along a straight line. Especially interesting is the fact that both the model compounds and the pigments as groups follow the same correlation pattern. This observation contradicts an alternative model of wavelength regulation in visual pigment and purple membrane system, namely twisting about double bonds (Kakitani and Kakitani, 1975). The effect of the double bond twist would be a bathochromic shift in the absorption maxima by raising the energy of the ground state. In addition, it should cause a significant decrease in bond order and consequently large lowering of the ethylenic frequency. The model compound data, however, arise from presumably strain free chromophores, as they are in solution. In addition, as we have previously discussed, the Raman spectra (fingerprint region) of the visual pigments and the purple membrane system indicate that, with the exception of bathorhodopsin (Oseroff and Callender, 1974), there is very little strain if any of the chromophore in the opsin matrix. Thus, the high degree of correlation of the model compounds and pigments, imply that mechanisms of electron delocalization is the main contributor in determining the color of the pigments.

A second conclusion is that the major source of wavelength shift in the metarhodopsin I to metarhodopsin II transition is the deprotonation of the Schiff base (Figures 21, 22). The same conclusion can be drawn for the PM568 to M412 transition (Figures 23, 24). It was the correlation between the absorption spectra of metarhodopsins and those of the Schiff bases, in the first place, that led to the speculation of the deprotonation of the Schiff base in this transition (Pitt et al., 1955; Matthews et al., 1963). The present Raman data confirm and prove this speculation by (a) demonstrating directly that there is a deprotonation and (b) measuring the degree of the electron delocalization of the ground state through the ethylenic mode frequency.

Summary

In conclusion, this work has been concerned with the development of a new technique that allows Raman measurements of photosensitive material. The resonance Raman spectra of rhodopsin, metarhodopsin I, metarhodopsin II, PM568 and M412 have been obtained in pure form. These spectra have been analyzed in terms of model compounds such as retinals protonated and unprotonated Schiff bases also obtained through the new technique. The analysis indicates that the chromophore in metarhodopsin I and metarhodopsin II assumes an essentially all-trans conformation. The main difference between the two forms as it concerns the chromophore lies in the deprotonation of the Schiff base in the metarhodopsin I to metarhodopsin II transition. An earlier finding that the conformation of the chromophore in rhodopsin is similar to that of 11-cis protonated Schiff base in solution has been confirmed.

The resonance Raman study of purple membrane system (PM568 and M412) contradicts earlier chemical-extraction experiments. The conformation of the chromophore in the two forms as indicated by the Raman spectra, does not resemble any of the proposed models. However, the deprotonation of the Schiff base in the PM568 to M412 transition has been confirmed. Finally, the mechanism by which the visual pigments and purple membrane system regulate their color has been studied. It has been confirmed that this regulation is achieved by delocalization of the π electrons of the chromophore. This explanation has also been extended to include metarhodopsin I and metarhodopsin II.

In bringing this work to conclusion we hope we have demonstrated that resonance Raman spectroscopy can be a useful tool in probing complex biological molecules and processes.

Appendix

The molecular flow technique can be characterized by two parameters. (a) The probability that a molecule will isomerize in the laser beam, (b) the fraction of the total sample photoisomerized. These two parameters were introduced in the experimental section. In what follows we present a detailed account of the derivation of them (Callender et al., 1976). Figure 26 shows the experimental configuration for this calculation. Assume the flow direction is parallel to the z axis, and the laser light parallel to the x axis. We assume the laser beam intensity profile is Gaussian. The beam flux in the yz plane then can be written as:

$$F(\bar{r}) = \frac{I_o}{\pi r_o^2} \exp-\left(\frac{y^2 + z^2}{r_o^2}\right) \tag{20}$$

where r_0 is the distance of 1/e points of the laser beam and can be taken to be the beam radius. A molecule will begin its transit along the z axis far from the beam center with a constant value of the y and constant bulk velocity U_b, so that $z = U_b t$. The probability of photoisomerization can be given as a function of time:

$$P(y,t) = \sigma_A \psi \int_{-\infty}^{t} \left[\frac{I_o}{\pi r_o^2} \exp-\left(\frac{y^2 + U_b^2 t'^2}{r_o^2}\right)\right] dt' \tag{21}$$

Figure 26

A schematic representation of the molecular flow experimental arrangement. The capillary tube is cylindrical with a radius of R. The arrows point along the direction of the molecular flow. Y axis points toward the spectrophotometer.

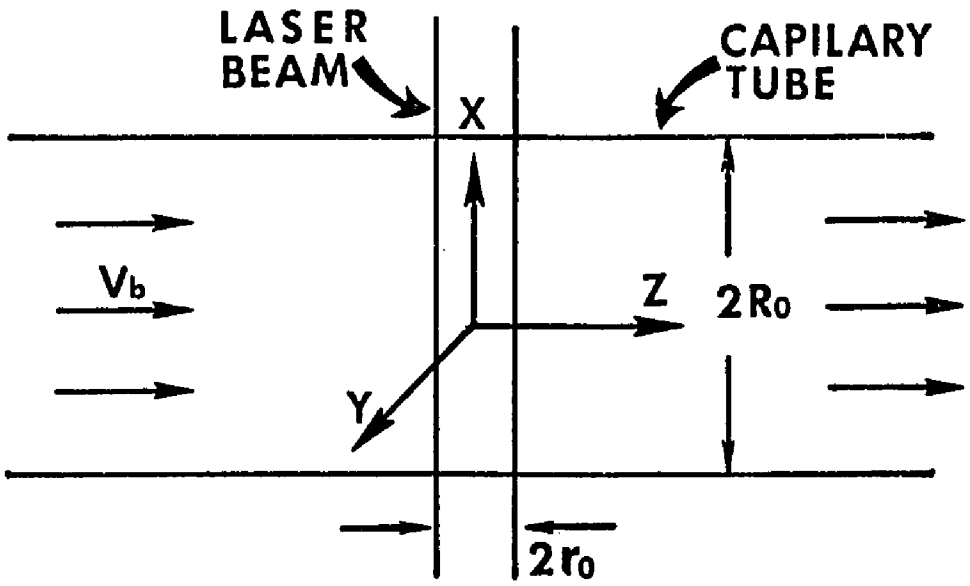
LASER
BEAM
CAPILARY
TUBE
X
Vb
Z
2Ro
Y
2ro

By extending the integral to infinity and taking $y = 0$ we obtain:

$$P_m = \frac{1}{\sqrt{\pi}} \frac{I_o \sigma_A \Psi}{U_b r_o} \tag{22}$$

This is identical with Equation 17, the probability of photoisomerization of a molecule during a single transit through the center of the laser beam.

So far, we have ignored any variation in the molecular flow velocities. It is well known, however, that the velocity profile for pipe flow is not uniform. The type of the flow velocity profile is categorized by the Reynold's number (Landau and Lifshitz, 1959).

$$K = \frac{2 \rho U_b R_o}{\eta} \tag{23}$$

where ρ and η are, respectively, the fluid density and viscosity and R_o is the radius of the pipe. For $K < 2000$, the fluid flow is said to be lamiiar and the velocity profile along the x axis is given by:

$$U(x) = \frac{2U_b}{R_o^2} \left(R_o^2 - x^2 \right) \tag{24}$$

For $K > 3000$, the fluid is turbulent, and the velocity profile, while not precisely known, is more uniform and equal to U_b across the pipe (Tennekes and Lumley, 1972). These divisions are, however, somewhat arbitrary and the pre-

cise experimental conditions influence the point of onset and degree of turbulence. We can estimate the influence of the non-uniform flow velocity by considering lamilar flow since this represents the worst possible case. It is clear that in this case, P_m is a function of x, and the probability of photoisomerization increases as we consider molecules travelling close to the wall of capillary tube. In fact, the flow velocity is zero next to the pipe wall making the probability of photoisomerization equal to unity. In what follows we approach the problem of photoisomerization in a more general way. We calculate the Raman scattering from photoisomerized sample, S', compared with that of the non-photoisomerized sample, S.

The number of Raman events, S, detected at the photomultiplier per second, of a particular species with a concentration $C(\bar{r})$ and Raman cross section σ_R is given by:

$$S = \sigma_R \Omega_o e_r \int F(\bar{r})\, C(\bar{r})\, dV \qquad (25)$$

where Ω_o the solid angle subtended by the collecting lens of the apparatus and e_r the total efficiency of the Raman apparatus. We consider that the system is composed of two species, photoisomerized and non-photoisomerized material with a total concentration of C_o. The probability of photoisomerization is given by Equation 21 as long as it is less than one. Otherwise, it is one. We explicitly discount, here, the possibility of multiple photon absorptions. Once

a molecule photoisomerizes, it is considered to give rise to spurious Raman scattering in our calculations.

It is convenient to rewrite Equation 21 in terms of the molecular position on the zy plane. Substituting Equation 22 in 21 we obtain:

$$P(y,z) = P_m \frac{1}{\sqrt{\pi}\, r_o} \int_{-\infty}^{z/v_b} \exp - \left(\frac{y^2 + z'^2}{r_o^2} \right) dz' \qquad (26)$$

where it is understood that P(y, z) is given by Equation 26 or unity, whichever is less. In this case, the concentration of the non-photoisomerized species $C(\bar{r}) = C_o \left[1 - P(y,z) \right]$. Substituting the concentration into Equation 25 performing the integrals and assuming uniform flow velocity and that P(y, z) is always much less than one (so that $C(\bar{r}) \approx C_o$) we find that:

$$\frac{S'}{S} = \frac{\sigma_R'}{\sigma_R} \frac{P_m}{\sqrt{8}} \qquad (27)$$

The contribution of the flow velocity profile on S'/S can be calculated as follows. Since the laser beam is very narrow in the zy plane, the velocity in this plane can be considered as constant. Thus, in evaluating Equation 21, the influence of the non-uniform flow is contained in performing the integral in the direction along the laser beam (x axis). The x dependence is then contained in the concentrations, $C(\bar{r})$ and $C'(\bar{r})$, since P(y, z) is now dependent on the x coordinate through P_m. P_m is a function of x by substituting the velocity profile (Equation

24) into Equation 22. Remembering that P(x,y,z) never exceeds one, the integrals (Equation 25) can be performed exactly. In the case where P_m evaluated using (uniform flow) is much less than one, a simple approximate form for S'/S can be derived.

$$\frac{S'}{S} = \frac{\sigma_R'}{\sigma_R} \frac{P_m}{\sqrt{8}} \left[\frac{1}{4} \left(\ln \frac{8}{P_m} + 1 \right) \right] \tag{28}$$

The effect of non-uniform flow is not very significant. For example, assuming $P_m = .14$ and $\sigma_R' / \sigma_R = 1$, we obtain S'/S = .05 for uniform flow and .06 for lamilar flow.

The fraction of the total sample photoisomerized can be derived in the following way. If A is the absorbance of the sample in the capillary tube, the $I_o(1-10^{-A})$ represents the total number of photons that are absorbed by the sample. The number of molecules photoisomerized is given by $I_o(1-10^{-A})\,\psi$ with the possibility of multiple absorptions being explicitly discounted. The fraction of the total sample photoisomerized is given by:

$$\bar{P} = \frac{I_o [1 - 10^{-A}] T \psi}{C_o V} \tag{29}$$

where T is the time of Raman measurement.

Bibliography

Abrahamson, E.W. (1973)
The Kinetics of Early Intermediate Processes in the Photolysis of Visual Pigments.
In "Biochemistry and Physiology of Visual Pigments" p. 47
Helmut Langer Ed. Springer-Verlag, N.Y., Heidelberg, Berlin

Abrahamson, E.W. & Ostroy, S.E. (1967)
The Photochemical and Macromolecular Aspects of Vision
Prog. Biophys, & Mol. Biol. 17, 181

Abrahamson, E.W. & Fager, R. S. (1973)
The Chemistry of Vertebrate and Invertebrate Visual Photoreceptors
Curr. Top. Bioenerg. 5, 125

Adar, F. & Erecinska, M. (1974)
Resonance Raman Spectra of the b - and c - Type Cytochromes of Succinate-Cytochrome c Reductase
Arch. Biochem. Biophys. 165, 570

Albrecht, A.C. (1961)
On the Theory of Raman Intensities
J. Chem. Phys. 34, 1476

Albrecht, A.C., & Hurtley, M.C. (1971)
On the Dependence of Vibrational Raman Intensity on the Wavelength of Incident Light
J. Chem. Phys. 55, 4438

Aton, B., Doukas, A.G., Callender, R.H., Becher, B., & Ebrey, T.G. (1977)
Resonance Raman Studies of the Purple Membrane
Biochem. in press

Becher, B., & Cassim, J.Y. (1975)
Improved Isolation Procedures for the Purple Membrane Protein of Halobacterium Halobium
Prep. Biochem. 5, 161

Becher, B., & Ebrey, T.G. (1977)
The Quantum Efficiency for the Photochemical Conversion of the Purple Membrane
Biophys. J. 17, 185

Becker, R.S., Berger, S., Dalling, D.K., Grant, D.M., & Pugmire, R.J. (1974)
Carbon-13 Magnetic Resonance Investigation of Retinal Isomers and Related Compounds
J. Am. Chem. Soc. 96, 7008

Blasie, J.K., Dewey, M.M., Blaurock, A.E., & Worthington, C.R. (1965)
Electron Microscope and Low Angle X-ray Diffraction Studies on Outer Segment Membranes from the Retina of the Frog
J. Mol. Biol. 14, 143

Blasie, J.K., & Worthington, C.R. (1969)
Planar Liquid-Like Arrangement of Photopigment Molecules in Frog Retinal Receptor Disk Membranes
J. Mol. Biol. 39, 417

Blatz, P.E. (1972)
The Formation of Long Wavelength Absorbing Species from Short Wavelength Absorbing Linear Conjugated Polyenes
Photochem. Photobiol. 15, 1

Blatz, P.E., Pippert, D.L., & Balasubramaniyan, V. (1968)
Absorption Maxima of Cations Related to Retinal and Their Implication to Mechanisms for Bathochromic Shift in Visual Pigment
Photochem. Photobiol. 8, 309

Blatz, P.E., Lin, M., Balasubramaniyan, P., Balasubramaniyan, V., & Dewhurst, P. (1969)
A New Series of Synthetic Visual Pigments from Cattle Opsin and Homologs of Retinal
J. Am. Chem. Soc. 91, 5930

Blatz, P.E., & Mohler, J.H. (1972)
Effect of Selected Hydrogen-Bonding Solvents on the Absorption Maxima of N-Retinylidene-N-Butylamonium Salts
Biochem. 11, 3240

Blatz , P.E., Mohler, J.H., & Navangul, H.V. (1972)
Anion Induced Wavelength Regulation of Absorption Maxima of Schiff Bases of Retinal
Biochem. 11, 848

Blaurock, A.E. (1975)
Bacteriorhodopsin: A Trans-Membrane Pump Containing α-Helix
J. Mol. Biol. 93, 139

Blaurock, A.E., & Stoeckinius, W. (1971)
Structure of the Purple Membrane
Nature (New Biol.) 233, 152

Blaurock, A.E., & Wilkins, M.H.F. (1969)
Structure of Frog Photoreceptor Membranes
Nature (London) 223, 906

Bonting, S.L. (1969)
Mechanism of Visual Processes
Curr. Top. Bioenerg. 3, 351

Bownds, D., & Wald, G. (1965)
Reaction of the Rhodopsin Chromophore with Sodium Borohydride
Nature (London) 205, 254

Bridges, C.D.B. (1970)
Biochemistry of Vision. In "Biochemistry of the Eye" p. 563-644
Graymore ed. Academic Press, London, N.Y.

Brown, P.K. (1972)
Rhodopsin Rotates in the Visual Receptor Membrane
Nature (New Biol.) 236, 35

Brown, T.K., & Murakami, M. (1964)
A New Receptor Potential of the Monkey Retina with No Detactable Latency
Nature (London) 201, 626

Brown, T.K., Watanabe, K , & Muracami, M. (1965)
The Early and Late Potential of Monkey Cones and Rods
Cold Spring Harbor Symposia on Quantitave Biology 30, 457

Brunner, H., Mayer, A., & Sussner, H. (1972)
Resonance Raman Scattering on the Haem Group of Oxy - and - Deoxyhaemoglobin
J. Mol. Biol. 70, 153

Brunner, H. (1973)
Resonance Raman Scattering on the Haem Group of Cytochrome
Biochem. Biophys. Res. Comm. 51, 888

Busch, G.E., Applenbury, M.L., Lamola, A.A., & Rentzepis, P.M. (1972)
Formation and Decay of Prelumirhodopsin at Room Temperatures
Proc. Natl. Acad. Scie. (USA) 69, 2802

Callender, R.H., Doukas, A., Crouch, R., & Nakanishi, K. (1976)
Molecular Flow Resonance Raman Effect from Retinal and Rhodopsin
Biochem. 15, 1621

Callender, R.H., & Honig, B. (1977)
Resonance Raman Studies of Visual Pigment
Ann. Rev. Biophys. & Bioeng. 6, 33

Chadwick, C.S., Johnson, P., & Richards, E.G. (1960)
Depolarization of the Fluorescence of Proteins Labelled with Various Fluorescence Dyes
Nature (London) 186, 239

Chan, W.K., Nakanishi, K., Ebrey, T.G., & Honig, B. (1974)
Properties of 14-Methylretinal, 13 Desmethyl-14-Methylretinal and Visual Pigments Formed Therefrom
J. Am. Chem. Soc. 96, 3642

Collins, D.W., Fitchen, D.B., & Lewis, A. (1973)
Resonant Raman Scattering from Cytochrome c Frequency Dependence of the Depolarization Ratio
J. Chem. Phys. 59, 5714

Cone, R.A. (1972)
Rotational Diffusion of Rhodopsin in the Visual Receptor Membrane
Nature (New Biol.) 236, 39

Cookingham, R.E., Lewis, A., & Kropf, A. (1977)
Resonance Raman Spectroscopy of Chemically Modified Retinals: Assigning the Carbon-Methyl Vibrations in the Resonance Raman Spectrum of Rhodopsin
Abstracts. 21st annual meeting of the Biophysical Society

Cooper, A., & Converse, C.A. (1976)
Energetics of Primary Processes in Visual Excitation: Photocalorimetry of Rhodopsin in Rod Outer Segment Membranes
Biochem. 15, 2790

Corless, J.M. (1972)
Lamilar Structure of Bleached and Unbleached Rod Photoreceptor Membranes
Nature (London) 237, 229

Crouch, R., Purvin, P., Nakanishi, K., & Ebrey, T.G. (1975)
Isorhodopsin II. Artificial Photosensitive Pigment Formed from 9, 13-dicis Retinal
Proc. Natl. Acad. Sci. (USA) 72, 1538

Daemen, F.J.M. (1973)
Vertebrate Rod Outer Segment Membranes
Biochem. Biophys. Acta 300, 255

Daemen, F., Rotmans, J., & Bonting, S. (1974)
On the Rhodopsin Cycle
Expl. Eye Res. 18, 97

Danon, A., & Stoeckinius, W. (1974)
Phosphorylation in Halobacterium Halobium
Proc. Natl. Acad. Sci. (USA) 71, 1234

Dartnall, H. (1972)
Handbook of Sensory Physiology. Vol. VII/1. Chapter 4: Photosensitivity
H. Dartnall ed. Springer-Verlag. Berlin, Heidelberg, N.Y.

DeGrip, W.J., Bonting, S.L., & Daemen, F.J.M. (1973)
The Binding Site of Retinaldehyde in Native Rhodopsin. In "Biochemistry and Physiology of Visual Pigments" p. 29
Helmut Langer ed. Springer, Verlag, N.Y., Heidelberg, Berlin

Dowling, J.E. (1960)
Chemistry of Visual Adaptation in the Rat
Nature (London) 188, 114

Ebrey, T.G. (1971)
Energy Transfer in Rhodopsin, N-Retinyl-Opsin and Rod Outer Segments
Proc. Natl. Acad. Sci, (USA) 68, 713

Ebrey, T.G., & Honig, B. (1972)
Ultraviolet Chromophore Transitions in the Rhodopsin Spectrum
Proc. Natl. Acad. Sci. (USA) 69, 1897

Ebrey, T.G., & Honig, B. (1975)
Molecular Aspects of Photoreceptor Function
Q. Rev. Biophys. 8, 124

Ebrey, T., Govindgee, B., Honig, B., Pollock, E., Chan, W., Crouch, R., Yudd, A., & Nakanishi, K. (1975)
Properties of Several Sterically Modified Retinal Analogs and their Photosensitive Pigments
Biochem. 14, 3933

Eisenger, J., & Dale, R. (1974)
Interpretation of Intramolecular Energy Transfer Experiments
J. Mol. Biol. 84, 643

Erickson, J.O., & Blatz, P.E. (1968)
N-Retinyledene-1-Amino-2-Propanol a Schiff Base Analog for Rhodopsin
Vision Res. 8, 1367

Fager, R.S , Sejnowski, P., & Abrahamson, E.W. (1972)
Aqueous Cyanohydridoborate Reduction of the Rhodopsin Chromophore
Biochem. Biophys. Res. Comm. 47, 1244

Fenstermacher, P.R., & Callender, R.H. (1974)
Resonant Raman Effect of I_2 Dissolved in Solution
Optics Comm. 10, 181

Gavin, Jr. R.M., & Rice, S.A. (1971)
Correlation of Pi-Electron Density with Vibrational Frequencies of Linear Polyenes
J. Chem. Phys. 55, 2675

Gill, D., Heyde, M.E., & Rinal, L. (1971)
Raman Spectrum of the 11-cis Isomer of Retinaldehyde
J. Am. Chem. Soc. 93, 6288

Giraldi, R., Karle, I.L., & Karle, J. (1971)
Crystal Structure of the Visual Chromophores, 11-cis and All-trans Retinals
Nature (London) 232, 187

Giraldi, R.D., Karle, I.L., & Karle, J. (1972)
The Crystal and Molecular Structure of 11-cis Retinal
Acta Cryst. B28, 2605

Goldstein, E.B. (1967)
Early Receptor Potential of the Isolated Frog Retina
Vision Res. 7, 837

Hagins, W.A. (1972)
The Visual Process: Excitatory Mechanisms in the Primary Receptor Cells
Ann. Rev. Biophys. & Bioeng. 1, 131

Hamanaka, T., Mitsui, T., Ashida, T., & Kakudo, M. (1972)
The Crystal Structure of All-trans Retinal
Acata Cryst. B28, 214

Hecht, S., Shlaer, S., & Pirenne, M.H. (1942)
Energy Quanta and Vision
J. Gen. Physiol. 25, 819

Heller, J., & Lawrence, M.A. (1970)
Structure of the Glycopeptide from Bovine Visual Pigment 500
Biochem. 9, 864

Henderson, R. (1975)
The Structure of the Purple Membrane from Halobacterium Halobium. Analysis of the X-ray Diffraction Pattern
J. Mol. Biol. 93, 123

Henderson, R., & Unwin, P.N.T. (1975)
Three Dimensional Model of Purple Membrane Obtained by Electron Microscopy
Nature (London) 257, 28

Henderson, R. (1977)
The Purple Membrane from Halobacterium Halobium
Ann. Rev. Biophys. Bioeng. 6, 87

Herzberg, G. (1945)
Infrared and Raman Spectra of Polyatomic Molecules. p. 227
Van Nostrand Reinhold Company, N.Y.

Heyde, M.E., Gill, D., Kilponen, R.G., & Rinal, L. (1971)
Raman Spectra of Schiff Bases of Retinal (Models of Visual Photoreceptors)
J. Am. Chem. Soc. 93, 6776

Hong, K., & Hubbel, W. (1973)
Lipid Requirements of Rhodopsin Regeneration
Biochem. 12, 4517

Honig, B., & Karplus, M. (1971)
Implications of Torsional Potential of Retinal Isomers for Visual Excitation
Nature (London) 229, 558
Erratum 231, 67

Honig, B., Hudson, B., Sykes, B.D., & Karplus, M. (1971)
Ring Orientation in β-Ionone and Retinals
Proc. Natl. Acad. Sci. (USA) 68, 1289

Honig, B., & Ebrey, T.G. (1974)
The Structure and Spectra of the Chromophore of the Visual Pigments
Ann. Rev. Biophys. & Bioeng. 3, 151

Honig, B., & Ebrey, T.G. (1976)
The Storage of Light Energy in the Bathoproduct of Rhodopsin
Abstracts. 20th Annual Meeting of the Biophysical Society

Honig, B., Greenberg, A.D., Dimur, U., & Ebrey, T.G. (1976)
Visual Pigment Spectra: Implications of the Retinal Schiff Base
Biochem. 15, 4593

Hubbard, R. (1954)
The Molecular Weight of Rhodopsin and the Nature of the Rhodopsin Digitonin Complex
J. Gen. Physiol. 37, 381

Hubbard, R. (1966)
The Stereoisomerization of 11-cis Retinal
J. Biol. Chem. 241, 1814

Hubbard, R., & Kropf, A. (1958)
The Action of Light on Rhodopsin
Proc. Natl. Acad. Sci. (USA) 44, 130

Hubbard, R., Brown, P.K., & Kropf, A. (1959)
Action of Light on Visual Pigments
Nature (London) 183, 442

Hubbard, R., Bownds, D., & Yoshizawa, T. (1965)
The Chemistry of Visual Photoreception
Cold Spring Harbor Symposia on Quantitative Biology 30, 301

Hubbard, R., Brown, P.K., & Bownds, D. (1971)
Methodology of Vitamin A and Visual Pigments. In "Methods in Enzymology"
V. 18 Vitamins and Coenzymes, Part C p. 615
McCormick and Wright eds. Academic Press, N.Y.

Inagaki, F., Tasumi, M., & Miyazawa, T. (1974)
Excitation Profile of the Resonance Raman Effect of β-Carotene
J. Mol. Spectr. 50, 286

Irving, C.S., Byers, G.W., & Leermakers, P.A. (1970)
Spectroscopic Model of the Visual Pigments.
Influence of the Microenvironmental Polarizability
Biochem. 9, 858

Johnson, B.B., & Peticolas, W.L. (1976)
The Resonant Raman Effect
Ann. Rev. Phys. Chem. 27, 465

Kakitani, T. (1974)
Theoretical Study of Optical Absorption Curves of Molecules. III
Prog. Theor. Phys. 51, 656

Kakitani, T., & Kakitani, H. (1975)
Molecular Mechanism for the Initial Process of Visual Excitation, I.
Model of Photoisomerization in Rhodopsin and its Theoretical Basis by Quantum
Mechanical Calculation of Adiabatic Potential
J. Phys. Soc. (Japan) 38, 1455

Kaufman, K.J., Rentzepis, P.M., Stoeckinius, W. & Lewis, A. (1976)
Primary Photochemical Processes in Bacteriorhodopsin
Biochem. Biophys. Res. Comm. 68, 1109

Kropf, A., Brown, P.K., & Hubbard, R. (1959)
Lumi-and Meta-Rhodopsins of Squid and Octopus
Nature (London) 183, 446

Kropf, A., & Hubbard, R. (1970)
The Photoisomerization of Retinal
Photochem. Photobiol. 12, 249

Landau, L.D., & Lifshitz, E.M. (1959)
Fluid Mechanics. Chapter 2. Pergamon Press, London

Lewin, D.R., & Thomson, J.N. (1967)
Light-Sensitive Pigments Formed from Retinaldehyde Epoxides
Biochem. J. 103, 36P

Lewis, A., Fager, R.S., & Abrahamson, E.W. (1973)
Tunable Laser Resonance Raman Spectroscopy of the Visual Process:
I. The Spectrum of Rhodopsin
J. Raman Spectr. 1, 145

Lewis, A., Spoonhower, J., Bogomolni, R.A., Lozier, R.H., & Stoeckinius, W. (1974)
Tunable Laser Resonance Raman Spectroscopy of Bacteriorhodopsin
Proc. Natl. Acad. Sci. (USA) 71, 4462

Lifson, S., & Warsel, A. (1968)
Consistent Force Fields for Calculations of Vibrational Spectra and Enthalpies
of Cycloalkane and N-Alkane Molecules
J. Chem. Phys. 49, 5116

Lozier, R.H., Bogomolni, R.A., & Stoeckinius, W. (1975)
Bacteriorhodopsin: a Light Driven Pump in Halobacterium Halobium
Biophys. J. 15, 955

Lunde, K., & Zeichmeister, L. (1955)
Infrared Spectra and Cis-Trans Configurations of Some Carotenoid Pigments
J. Am. Chem. Soc. 77, 1647

Lutz, M. & Breton, J. (1973)
Chlorophyl Associations in the Chloroplast. Resonance Raman Spectroscopy
Biochem. Biophys. Res. Comm. 53, 413

Mason, W.T., Fager, R.S., & Abrahamson, E.W. (1974)
Ion Fluxes in Disk Membranes of Retinal Rod Outer Segment
Nature (London) 247, 562

Mathies, R., Oseroff, A.R., & Stryer, L. (1976)
Rapid-Flow Resonance Raman Spectroscopy of Photolabile Molecules:
Rhodopsin and Isorhodopsin
Proc. Natl. Acad. Sci. (USA) 73, 1

Mathies, R., Freedman, T.B., & Stryer, L. (1977)
Resonance Raman Studies of the Conformation of Retinal in Rhodopsin and Isorhodopsin
J. Mol. Biol. 109, 367

Matthews, R.G., Hubbard, R., & Brown, P.K. (1963)
Tautomeric Forms of Metarhodopsins
J. Gen. Physiol. 47, 213

Mendelsohn, R., Verna, A.L., Bernstein, H.J., & Kates, M. (1974)
Structural Studies of Bacteriorhodopsin from Halobacterium Cutirubrum by Resonance Raman Spectroscopy
Can. J. Biochem. 52, 774

Mendelsohn, R. (1976)
Thermal Denaturation and Photochemistry of Bacteriorhodopsin from Halobacterium Cutirubrum as Monitored by Resonance Raman Spectroscopy
Biochem. Biophys. Acta 427, 295

Mingardi, M., & Siebrand, W. (1973)
Vibrational Structure of Resonance Raman Spectra
Chem. Phys. Letts. 23, 1

Mingardi, M., & Siebrand, W. (1974)
Generalizations of Raman Intensity Expressions as to Include Resonance
Chem. Phys. Letts. 24, 492

Mingardi, M., & Siebrand, W. (1975)
Theory of Resonance Raman Scattering. An Improved Formulation of the Vibronic Expansion Method
J. Chem. Phys. 62, 1074

Mitchell, P. (1972)
Chemiosmotic Coupling in Energy Transduction: A Logical Development of Biochemical Knowledge
J. Bioenerg. 3, 5

Mitsui, T., & Hamanaka, T. (1975)
Structures of All-Trans Retinal and its Unprotonated and Protonated Schiff Base
US-Japan Conference on Visual Pigments.
Allerton House. University of Illinois

Nafie, L.A., Pezolet, M., & Peticolas, W.L. (1973)
On the Origin of the Intensity of the Resonant Raman Bands of Differing Polarization in Heme Proteins
Chem. Phys. Letts. 20, 563

Nelson, R., DeRiel, J.K., & Kropf, A. (1970)
13-Desmethyl Rhodopsin and 13-Desmethyl Isorhodopsin Visual Pigment Analogues
Proc. Natl. Acad. Sci. (USA) 66, 531

Oesterhelt, D. (1971)
The Binding Site of Retinal in the Purple Membrane of Halobacterium Halobium
Absst. Comm. 7th meet. Eur. Biochem. Soc. #517

Oesterhelt, D., & Stoeckinius, W. (1971)
Rhodopsin-Like Protein from the Purple Membrane of Halobacterium Halobium
Nature (New Biol.) 233, 149

Oesterhelt, D., & Stoeckinius, W. (1973)
Functions of a New Photoreceptor Membrane
Proc. Natl. Acad. Sci. (USA) 70, 2853

Oseroff, A.R., & Callender, R.H. (1974)
Resonance Raman Spectroscopy of Rhodopsin in Retinal Disk Membranes
Biochem. 13, 4243

Papermaster, D.S., & Dryer, W.J. (1974)
Rhodopsin Content in the Outer Segment Membranes of Bovine and Frog Retinal Rods
Biochem. 13, 2438

Patel, D.J. (1969)
220 MHz Proton Nuclear Magnetic Resonance Spectra of Retinals
Nature (London) 221, 825

Peticolas, W.L., Nafie, L., Stein, R., & Fanconi, B. (1970)
Quantum Theory of the Intensities of Molecular Vibrational Spectra
J. Chem. Phys. 52, 1576

Pettei, M.J., Yudd, A.P., Nakanishi, K., Henselman, R., & Stoeckinius, W. (1977)
Identification of Retinal Isomers Isolated from Bacteriorhodopsin
Biochem. 16, 1955

Pezolet, M., Nafie, L.A., & Peticolas, W.L. (1973)
Complete Polarization Measurements for Non-Symmetric Raman Tensors.
Symmetry Assignments of Ferrocytochrome C Vibrations
J. Raman Spectr. 1, 455

Pilkiewicz, F., Pettei, M.J., Yudd, A.P., & Nakanishi, K. (1977)
Simple and Non-Isomerizing Procedure for the Identification of Protein-Linked Retinals
Expl. Eye Res. in press.

Pitt, G.A.J., Collins, F.D., Morton, R.A., & Stoc, P. (1955)
Studies of Rhodopsin. 8. Retinyledene Methylamine, an Indicator Yellow Analogue
Biochem. J. 59, 122

Placzek, G. (1934)
Handbach der Radiologie. E. Marx ed. V2 p. 209-374
"Rayleigh and Raman Scattering" UCRL translation #526L

Poo, M., & Cone, R.A. (1974)
Lateral Diffusion of Rhodopsin in the Photoreceptor Membrane
Nature (London) 247, 438

Racker, E., & Stoeckinius, W. (1974)
Reconstitution of Purple Membrane Vesicles Catalysing Light-Driven Proton Uptake and Adenosine Triphosphate Formation
J. Biol. Chem. 249, 662

Radding, C.M., & Wald, G. (1956a)
Stability of Rhodopsin and Opsin. Effects of pH and Aging
J. Gen. Physiol. 39, 923

Radding, C.M., & Wald, G. (1956b)
Acid Base Properties of Rhodopsin and Opsin
J. Gen. Physiol. 39, 909

Raman, C.V., & Krishnan, K.S. (1928)
A New Type of Secondary Radiation
Nature (London) 121, 501

Rea, D.G. (1960)
On the Theory of the Resonance Raman Effect
J. Mol. Spectr. 4, 499

Renthal, R., Steinemann, A., & Stryer, L. (1973)
The Carbohydrade Moiety of Rhodopsin: Lectin-Bindings, Chemical Modification and Fluorescence Studies
Expl. Eye Res. 17, 511

Rinai, L., Heyde, M.E., Heller, H.C., & Gill, D. (1971a)
Raman Excitation Profiles as Probes for Inaccessible Electronic Levels in Molecules: Retinol and Naphthalene
Chem. Phys. Letts. 10, 207

Rinai, L., Gill, D., & Parsons, J.L. (1971b)
Raman Spectra of Dilute Solutions of some Stereoisomers of Vitamin A Type Molecule
J. Am. Chem. Soc. 93, 1353

Rinal, L., Heyde, M.E., & Gill, D. (1973)
Vibrational Spectra of Some Carotenoids and Related Linear Polyenes.
A Raman Spectroscopic Study
J. Am. Chem. Soc. 93, 4493

Robertson, J.D. (1966)
Granulo-Fibrillar and Globular Substructure in Unit Membranes
N.Y. Ann. Sci. 137, 421

Rosenfeld, T., Honig, B., Ottolengi, M., & Ebrey, T.G. (1977a)
Cis-Trans Isomerization in the Photochemistry of Vision
Pure Appl. Chem. 49, 341

Rosenfeld, T., Honig, B., Ottolengi, M., & Ebrey, T.G. (1977b)
On the Role of the Protein in the Photoisomerization of the Visual Pigment Chromophore
In press.

Rowan, III.R., Warshel, A., Sykes, B.D., & Karplus, M. (1974)
Conformation of Retinal Isomers
Biochem. 13, 970

Rowan, III.R., & Sykes, B.D. (1974)
A Carbon-13 Nuclear Magnetic Resonance Study of the Visual Model Compounds
J. Am. Chem. Soc. 96, 7000

Shepard, N., & Sutherland, G.B.B.M. (1949)
Vibration Spectra of Hydrocarbon Molecules: Frequencies Due to Deformation Vibration of Hydrogen Atoms Attached to a Double Bond
Proc. R. Soc. (London) A196, 195

Shichi, H. (1971)
Biochemistry of Visual Pigments II. Phospholipid Requirement and Opsin Conformation for Regeneration of Bovine Rhodopsin
J. Biol. Chem. 246, 6178

Smith, Jr. H.G., Fager, R.S., & Litman, B.J. (1977)
Light Activated Calcium Release from Sonicated Bovine Retinal Rod Outer Segment Disks
Biochem. 16, 1399

Spiro, T.G. (1975a)
Resonance Raman Studies of Heme Protein
Biochim. Biophys. Acta 416, 169

Spiro, T.G. (1975b)
Biological Applications of Resonance Raman Spectroscopy: Haem Proteins
Proc. R. Soc. (London) A345, 89

Spiro, T.G., & Strekas, T.C. (1972)
Resonance Raman Spectra of Hemoglobin and Cytochrome c Inverse Polarization and Vibronic Scattering
Proc. Natl. Acad. Sci. (USA) 69, 2622

Spiro, T.G., & Strekas, T.C. (1974)
Resonance Raman Spectra of Heme Protein. Effects of Oxidation and Spin State
J. Am. Chem. Soc. 96, 338

Stoeckinius, W. (1975)
The Photoreaction Cycle of Bacteriorhodopsin
US-Japan Conference of Visual Pigments
Allerton House. University of Illinois

Stoeckinius, W. (1976)
The Purple Membrane of Salt-Loving Bacteria
Sci. Am. 234(6), 38

Strekas, T.C., & Spiro, T.G. (1972a)
Hemoglobin: Resonance Raman Spectra
Biochim. Biophys. Acta 263, 830

Strekas, T.C., & Spiro, T.G. (1972b)
Cytochrome c: Resonance Raman
Biochim. Biophys. Acta 278, 188

Sulkes, M., Lewis, A., Lemley, A.T., & Cookingham, R. (1976)
Modelling the Resonance Raman Spectrum of Metarhodopsins: Implications for the Color of Visual Pigments
Proc. Natl. Acad. Sci. (USA) 73, 4266

Suzuki, H., Komatsu, T., & Kitajima, H. (1974)
Theory of the Optical Property of Visual Pigment
J. Phys. Soc. (Japan) 37, 177

Tang, J., & Albrecht, A.C. (1968)
Studies in Raman Intensity Theory
J. Chem. Phys. 49, 1144

Tang, J., & Albrecht, A.C. (1970)
Developments in the Theories of Vibrational Raman Intensities. In "Raman Spectroscopy" V2 p. 33-68. Szymanski, H.A. ed. Plenum, N.Y.

Tennekes, H., & Lumley, J.L. (1972)
A First Course in Turbulence. Chapter 5. MIT Press, Cambridge, Mass.

Trissl, H.W., Darszon, A., & Montal, M. (1977)
Rhodopsin in Model Membranes: Charge Displacements in Interfacial Layers
Proc. Natl. Acad. Sci. (USA) 74, 207

Udefriend, S. (1969)
Fluorescence Assay in Biology and Medicine. Chapter 6: Proteins.
Academic Press, N.Y., London

Van Vleck, J.H. (1929)
On the Vibrational Selection Principles in the Raman Effect
Proc. Natl. Acad. Sci. (USA) 15, 754

Wagoner, A.S., & Stryer, L. (1971)
Induced Optical Activity in Metarhodopsins
Biochem. 10, 3250

Wald, G. (1968)
Molecular Basis of Visual Excitation
Science 162, 230

Wald, G., & Hubbard, R. (1960)
Enzymic Aspects of Visual Processes. In the "Enzymes" V. 3 Part B
p. 369-386. P.D. Bayer, H. Lardy, & K. Myrback eds.
Academic Press, N.Y.

Waleh, A., & Ingraham, L.L. (1973)
A Molecular Orbital Study of the Protein-Controlled Bathochromic Shift in a Model of Rhodopsin
Arch. Biochem. Biophys. 156, 261

Warshel, A. (1973)
Quantum Mechanical Consistent Force Field (QCFF/PI) Method: Calculations of Ground and Excited States of Conjugated Molecules
Israel J. Chem. 11, 709

Warshel, A. (1977)
Interpretation of Resonance Raman Spectra of Biological Molecules
Ann. Rev. Biophys. & Bioeng. 6, 273

Warshel, A., & Karplus, M. (1972a)
Vibrational Structure of Electronic Transitions in Conjugated Molecules
Chem. Phys. Letts. 17, 7

Warshel, A., & Karplus, M. (1972b)
Calculations of Ground and Excited State Potential Surfaces of Conjugated Molecules I. Formulation and Parametrization
J. Am. Chem. Soc. 94, 5612

Warshel, A., & Karplus, M. (1974)
Calculation of Excited State Conformation and Vibronic Structure of Retinal and Related Molecules
J. Am. Chem. Soc. 96, 5677

Warshel, A., & Karplus, M. (1977)
Calculation of the Resonance Raman Intensities of Schiff Bases of Retinal as a Tool for Interpretation of the Resonance Raman Spectra of Photoreceptor Pigments
J. Am. Chem. Soc. in press.

Weber, G., & Teale, F.J.W. (1959)
Electronic Energy Transfer in Haem Protein
Discussions Faraday Soc. 27, 134

Wiesenfeld, J.R., & Abrahamson, E.W. (1968)
Visual Pigments: Their Spectra and Isomerizations
Photochem. Photobiol. 8, 487

Worthington, C.R. (1971)
Structure of Photoreceptor Membranes
Fed. Proc. 30, 57

Worthington, C.R. (1973)
X-ray Diffraction Studies on Biological Membranes
Curr. Top. Bioenerg. 5, 1

Worthington, C.R. (1974)
Structure of Photoreceptor Membranes
Ann. Rev. Biophys. & Bioeng. 3, 53

Wu, C.W., & Stryer, L. (1972)
Proximity Relations in Rhodopsin
Proc. Natl. Acad. Sci. (USA) 69, 1104

Yamamoto, T., Palmer, G., Gill, D., Salmeen, I.T., & Rinai, L. (1973)
The Valence and Spin State of Iron in Oxyhemoglobin as Inferred from Resonance Raman Spectroscopy
J. Mol. Biol. 248, 5211

Yoshizawa,T., & Wald, G. (1963)
Prelumirhodopsin and the Bleaching of Visual Pigments
Nature (London) 197, 1279

Yoshizawa, T., & Horiuchi, S. (1973)
Studies of Intermediates of Visual Pigments by Absorption Spectra at Liquid Helium Temperature and Circular Dichroism at Low Temperatures.
In "Biochemistry and Physiology of Visual Pigments" p. 69
Helmut Langer ed. Springer-Verlag, N.Y., Heidelberg, Berlin

Zimmerman, W., Yost, M., & Daemen, F. (1974)
Dynamics and Function of Vitamin A Compounds in the Rat Retina After a Small Bleach of Rhodopsin
Nature (London) 250, 66

Zorn, M., & Futterman, S. (1971)
Properties of Rhodopsin Dependent on Associated Phospholipid
J. Biol. Chem. 246, 881